PROGRESSIVE COLLAPSE TESTING AND ANALYSIS OF A STEEL BUILDING

HONORS THESIS

Presented in Partial Fulfillment of the Requirement to Graduate with Honors Research Distinction from the Civil, Environmental and Geodetic Engineering Department at The Ohio State University

By

Ebiji Anthony Akah

The Ohio State University

2013

Undergraduate Honors Examination Committee:

Dr. Halil Sezen, Advisor

Dr. Shive K. Chaturvedi

ABSTRACT

This research investigates the progressive collapse vulnerability of an existing steel building, Haskett Hall, on the Ohio State University (OSU) campus. The building was tested by removing one of the first-story columns to observe its collapse resistance and to evaluate the effectiveness of current modeling and analysis guidelines. Progressive collapse is a partial or complete collapse of a structure due to the loss of a supporting element, a column in this case. Few researchers have been able to conduct full-scale experiments to understand the progressive collapse mechanism. One previous OSU study tested the vulnerability for progressive collapse of a steel building in Northbrook, Illinois, and another building on the OSU campus. It was concluded that more detailed models are needed to account for nonlinearity, three-dimensional and dynamic effects in analysis of a building frame including beams and columns surrounding the removed column. To address these issues, in this research deflections and deformations within the neighboring beams and columns were measured during column removal. A structural analysis program, SAP2000, is used to predict building response which is then compared to the experimental data. The goal of this study is to develop recommendations for improved procedures for static progressive collapse analysis of buildings.

ACKNOWLEDGEMENTS

I would like to thank my advisor, Associate Professor Halil Sezen, for his wisdom, support, and guidance. Without his aid and dedication, this honors thesis would not have been possible. He continues to mentor me to improve my research capabilities, writing, and overall knowledge of the civil engineering field. Furthermore, he always makes an effort to meet with me to answer any questions while allowing me to lead the project progression.

I want to thank doctorate students, C. Wood and S. Lodhi, graduate student, N. Savage, and undergraduate student, J. Wade for their contribution to this research. Without the help of C. Wood, S. Lodhi and N. Savage, the instrumentation process and pictorial documentation for the experiment would not have been possible. Furthermore, I thank C. Wood and S. Lodhi for getting me acquainted with architectural building layouts and SAP2000. I want to thank J. Wade for his help in calculating loads, determining member sizes, and interpreting data. I also thank J. Wade for being flexible about meeting times.

I want to thank the Loewendick Demolition Company for allowing the project team to work on-site before demolishing the buildings. I thank the company for removing part of the façade to expose beams and columns for instrumentation. Furthermore, I thank Loewendick for removing a single column for the experiment before continuing with the demolition.

Lastly, I want to thank the Undergraduate Research Office (URO) and College of Engineering for supplying funding. Their scholarships and research fellowships provided focused time to work on this research during the summer of 2012 and throughout the 2012-2013 academic year. I would not have been where I am today without their support.

VITA

August 21, 1991……Born – Upper Arlington, Ohio

May 5, 2013……B.S. Civil Engineering

FIELD OF STUDY

Major Field: Civil, Environmental and Geodetic Engineering

TABLE OF CONTENTS

LIST OF FIGURES

LIST OF TABLES

CHAPTER 1: INTRODUCTION

1.1 Background

The term “Progressive Collapse” is defined as the collapse of all or part of a structure resulting from a small or local structural failure [9]. When a column is removed, the load that the column supports is then distributed through the structure into nearby slabs, beams and columns until equilibrium is once again obtained. When the neighboring elements are not designed to redistribute the load a disproportionate part of the structure could collapse.

The General Services Administration (GSA), American Society of Civil Engineers (ASCE), and the Unified Facility Criteria (UFC) all have guidelines to evaluate, design and improve progressive collapse resistance of existing and new buildings. GSA (2003) outlines procedures to evaluate whether a building, based on its size and shape, is vulnerable to progressive collapse [7]. ASCE 7 (2010) outlines approaches to ensure structural integrity when a load-carrying member is damaged [3]. Lastly, UFC 4-023-03 outlines how to prevent progressive collapse in multi-story buildings [4]. This research will use these guidelines to test and analyze whether a given structure was susceptible to progressive collapse, and whether these guidelines require simplifications or improvements.

This research focuses on progressive collapse modeling and analysis of Haskett Hall. Haskett Hall was a four-story building built in 1925 on the Ohio State University

(OSU) campus in Columbus, Ohio. It was composed of built-up steel columns using rivets and channels, reinforced concrete slabs for the flooring, and steel I-beams filled with concrete [8]. One column within Haskett Hall was removed within a short time period, as recommended by the GSA design guidelines, by Loewendick Demolition Contractors. The building was demolished on December 19, 2011.

Strain gauges, installed on three neighboring columns and three connecting beams, measured the change in axial strains during the column removal. Furthermore, displacement sensors (LVDT's) measured the vertical and horizontal vibrations and displacements. Haskett Hall was modeled in the computer program, SAP2000 (2012), to analyze progressive collapse performance by following GSA guidelines. In the analyses, the effects of steel yielding, and load redistribution were considered. Strain and moments calculated from the SAP2000 model are compared with the measured strains and displacements.

This research is part of a large research program at OSU that includes theses by K. Giriunas, B. Song and S. Lodhi, and a paper by C. Wood. Each graduate student researcher is analyzing the progressive collapse performance of the other buildings demolished in the area, including Johnston Laboratory, Boyd Laboratory, and Aviation Building in order to prepare construction for the new Chemical and Biomolecular Engineering and Chemistry Building on the OSU campus.

In addition, this research is in partial collaboration with undergraduate student, J. Wade, who calculated load distributions resulting from the roof and walls of Haskett Hall. Wade also helped with determining the section properties of the various columns used for analysis.

1.2 Previous Research

Following the ASCE, GSA and UFC guidelines, research was conducted in 2007 to test the vulnerability for progressive collapse of the steel Ohio Union Building in Columbus, Ohio [11]. The building was scheduled for demolition in order to start constructing a newly renovated Ohio Union, and was therefore tested for progressive collapse by removing four steel columns. From its first story a similar experiment was conducted in 2009 on the steel Bankers Life and Casualty Company building in Northbrook, Illinois, [5, 11]. Research on these steel buildings provided experimental collapse data from real buildings; full-scale experiments that few researchers have been able to conduct to understand progressive collapse mechanism. During field testing of these buildings, column axial forces were measured through recorded strains and compared with analysis results from two- and three-dimensional computer models. It was concluded that more detailed models are needed to account for nonlinearity, three-dimensional and dynamic effects. Furthermore, it is suggested that experimental deflection data be gathered while analyzing the beams and columns surrounding the removed columns to validate the vertical displacements and overall computational analysis for the progressive collapse [11].

1.3 Scope and Objectives

The purpose of this research is to analyze the demolished building, Haskett Hall, to determine the potential for progressive collapse of the building. The objectives are as follows:

- Implement and evaluate current design methodologies.

- Test and collect data of the structural response resulting from removing a first-story column.
- Perform linear static analyses of the two-dimensional computer model.
- Compare predicted and experimental response of the building.

CHAPTER 2: BUILDING DESCRIPTION

2.1 Introduction

Chapter 2 discusses the building details of Haskett Hall. This chapter includes the roof layout, floor plan and elevation, wall details, beam and column properties and element connections. The details provided within Chapter 2 are used to develop the building's two-dimensional Western frame model and structural load values for analysis described in Chapter 5.

2.2 Building Description

The Ohio State University's Haskett Hall, located in Columbus, Ohio was completed in 1925 (Figure 2.1). Haskett Hall was a four-story building without a basement. Haskett Hall included entrances on each side of the building on the grade level and had one elevator that was replaced in 1973 [8]. The building consisted of classrooms, offices and laboratories. A section on the North side of the building was used as a three-story testing laboratory (Figure 2.2). The building layout is detailed in 20 original structural plan sheets from when the building was being erected in 1924. These structural plans were acquired from the Ohio State University's Facilities Operations and Development Archives and are included in Appendix A. Only the Western perimeter frame of Haskett Hall, where a column was removed from the building, is considered in the analysis of the progressive collapse.

2.3 Roof Layout

The roof consisted of steel trusses, a wood tongue and a groove deck (Figure A.16 in Appendix A). From Figure A.16, the "Longitudinal Section on CL (Cross Section)" detail shows that the elevations vary. The elevation difference is because the South half of the building included a three beam arc, while the North half used a crane rail system for the test facility. Along the North and South frames of the building were sway frames which consist of truss systems and are detailed in Figure A.18. Steel trusses were also used for the crane rail system along the North test facility roofing. Beams ran in the North-South direction between columns. From Figure A.16, the "Roof Framing Plan" details the numerous purlins that ran in the East-West direction between these beams. Each purlin was connected with a countersink to the composition roofing – combining the wood tongue and groove sheathing. Lastly, angle bracings existed diagonally between select columns.

2.4 Floor Layout

The building included a grid of seven columns that ran in the North-South direction and six columns that ran in the East-West direction. The total number of columns was 38 for the building (Figure 2.3). Figure 2.4 shows the typical elevation of the building frame and details the bay dimensions and elevations for each of the four floors based on distances between floor columns and beams, respectively. Figures A.13 through A.15 detail floors two, three and four, respectively. Throughout each floor were slabs that are labeled alphabetically and correspond to the respective floor level (example, 3B). Occasionally, trapezoidal joists below floor slabs were used in the East-

West direction (Figure 2.5). Joists were typically spaced at 2 ft-1 in. Typical reinforced concrete slab thickness was seven inches without joists and three inches with joists.

2.5 Wall Details

The exterior of the building had a masonry skin combining brick and limestone. Floor slabs rested on the exterior floor beams and extended into the façade (Figure 2.6). Limestone extended above floor beams and slabs and provided architectural designs along the façade. The brick extended above the limestone until the next floor beam. Brick was also inserted into external column webs (Figure 2.7). The main entrances to the building were lined by limestone for architectural designs. All secondary doors were lined with brick. Rectangular windows existed throughout the exterior walls (Figure A.7 in Appendix A). Brick lined the top and sides of each window while the bottom had limestone. The door and window schedules are included in Figure A.4.

2.6 Beam and Column Details

Beams and columns consisted of A36 steel with specific yield strength of 36,000 pounds per square inch (psi). The majority of beams on each floor ran in the East-West direction (Figure A.19). Some of these beams were encased with 4000 psi concrete, the cross-sections being detailed on each respective floor (Figure 2.8). Steel beams located in the perimeter frames were partially encased in concrete for fireproofing (Figure 2.6). Beams were connected to columns using rivets through angles that were located on the bottom flanges and internal webs (Figure B.5.1 in Appendix B). The reinforced concrete slab on beams created a more rigid connection. The columns within the building were built-up sections – I-sections bracketed by two channel sections that were connected with

rivets (Figure 2.9). Each column ran continuously throughout each floor of the building and spliced at 14 feet from the ground elevation (Figure A.17).

2.7 Foundation Details

The first floor columns were connected rigidly to the ground with rivets and angles (Figure 2.10). Typical footing for columns were designed with #6 bars that ran parallel and perpendicular to each other to create a square base (Figure A.12). At edges, bars were bent up to be hooked. Select columns extended its footing to create trapezoidal cross-sections (Figure 2.11).

Figure 2.1: Completed Haskett Hall building in 1925

Figure 2.2: North testing facility

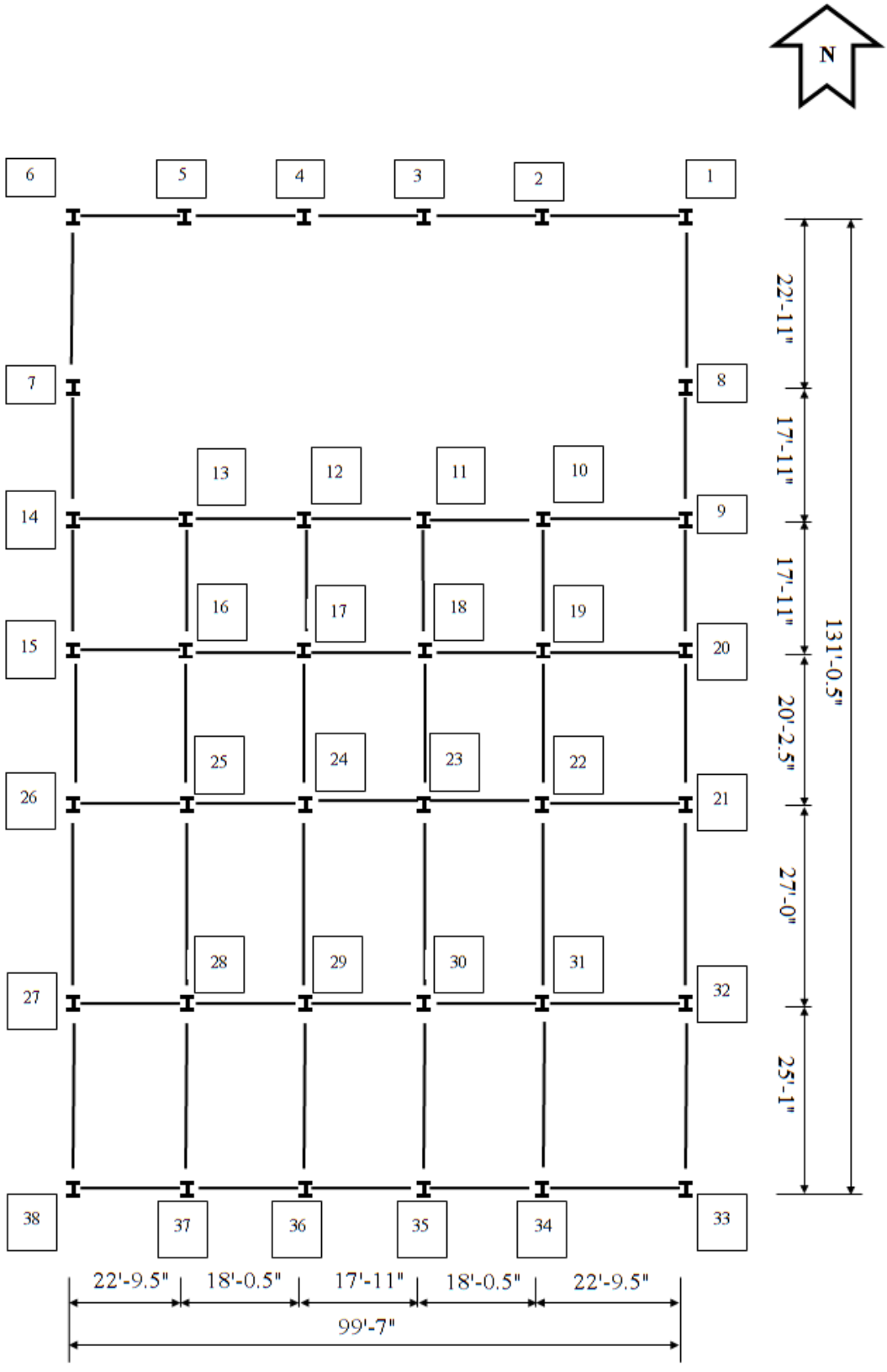

Figure 2.3: Haskett Hall floor layout (column numbers shown in rectangular boxes)

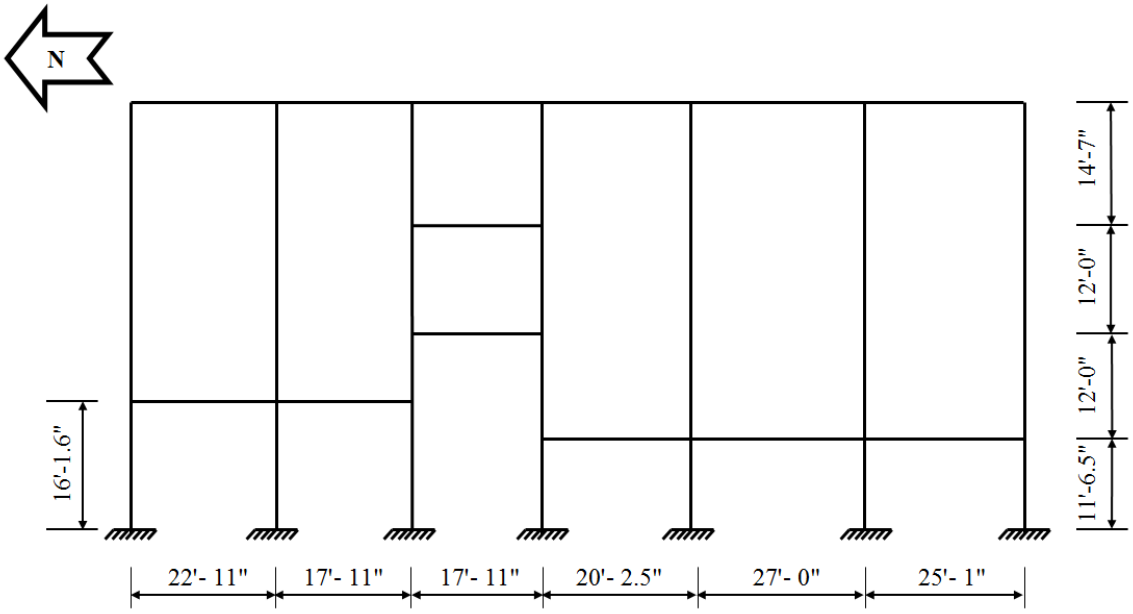

Figure 2.4: Haskett Hall elevation and bay layout

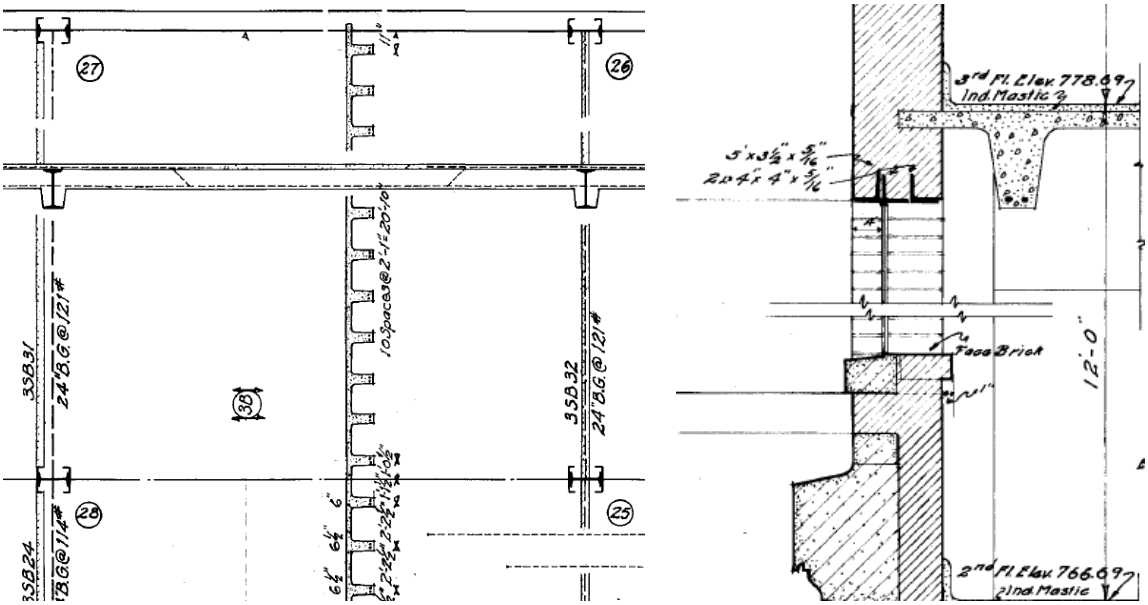

(a) (b)

Figure 2.5: Third floor joists (a, from Figure A.14) and elevation (b, from Figure A.9)

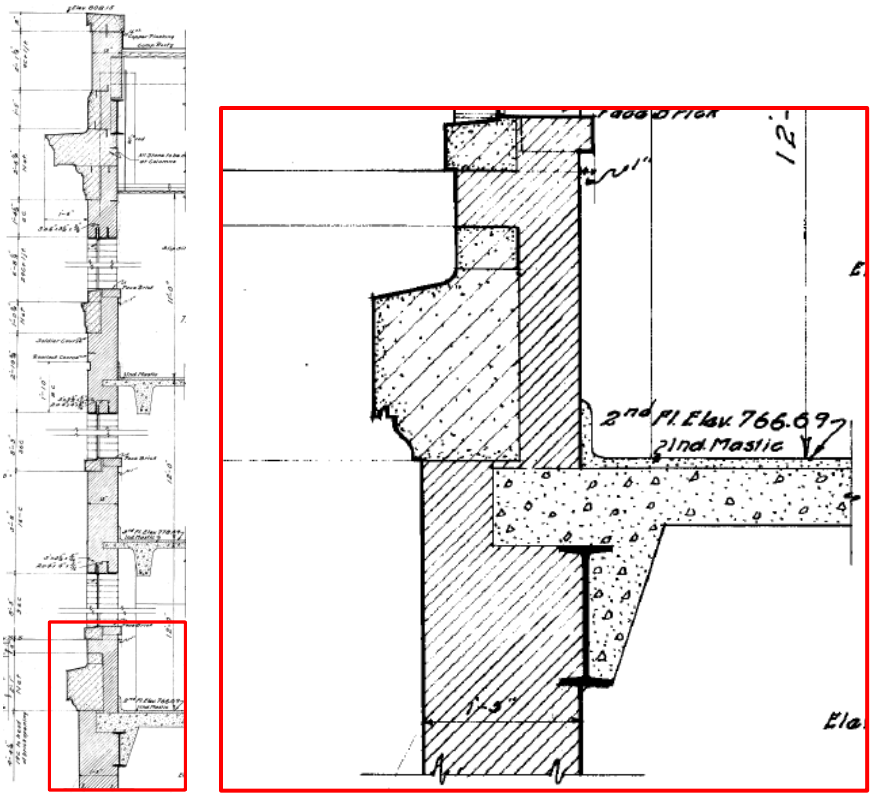

(a) (b)

Figure 2.6: Façade cross-section (a) and (b) close-up of second floor slab running into façade (taken from Figure A.9)

Figure 2.7: Brick inserted into external column webs

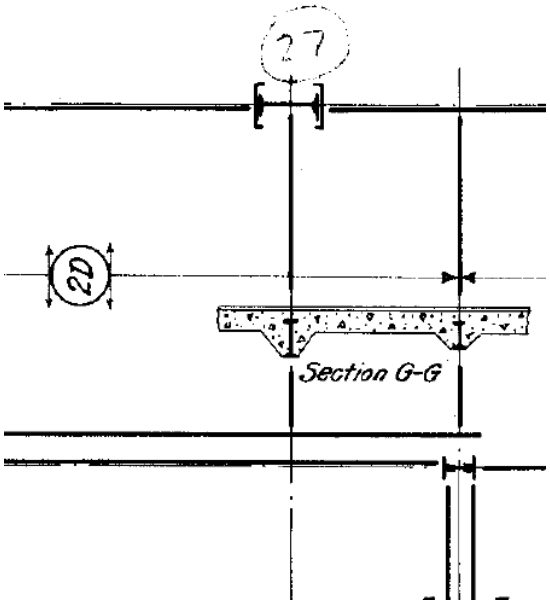

Figure 2.8: Close-up of beams encased in concrete (taken from Figure A.13)

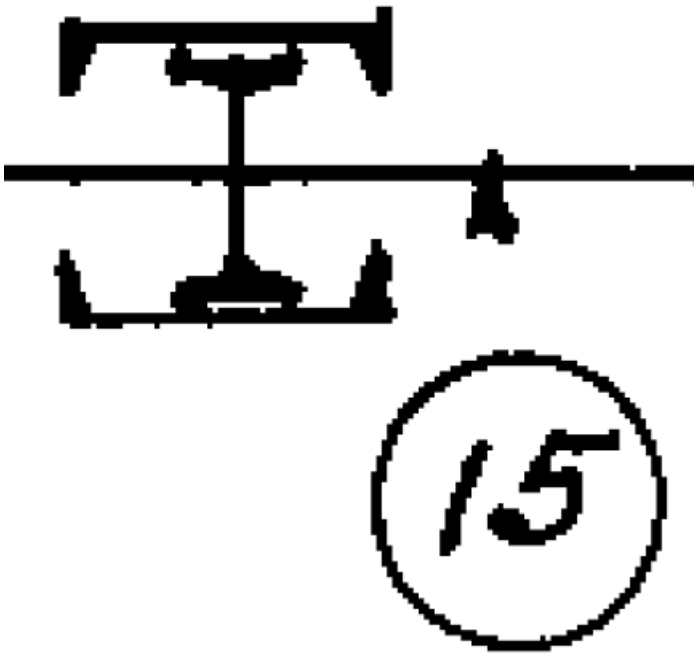

Figure 2.9: Close-up of built-up column 15 (taken from Figure A.15)

Figure 2.10: Rigid column footing

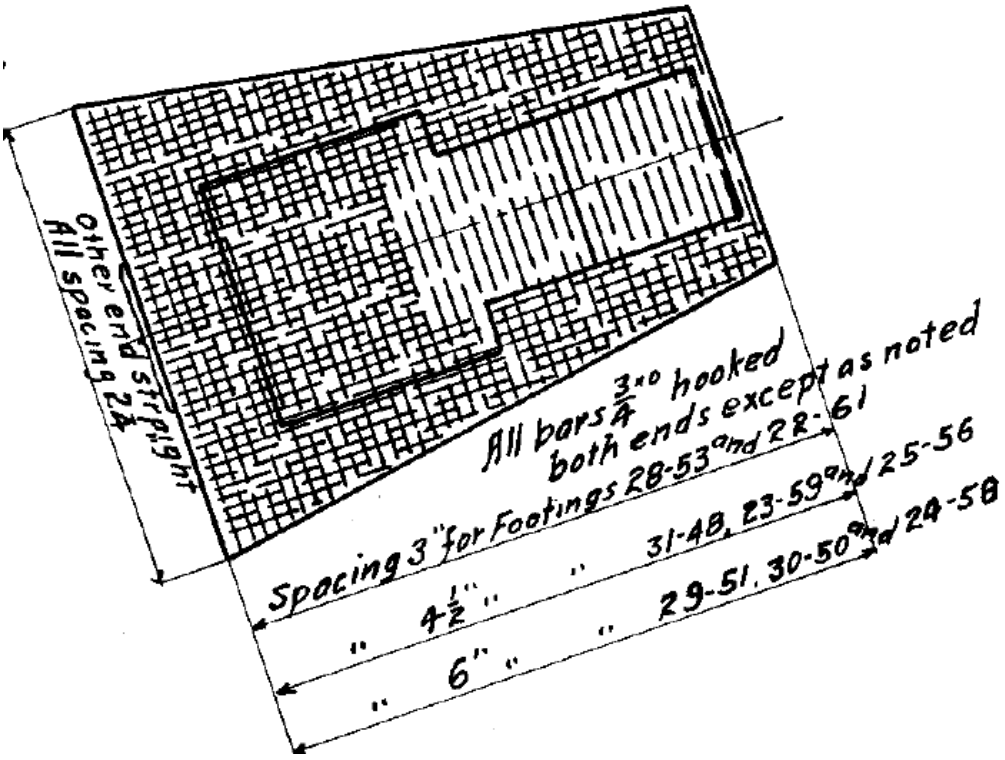

Figure 2.11: Close-up of trapezoidal footing for select columns (from Figure A.12)

CHAPTER 3: INSTRUMENTATION AND TESTING

3.1 Introduction

Chapter 3 discusses the experiment conducted on Haskett Hall. This chapter details the application and locations of the strain gauges and displacement sensors on the beams and columns neighboring the removed column. Measured data from the instrumented strain gauges and displacement sensors is presented in Chapter 4.

The experiment involved removal of a first floor column from Haskett Hall. Loewendick Demolition Contractors was hired by the university to demolish Haskett Hall. Loewendick agreed to help with the experiment by partially tearing down the exterior walls on each side of the first-story column to be removed in order to create clearance to apply strain gauges. Loewendick then removed the column using a processor. Strain gauges were attached on three columns and three beams to record the strains and deflections at various locations while one of the columns was removed. Column 27 along the Western perimeter frame was removed at the first floor level (Figure 3.13). Two displacement sensors were used to measure vertical displacements on each side of the removed column. The column removal process is described in Section 3.5.

3.2 Strain Gauges

In order to understand the consequences of removal of a steel column, each of the three steel beams connected to the removed column, as well as the three neighboring steel columns were instrumented with strain gauges and displacement sensors. The CEA-06-250UW-120/P2 strain gauges had a resistance of 120 ± 0.3% Ohms and a strain range of ±3%. They measure the strain in uniaxial direction caused by the compressive and tensile forces.

The first step to the strain gauge instrumentation was to create a smooth surface with a grinder with sand paper. The steel surface was smoothed further by applying CSM-2 degreaser while hand-sanding with 220 grit sand paper. Next, an M-Prep Conditioner A chemical was applied to the surface while using 320 and 400 grit sand papers. Q-tips were used to wipe the surface clean, swabbing from the center and moving out to the edges in order to avoid bringing dirt to the application site. Once the Q-tips showed that all dirt was cleared (i.e., the Q-tip remained white), a gauze strip was used to wipe the surface clean of the solution. After the surface was clean with the M-Prep Conditioner A, the process of cleaning with Q-tips and gauze was repeated with M-Prep Neutralizer 5A.

Once the surface was completely smoothed and cleaned, the strain gauge could be applied. To apply the strain gauge, the sensors on the gauge were placed on a strip of scotch tape. While on the tape, M-Bond 200 Catalyst was brushed onto the back of the strain gauge, making sure to wipe the excess solution along the sides of the bottle (approximately ten times). Quickly after the catalyst is applied, two drops of M-Bond 200 Adhesive were placed onto the gauge to react with the catalyst in order to create a

stronger bond to the steel surface. The strain gauge was then placed and firmly pressed against the cleaned surface of the steel element. Typically the strain gauge needs to be applied for two minutes in 70-degree-Fahrenheit weather. Because the experiment was conducted on December 19, 2011, when the temperature was around 40-degrees-Fahrenheit, each strain gauge was held against the surface for approximately five minutes to ensure a strong bond. Some vinyl mastic tape can be applied over the gauge in order to protect the strain gauge from debris, but for this experiment mastic tape was not used. Figure 3.1 shows an applied strain gauge to a column.

3.3 Strain Gauge Locations

A total of 16 strain gauges were used in the experiment: seven were applied to columns and nine were applied to beams. Figures 3.2 and 3.3 show the columns that were instrumented with strain gauges: one corner column, one column along the face of the building and one interior column. In the Haskett building layout (Figure 2.3), the removed column is labeled 27. The columns that were instrumented with strain gauges – located to the North, East, and South of the test column – were labeled 26, 28 and 38, respectively (Figure 2.3). Figure 3.2 shows the strain gauge locations. Column 26, to the North of the removed column, had two strain gauges: one on the South flange face (gauge #1) and one on the North flange face (gauge #2), each located at one-third height of the column (3 ft-1 in. above the column base). Column 28, to the East of the removed column, had one strain gauge on the West web face located at one-half height of the column (gauge #3, 4 ft-7 in.). Column 38, the corner column located to the South of the removed column, had four strain gauges: three at two-thirds height of the column (6 ft-2 in.) located on the South flange face (gauge #4), East web face (gauge #5), and North

flange face (gauge #6), and one gauge on the North flange face at one-half height of the column (gauge #7, 4 ft-7 in.). Figure 3.4 shows the strain gauge locations on the columns.

All strain gauges located on beams were on the bottom face of flanges. The orientation of each strain gauge was parallel to the beam longitudinal direction and located on the centerline or no more than two inches off-center. The beams connected to the removed column in the North-South direction each had three strain gauges. On the North-directed beam (beam between columns 26 and 27 in Figure 3.2), two gauges were located at the beam-column connection (gauge #11, East of the beam's centerline and gauge #12, West of the centerline seen in Figure 3.5). A third gauge on the North-directed beam was placed at approximately one-half the beam length from the removed column (gauge #16 at 12 ft-9 in. seen in Figure 3.6). On the South-directed beam (beam between columns 27 and 38 in Figure 3.2), two gauges were located at the beam-column connection (gauge #13, East of the centerline and gauge #14, West of the centerline seen in Figure 3.7). A third gauge on the South-directed beam was placed at approximately one-half the beam length from the removed column (gauge #15 at 12 ft-9 in. seen in Figure 3.8). The beam connected to the removed column in the East-West direction (beam between columns 27 and 28 in Figure 3.2) also had three strain gauges. Two gauges were located at the beam-column connection (gauge #9, South of the centerline and gauge #10, North of the centerline seen in Figure 3.9). A third gauge on the East-directed beam was placed at one-half of the beam length from the test column (gauge #8 at 11 ft-4.75 in. seen in Figure 3.10). Tables 3.1 and 3.2 outline the numbering and locations of the strain gauges on the beams and columns.

Table 3.1: Numbering and location of strain gauges on columns

Strain Gauge #	Steel Member	Location	Height on Column
1	(N) Column 26	(S) Flange	3 ft-1 in.
2	(N) Column 26	(N) Flange	3 ft-1 in.
3	(E) Column 28	(W) Web	4 ft-7 in.
4	(S) Column 38	(S) Flange	6 ft-2 in.
5	(S) Column 38	(E) Web	6 ft-2 in.
6	(S) Column 38	(N) Flange	6 ft-2 in.
7	(S) Column 38	(N) Flange	4 ft-7 in.

Table 3.2: Numbering and location of strain gauges on beams

Strain Gauge #	Steel Member	Location on Flange	Distance from Column 27
8	(E) Beam	On centerline	11 ft-4.75 in.
9	(E) Beam	(S) of centerline	1 ft-0.65 in.
10	(E) Beam	(N) of centerline	1 ft-0.65 in.
11	(N) Beam	(E) of centerline	1 ft-0.65 in.
12	(N) Beam	(W) of centerline	1 ft-0.65 in.
13	(S) Beam	(E) of centerline	1 ft-0.65 in.
14	(S) Beam	(W) of centerline	1 ft-0.65 in.
15	(S) Beam	On centerline	12 ft-9 in.
16	(N) Beam	On centerline	12 ft-9 in.

To elaborate on the distance of strain gauges #9 through #14, a steel angle connected the beams to the column, resulting in instrumentation being located at approximately one foot from the test column.

3.4 Displacement Sensor Instrumentation and Location

Along with the 16 strain gauges, three Linear Variable Differential Transformers (LVDTs) were used to collect vertical and horizontal displacement measurements surrounding the removed column. During the experiment, two LVDTs were used to measure vertical displacements – one to the North and one to the South of the removed column. The third LVDT was placed on the North side of the test column in the horizontal direction. The major objective of this horizontal LVDT was to measure any potential slippage at the bottom of the beam-column connection. To hold the two vertical LVDTs right under the beams connected to the removed column's North and South faces, two wooden towers (designed and built by OSU graduate students C. Wood, S. Lodhi and N. Savage) were used. Figure 3.11 shows the layout of the three displacement sensors around the test column. Table 3.3 details the distance of the LVDTs from the removed column.

Table 3.3: Numbering and location of LVDTs

LVDT #	Steel Member	Orientation	Distance from Column
1	(N) Beam	Vertical	1 ft-6 in.
2	(S) Beam	Vertical	2 ft-4.75 in.

3	(N) Beam	Horizontal	At face of removed column

3.5 Column Removal and Data Collection

The demolition company, Loewendick, first removed the walls on each side of the column to be removed from the first story of Haskett Hall. Then the columns and beams were instrumented as described in Section 3.2. The demolition company removed the column using a processor. A processor is a machine that has a claw to twist, pull and pinch a column. The processor used by Loewendick can be seen in Figure 3.12. Figure 3.13 shows the process of column removal and after the column is cut. While the column was being removed, the strain gauges and displacement sensors were measuring data to capture the change in displacement and strains in neighboring beams and columns.

Each strain gauge and displacement sensor had lead wires that were connected to a gauge detector by soldering the ends of the wire (all soldering was performed by graduate students Lodhi and Wood). The gauge detector fed into a portable data acquisition system which was connected to a laptop computer. Strain data from numbered strain gauge channels (detailed in Figure 3.2 and Tables 3.1 and 3.2) and displacement data from three displacement sensors (Figure 3.11 and Table 3.3) were recorded during the entire column removal process. The laptop computer and data acquisition program was operated by graduate student Lodhi, while I kept lap-times of when the processor was in contact with the column. For safety measures, all researchers remained at least 100 feet away from the test building. Pictures were taken and video was recorded by graduate students N. Savage, C. Wood and J. Morone. Once the steel column was cut through, data recording was terminated. The experimental data was stored in a Microsoft Excel file.

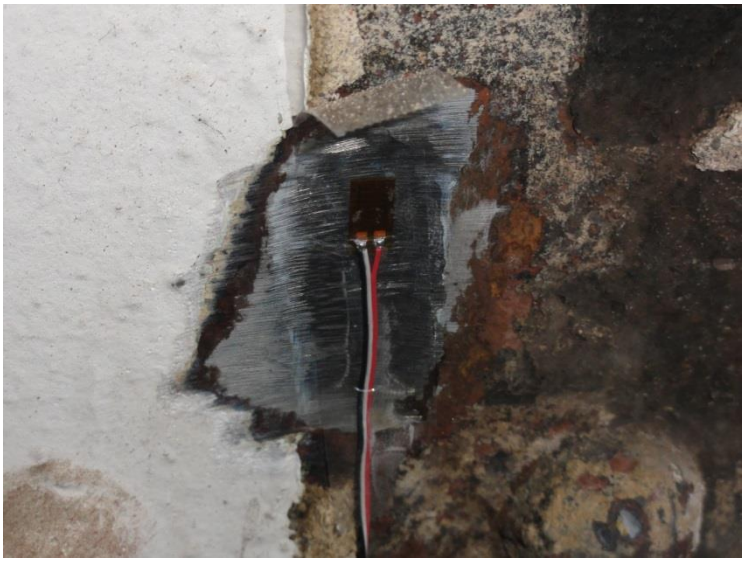

Figure 3.1: Strain gauge attached to a steel surface

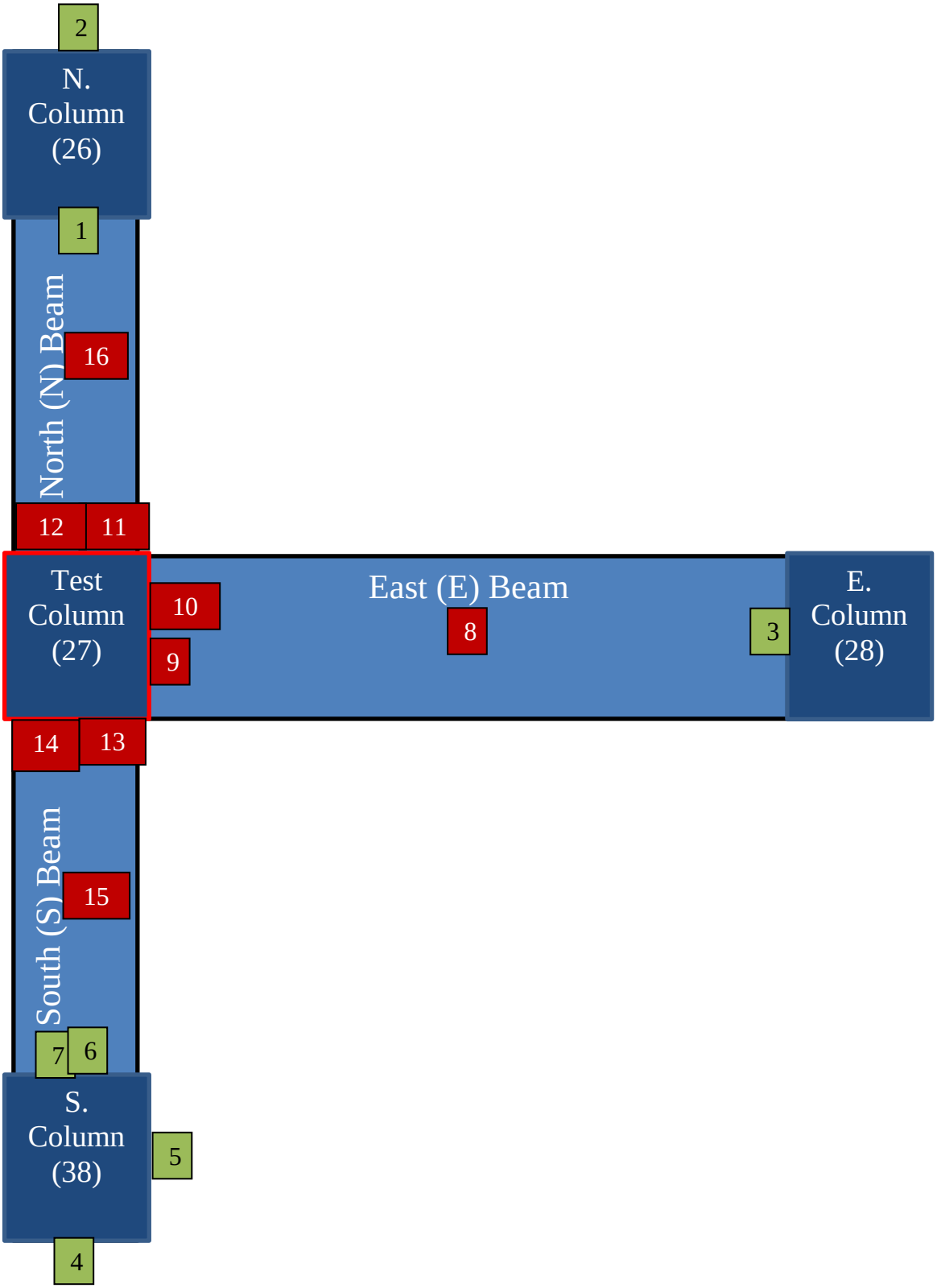

Figure 3.2: Strain gauge layout on beams (red) and columns (green)

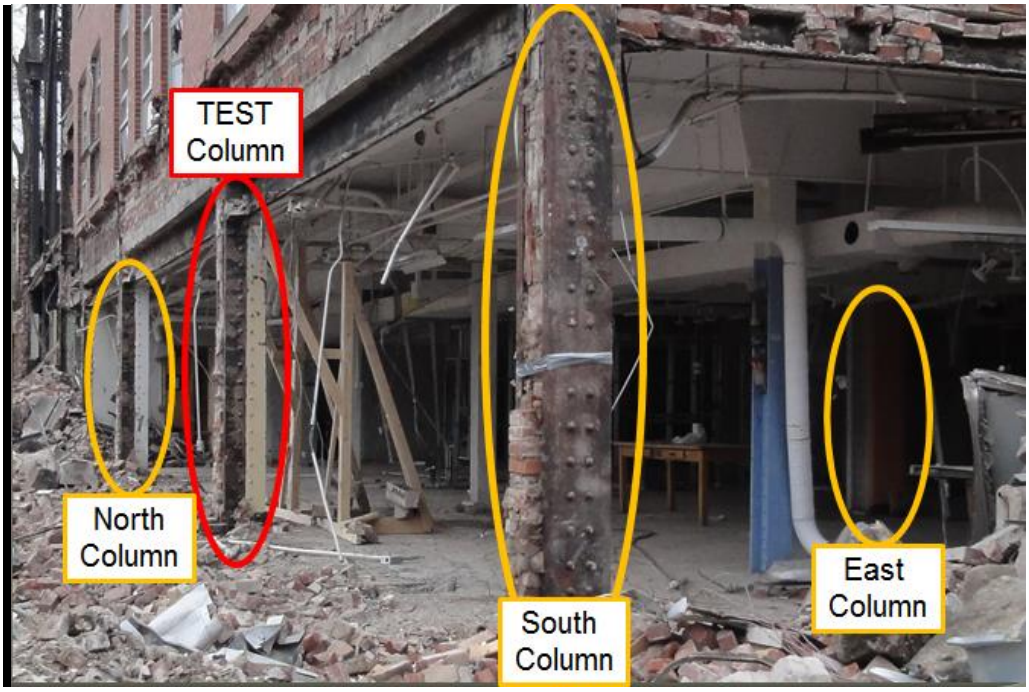

Figure 3.3: Test column (red) and neighboring columns (yellow) to be instrumented

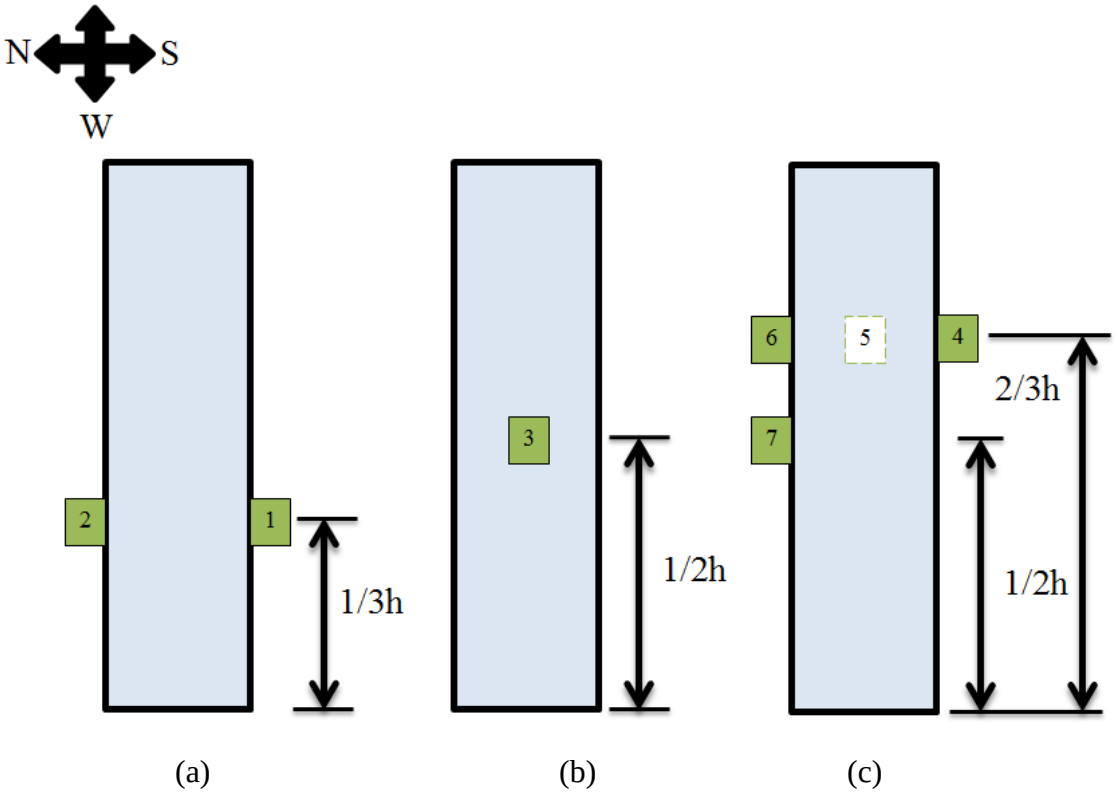

Figure 3.4: Strain gauge location on the North (a), East (b), and South (c) columns

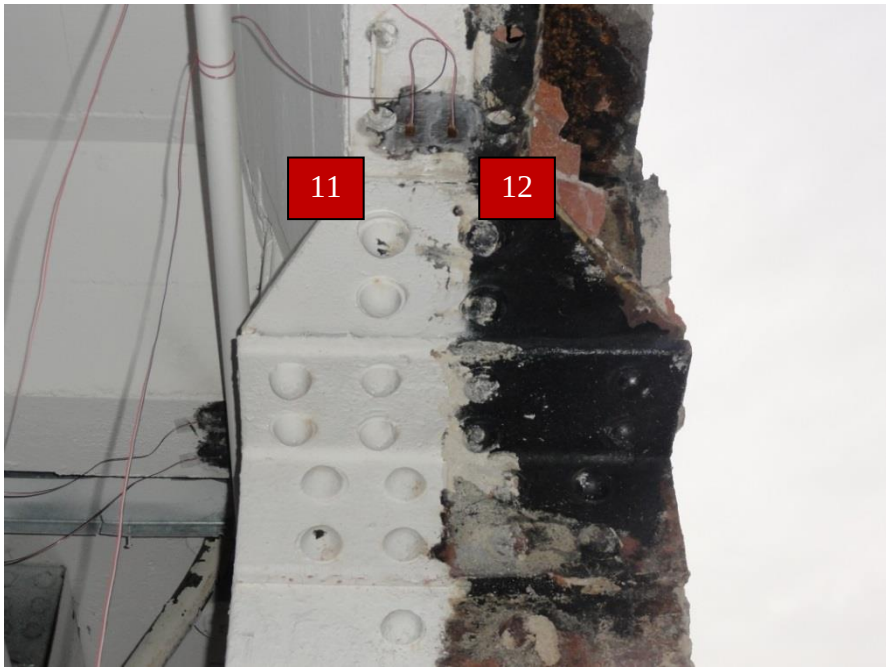

Figure 3.5: North-directed beam instrumented with strain gauges #11 and #12

Figure 3.6: North-directed beam instrumented with strain gauge #16

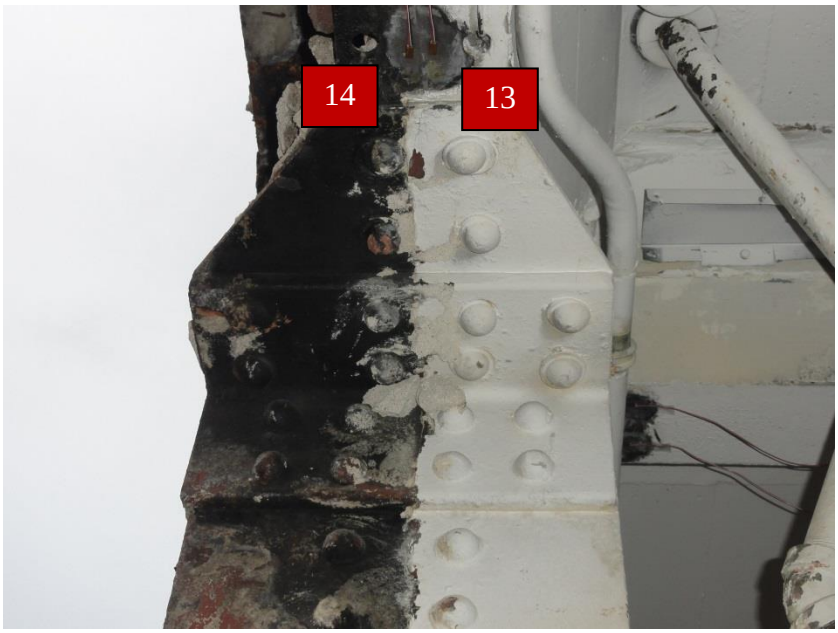

Figure 3.7: South-directed beam instrumented with strain gauges #13 and #14

Figure 3.8: South-directed beam instrumented with strain gauge #15

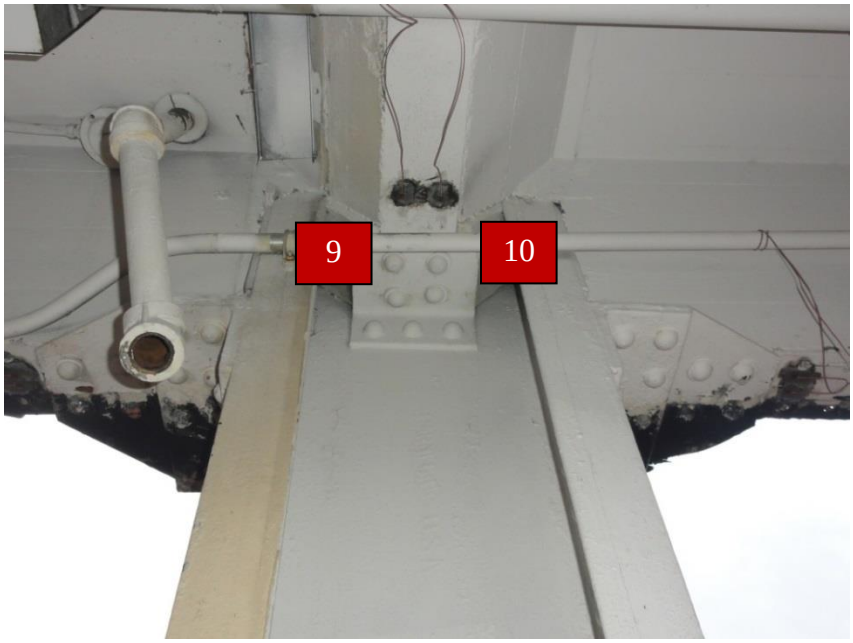

Figure 3.9: East-directed beam instrumented with strain gauges #9 and #10

Figure 3.10: East-directed beam instrumented with strain gauge #8

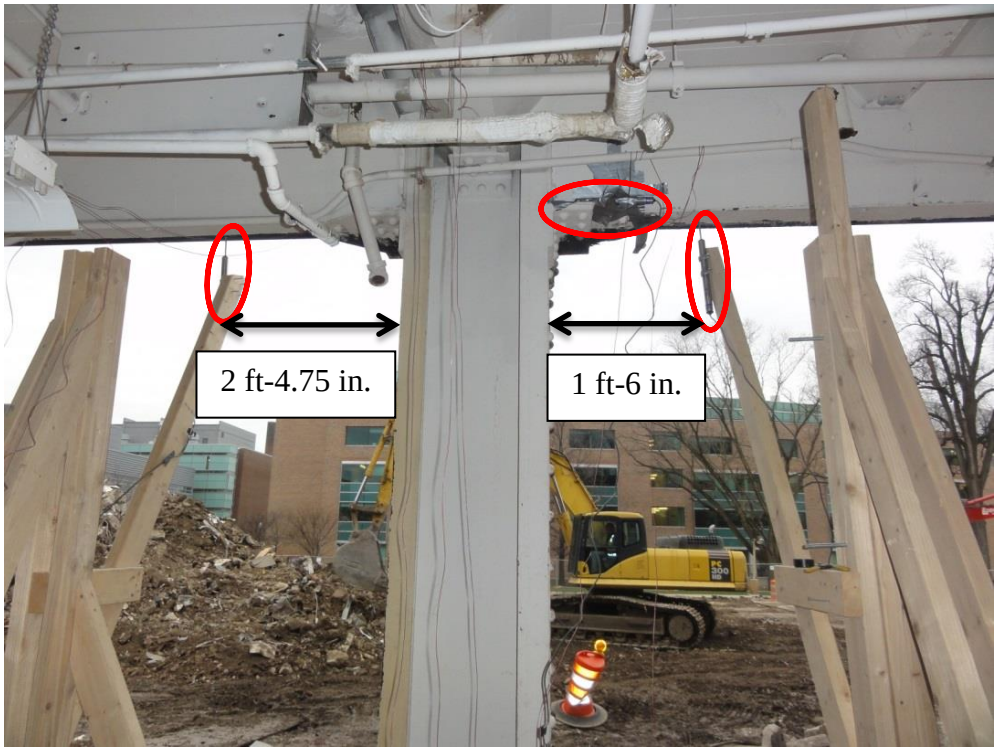

Figure 3.11: Displacement sensor positions with respect to the removed column

Figure 3.12: Loewendick Demolition Company's processor used to cut the column

(a) (b)

Figure 3.13: (a) Column removal process and (b) removed first-story test column

CHAPTER 4: EXPERIMENTAL DATA AND ANALYSIS

4.1 Introduction

Chapter 4 discusses the experimental data measured by the strain gauges and displacement sensors. This chapter details the time intervals that the processor made contact with the test column and how those intervals affected the strain and displacement values measured. Furthermore, this chapter includes how strain and displacement values are related to the building's response to removing the first-floor column.

4.2 Measured Strain Data

Strain can be defined as the change in length divided by the original length of a structural member. When the structural element experiences positive strain, that element is being stretched under tensile force. When the structural element experiences negative strain, that element is being contracted under compressive force. When the strain history is plotted as a function of time, a change in slope represents deformation and a lack of static equilibrium. Therefore, when the slope is zero, equilibrium within an element has been established.

All but one strain gauge described in Section 3.3 worked well and reliable dynamic strain data was recorded during column removal. Strain gauge #8, located at the midpoint of the Eastern beam between the test column 27 and column 28 (Figure 3.2) was the only gauge that failed to collect data during the column removal process. There

were five distinct physical events and the corresponding measured strain helped understand the behavior of the building during those events. Initially, all strain gauges and sensors had stable readings, ideally at zero strain. When the processor made contact with the test column, strain values started to increase. A period for the processor began when the claw closed, making contact with the column, and ended when the claw opened and was no longer in contact with the column. These five periods are shown in Table 4.1.

Table 4.1: Times that the processor made contact with the test column

Contact # and Event	**Contact Start Time (s)**	**Contact End Time (s)**
1. Strain and displacement values increased from zero	168.49	177.65
2. Bricks inserted into external column web crumbled	184.61	191.17
3. Column became bent inward	208.62	218.54
4. Column became warped, twisted by the processor	221.60	231.76
5. Column was cut through and 2nd floor beams visibly deflected downward	247.77	251.74

The measured strain versus time plots can be seen in Figures 4.1 through 4.8. From the plots, dynamic measurements of strain that appear after 300 seconds are a result of the processor making contact with the test column, but for the sake of the experiment, data measurements were meant to be terminated once the column was removed.

4.3 Analysis of Measured Strains

The strain gauge measurements were directly affected by the processor movements. In order to describe how the times that the processor made contact with the column affected the measured strain values, Figure 4.2, the strain versus time plot of strain gauge #3 located at one-half height (4 ft-7 in.) on the East column 28 will be referenced as an example. As seen in this plot, at each time that the processor made contact with the column there existed a jump in strain. With this specific strain gauge, the first contact time started at 168.49 seconds with the processor closing its claw and resulted in the strain gauge recording a jump to a strain value of approximately -20×10^{-6} inch/inch. Once the processor opened its claw and was no longer in contact with the column at a time of 177.65 seconds, the strain fell to a value of -15×10^{-6} in./in. This overall decrease in strain exhibits the change, and overall increase, in axial load on column 28. The same effect is apparent from when the processor closed and opened its claw three more times: from 184.61 seconds to 191.17 seconds, 208.62 seconds to 218.54 seconds, and 221.60 seconds to 231.76 seconds. During these contact times the column's inserted bricks began to crumble, the column became bent inward and started to become warped by the processor's twisting. At the beginning of these contact times there resulted in a negative strain measurement, while at the end of the contact times there was a marginal decrease in overall strain in the column. With each period the overall measured strain in the column became more negative with a smaller marginal value. This was in result of the test column providing less support for the building with each time the processor made contact to cut the column.

During the last processor contact time, which lasted from 247.77 seconds to 251.74 seconds, the test column was completely cut through and the connecting beams

deflected downward. It should be noted that the test column was cut by altering the position of the processor, meaning there existed a three-dimensional cutting plane. Analyzing the data from strain gauge #3, once the column was cut, the measured stain value drastically increased momentarily. Once the processor was no longer in contact with the cut column, the measured strain leveled out to a negative value of $-31x10^{-6}$ in./in. This negative strain value, by definition, means that the column at one-half of its height was in compression. The remaining strain gauge measurements at 300 seconds, after the last contact time, can be seen in Tables 4.2 and 4.3 which expand on Tables 3.1 and 3.2. Negative strain values indicate compression and positive strain values indicate tension.

Table 4.2: Strain values at 300 seconds from strain gauges on columns

Gauge #	**Steel Member**	**Location**	**Height on Column**	**Strain ($x10^{-6}$ in./in.)**
1	(N) Column 26	(S) Flange	3 ft-1 in.	-32
2	(N) Column 26	(N) Flange	3 ft-1 in.	-54
3	(E) Column 28	(W) Web	4 ft-7 in.	-31
4	(S) Column 38	(S) Flange	6 ft-2 in.	-7
5	(S) Column 38	(E) Web	6 ft-2 in.	-61
6	(S) Column 38	(N) Flange	6 ft-2 in.	-103
7	(S) Column 38	(N) Flange	4 ft-7 in.	-93

Table 4.3: Strain values at 300 seconds from strain gauges on beams

Gauge #	Steel Member	Location on Flange	Distance from Column 27	Strain ($x10^{-6}$ in./in.)
8	(E) Beam	On centerline	11 ft-4.75 in.	Not Available
9	(E) Beam	(S) of centerline	1 ft-0.65 in.	26
10	(E) Beam	(N) of centerline	1 ft-0.65 in.	-42
11	(N) Beam	(E) of centerline	1 ft-0.65 in.	136
12	(N) Beam	(W) of centerline	1 ft-0.65 in.	171
13	(S) Beam	(E) of centerline	1 ft-0.65 in.	252
14	(S) Beam	(W) of centerline	1 ft-0.65 in.	272
15	(S) Beam	On centerline	12 ft-9 in.	81
16	(N) Beam	On centerline	12 ft-9 in.	-10

Table 4.2 shows that each strain gauge measured a negative strain value, indicating that each column underwent compression once the test column was removed. This is due to the axial loads being transferred from the test column to the neighboring columns in order to reach equilibrium within the building. The magnitude of the strain indicates the amount of axial load that was transferred to the column. As strain measures the change in length divided by the original length, a greater axial load will result in a greater compressive force and strain value. As seen in Table 4.2, the South column 38 – which measured the largest negative strain values – was transferred a greater axial force than the East column 28 or North column 26. Furthermore, the magnitude of strain values

on the columns increased from South to North and West to East, exhibiting that the axial loads were being transferred into the building.

Analyzing Table 4.3, the beam in the East-West direction between test column 27 and column 28 indicates that North of the beam's centerline on the face of the bottom flange was in compression (gauge #10, with a negative strain value) and South of the beam's centerline was in tension (gauge #9, with a positive strain value). All of the strain gauges located at the test column-beam connection (gauges #9 through #14) measured positive strain except for strain gauge #10. Strain gauge #16 measured negative – compression – at 12 feet-9 inches North of the test column. Strain gauge #15 measured positive – tension – at 12 feet-9 inches South of the test column. Analyzing the response of strain gauges #15 and #16, each time the processor made contact with the test column, the strain response of gauge #15 was similar to other strain gauges by marginally increasing in value. Whereas strain gauge #16 measured strain response oscillated between being positive and negative.

Lastly, to test for progressive collapse, the strain gauge measurements were compared with the yield strain. The yield strain defines when an element has hit its yield point – a strain value greater than the yield strain indicates that the element is being overstrained and is potentially going to fail. For steel, the yield strain is calculated by using Equation 4.1.

$$\varepsilon_y = \frac{f_y}{E} \tag{4.1}$$

In Equation 4.1, ε_y is the yield strain (in./in.), f_y is the yield strength of the steel material and E is the modulus of elasticity for steel (29,000 ksi). For A36 steel, the yield strength is 36 kips per square inch (ksi), therefore the yield strain is calculated to be 0.00124

in./in. or $1240x10^{-6}$ in./in. The maximum measured strain value was $272x10^{-6}$ in./in. Compared to the yield strain, the experimental strain values measured from Haskett Hall did not exceed the yield strain, indicating that the building was not susceptible to progressive collapse.

4.4 Measured Displacement Data

Displacement can be defined as the change in position. Displacement sensors measure displacements using a plum bob (Figure C.1.1 in Appendix C). The displacement measured either pushes the plum bob inward (indicating displacement in this research) or is allowing the plum bob to extend (indicating displacement). The reference point for measured data was zeroed for each displacement sensor by slightly pushing the plum bob inward to allow for negative measurements. When the displacement is plotted as a function of time, when the slope is zero, equilibrium within an element has been established.

All three displacement sensors described in Sections 3.4 worked well and reliable dynamic displacement data was recorded during column removal. Similar to the strain gauge data, there were five distinct physical events and the corresponding measured displacements help understand the behavior of the building during those events. Initially, all displacement sensors had stable readings, ideally at zero displacement. When the processor made contact with the test column, displacement values started to increase. The five times the processor made contact with the column are described in Table 4.1. The displacement measurements can be seen in Figure 4.9. Displacement measurements were converted from millimeters to inches from the original experimental data which is plotted in Figure C.1.2 in Appendix C. An individual plot of the horizontal displacement sensor

can be seen in Figure C.1.3. From the plots, dynamic measurements of displacement that appear after 300 seconds were a result of the processor making contact with the test column, but for the sake of the experiment, data measurements were meant to be terminated once the column was removed. Table 4.4 expands on Table 3.3 and shows the displacement values of each sensor at a time of 300 seconds.

Table 4.4: Displacement values at 300 seconds from LVDTs

LVDT #	**Steel Member**	**Orientation**	**Distance from Column**	**Displacement (in.)**
1	(N) Beam	Vertical	1 ft-6 in.	0.474
2	(S) Beam	Vertical	2 ft-4.75 in.	0.659
3	(N) Beam	Horizontal	At face of removed column	-5.91×10^{-3}

Negative displacement values indicate that the plum bob is moving outward, away from the displacement sensor, while positive values indicate that the plum bob is moving inward, toward the displacement sensor, i.e., the beam is deflecting downward.

4.5 Analysis of Measured Displacement Data

The general trend of the measured vertical displacements was similar to strain gauge measurements. With each processor contact time the overall measured displacement on the beams connected to the test column became more positive. This is a result of the test column providing less support for the building – and connecting beams

deflecting downward – as the column was being cut each time the processor closed its claw on the column. During the last processor contact time with the column (from 247.77 seconds to 251.74 seconds), the test column was completely cut through and the measured displacement drastically varied momentarily. Analyzing Table 4.4, at a time of 300 seconds, after the column was cut through, the measured vertical displacements leveled out to positive values and downward deflections. Without the support provided by the test column 27, the two beams moved downward and elongated.

The horizontal displacement sensor was used to measure any potential slippage at the bottom of the beam-column connection. The behavior of the horizontal displacement sensor was quite dynamic – the displacement values measure to be positive and negative in Figure C.1.3 in Appendix C. This dynamic response indicates that the column shifted in the North-South direction. As the displacement measurement is relatively small (Table 4.4) no substantial slippage resulted from deflection of beams and removal of the column.

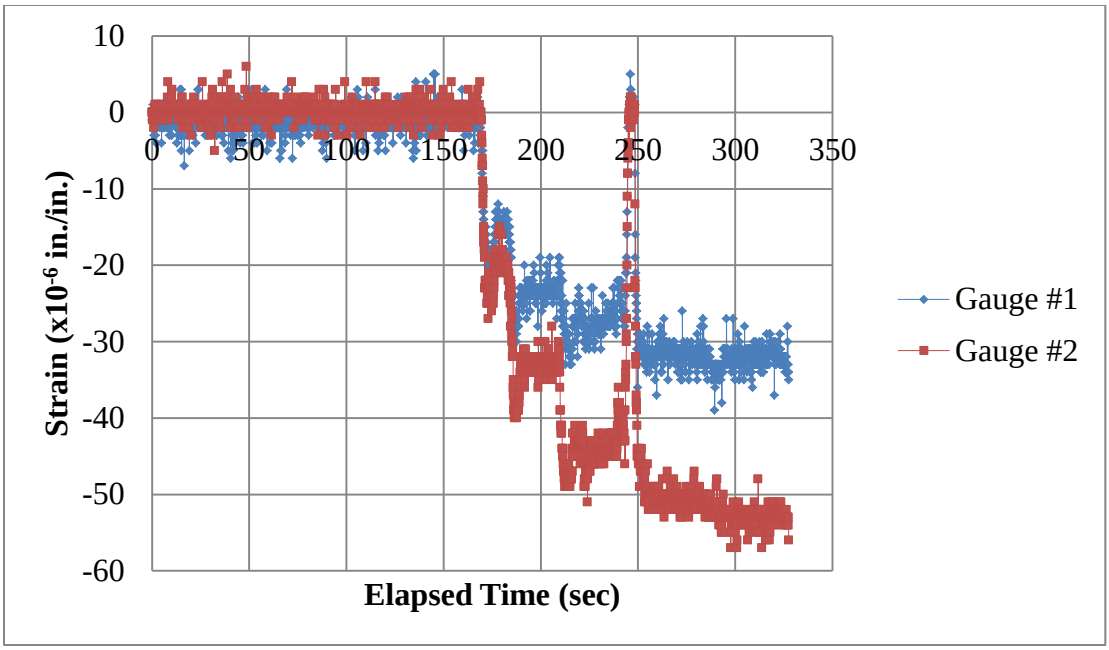

Figure 4.1: Strain versus time plot from gauges #1 and #2 on North column 26

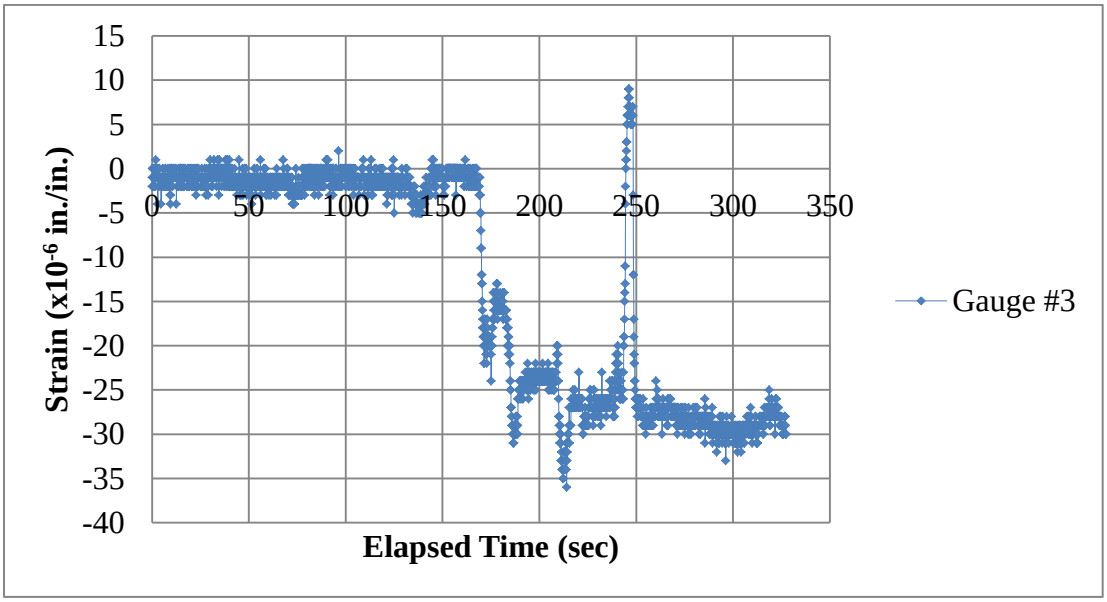

Figure 4.2: Strain versus time plot from gauge #3 on East column 28

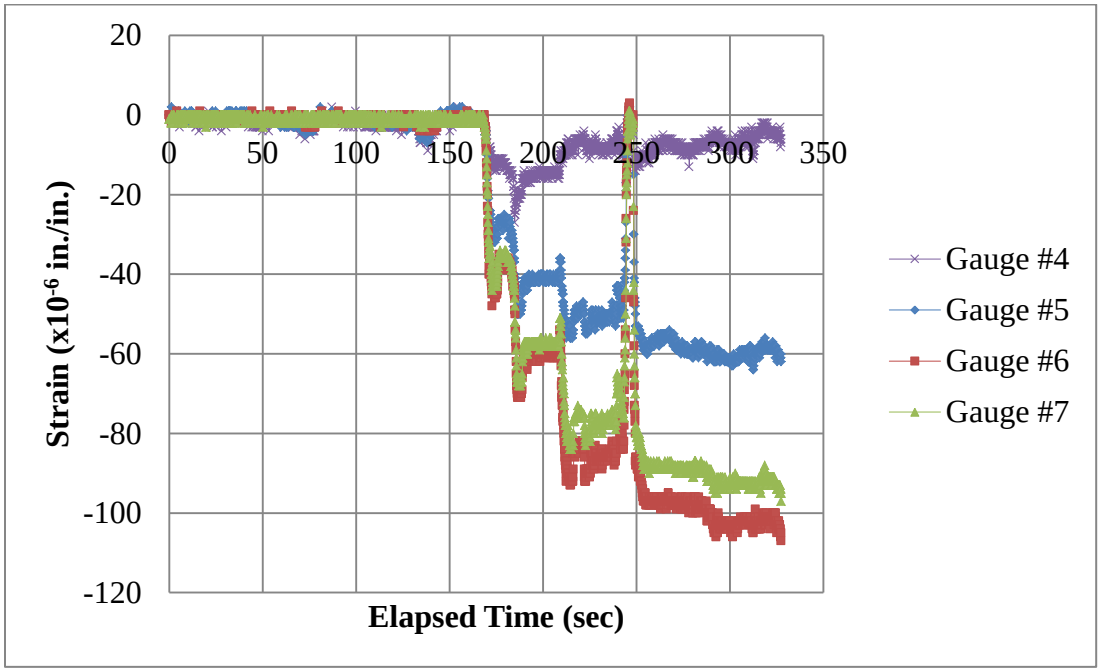

Figure 4.3: Strain versus time plot from gauges #4 through #7 on South column 38

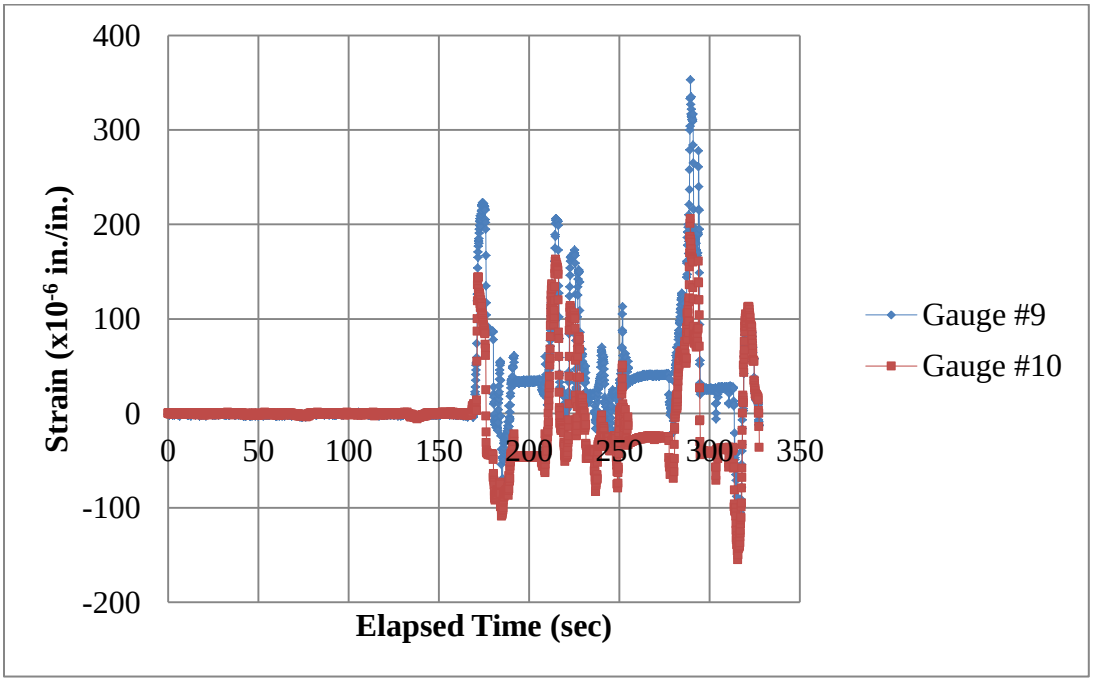

Figure 4.4: Strain versus time plot from gauges #9 and #10 on Eastern beam

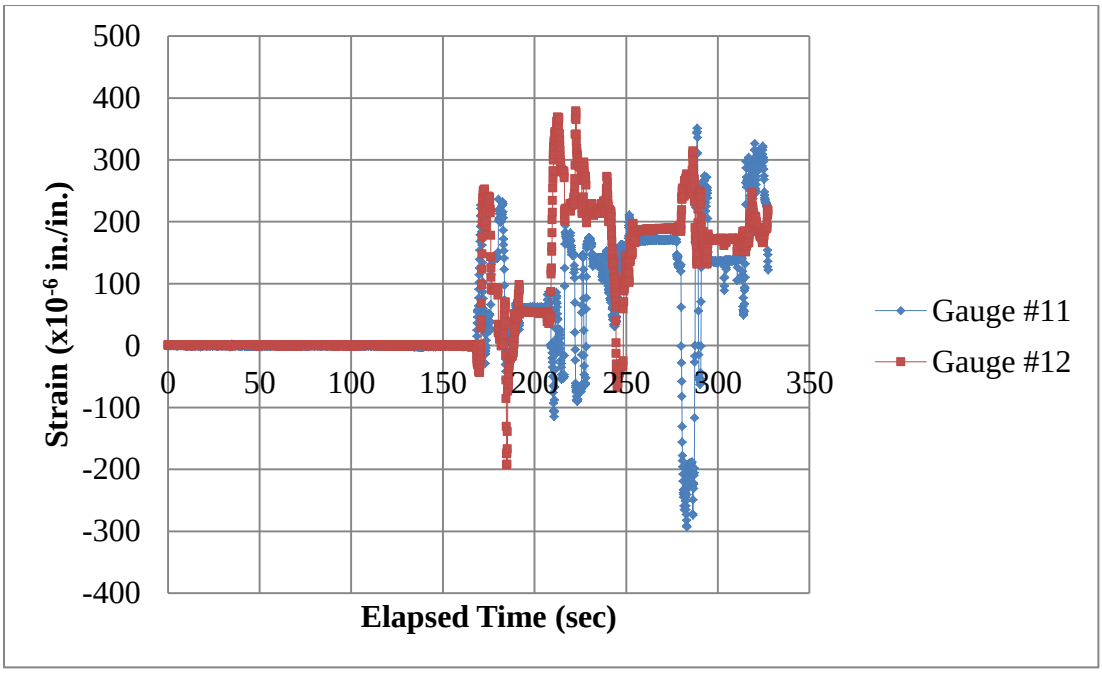

Figure 4.5: Strain versus time plot from gauges #11 and #12 on Northern beam

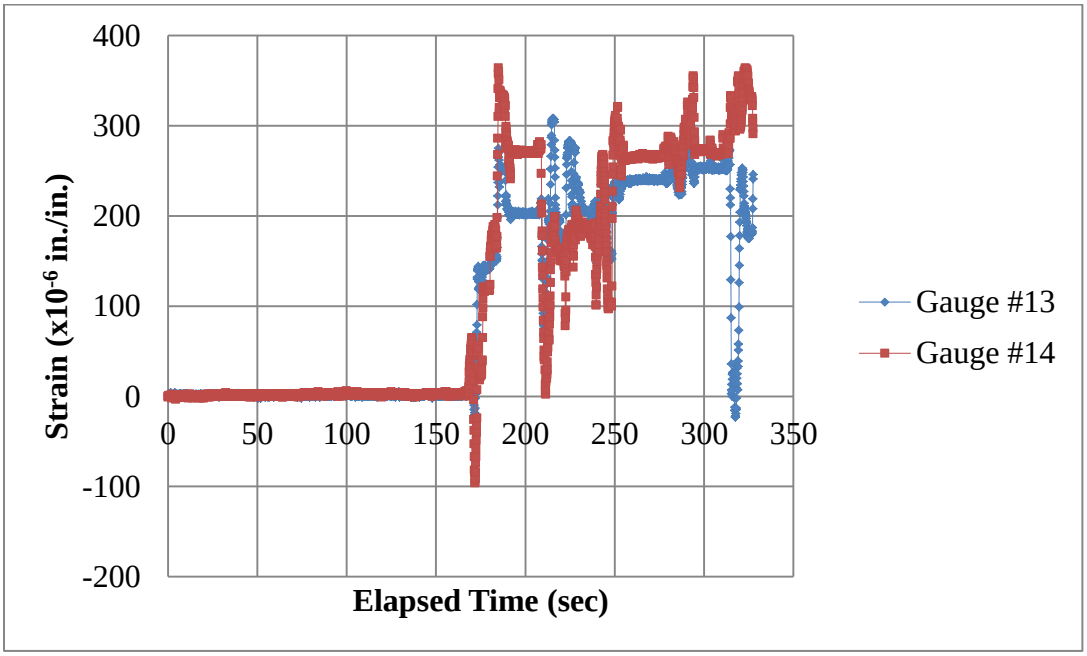

Figure 4.6: Strain versus time plot from gauges #13 and #14 on Southern beam

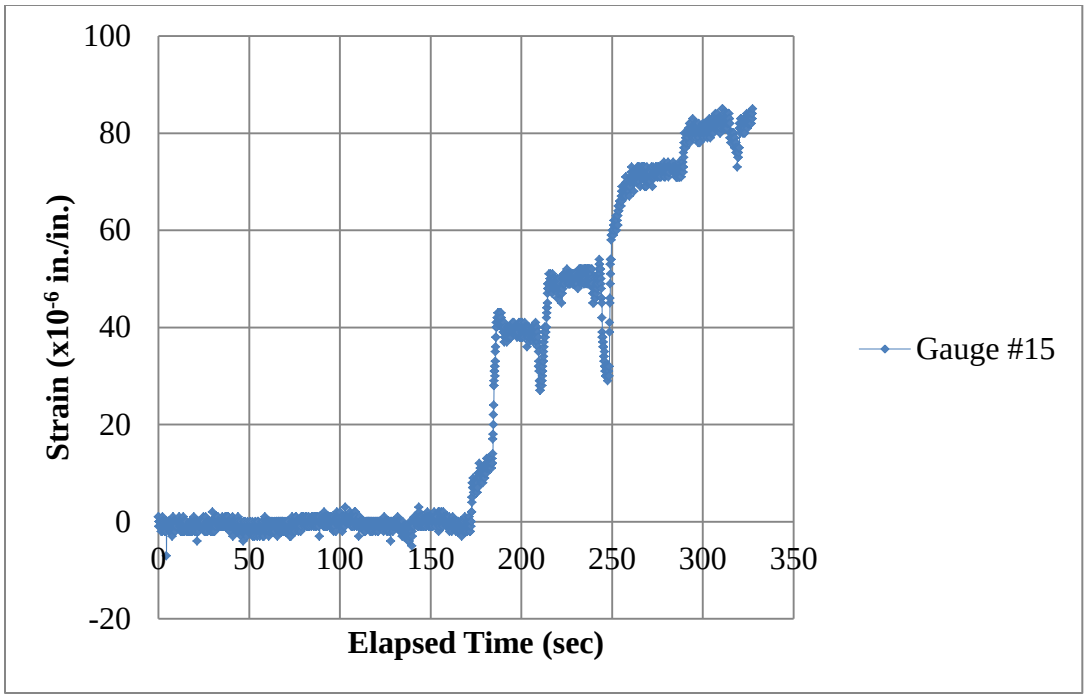

Figure 4.7: Strain versus time plot from gauge #15 on Southern beam

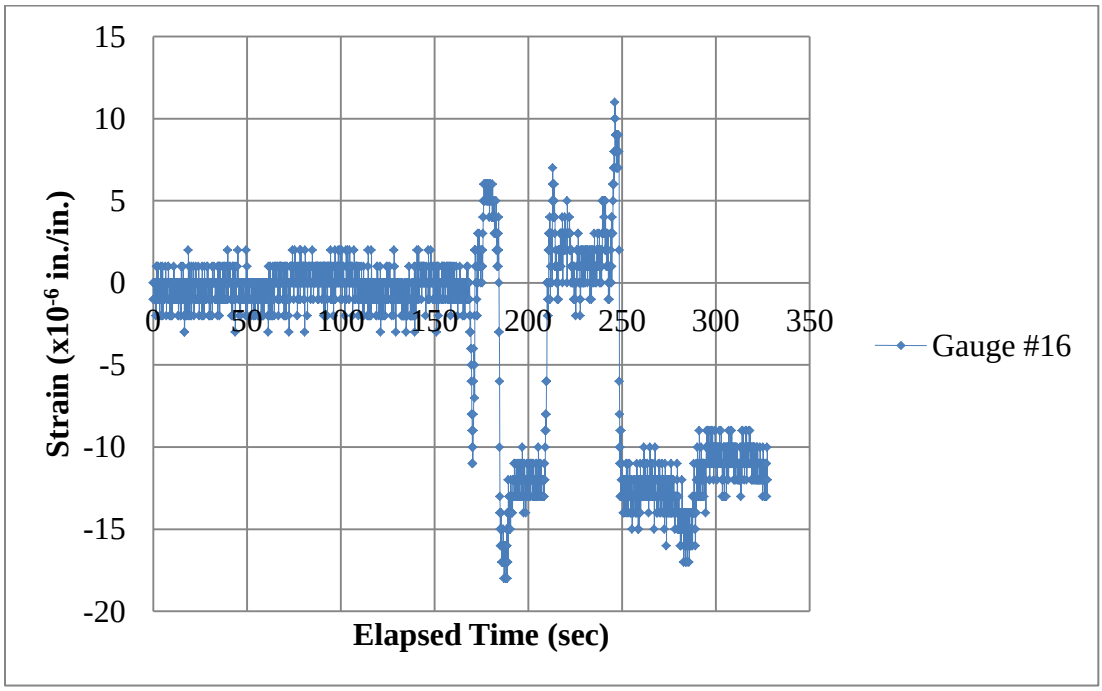

Figure 4.8: Strain versus time plot from gauge #16 on Northern beam

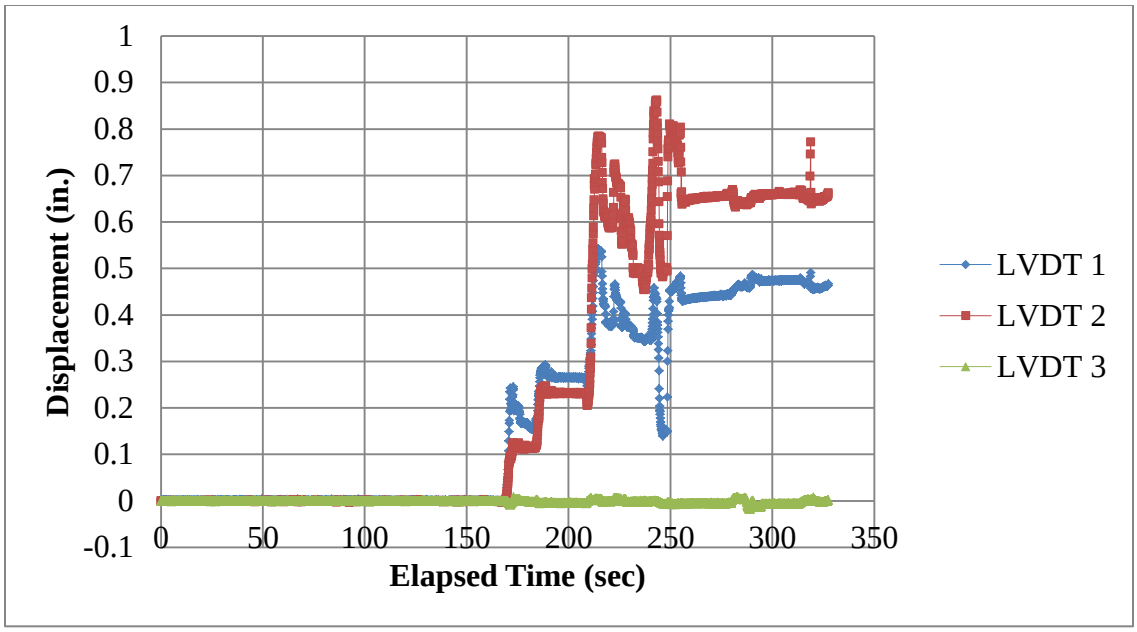

Figure 4.9: Displacement versus time plot of vertical (1 and 2) and horizontal (3) Linear Variable Differential Transformers (LVDTs)

CHAPTER 5: PERIMETER FRAME DETAILS

5.1 Introduction

This chapter discusses how the details of the Western frame of the Haskett Hall were determined. This chapter details the Western frame elevation, bay width layout, connections, beam and column property estimates, and load values. Beam and column properties as well as load calculations were determined with the aid of undergraduate student, J. Wade. Lastly, the information within this chapter is used to model the perimeter frame in SAP2000 which is discussed in Chapter 6.

5.2 Frame Layout

The perimeter frame on the West side of the Haskett Hall is detailed in Figure A.17. This figure indicates that the Western frame includes columns 6, 7, 14, 15, 26, 27, and 38, numbered from North to South. Columns ran continuously through each floor. Columns 7 and 15 were oriented with their minor axes being parallel with the frame. All other columns were oriented with their major axes being parallel with the frame. The elevations of each floor are also detailed in Figure A.17, matching the overall elevations for the building (Figure 2.4). The beam layout within Haskett Hall was detailed and discussed in Sections 2.4 and 2.6. The majority of floor beams ran in the East-West direction. Figure A.17 shows that beams ran in the North-South direction in the second

floor except between columns 14 and 15. The North part of the frame, between columns 6 and 14, is the three-story testing laboratory. The beams on the second floor along the testing laboratory had a greater elevation than other beams on the floor (Figure 2.4). The third and fourth floors each had one beam located between columns 14 and 15, while the roof had beams along the entire frame. The structural details of the roof of the building were discussed in Section 2.3.

5.3 Beam Dimensions and Properties

Minimal section properties or other details of the beams within the building were provided in the original building plans provided in Appendix A. The beam details were determined in collaboration with the undergraduate student, J. Wade. In order to determine the geometry of the beams within the perimeter frame, original building plans were used as well as the pictures taken during the experiment. The pictures showed most details of the beams in the first floor level because those beams were exposed before the test.

Figure A.17 shows that the perimeter frame included three different types of beams: 15" I @42$^{\#}$, 18" I @55$^{\#}$ and 24" BI @73.5$^{\#}$. Therefore, the beams had overall depths of 15-inches, 18-inches and 24-inches and were rated at 42-pounds per foot (lb/ft), 55 lb/ft and 73.5 lb/ft, respectively. Since this information did not detail what type of I-beam to use – Wide (W), Standard (S), or light (B) – pictures of the beams that were used for pictorial analysis. All photos are included in Appendix B. Pictorial analysis was relatively accurate by knowing that the actual diameter of the rivets that were used in connections was 1.5 inches. The width, depth or other dimensions of a beam can be

estimated in relation to the size of a rivet on the same photograph. Based on the actual dimension of a rivet, the pictorial analysis is set up in Equation 5.1:

$$\text{Distance}_{\text{actual}} = \frac{\text{Rivet}_{\text{actual}}}{\text{Rivet}_{\text{measured}}} \times \text{Distance}_{\text{measured}} \tag{5.1}$$

In Equation 5.1, $\text{Distance}_{\text{actual}}$ is the actual dimension of a beam, $\text{Distance}_{\text{measured}}$ is the scaled size of a beam's dimension from a photograph, $\text{Rivet}_{\text{measured}}$ is the scaled size of a rivet from a photograph, and $\text{Rivet}_{\text{actual}}$ is the actual diameter of a rivet (1.5 inches). By analyzing Figure B.2.1 in Appendix B, which shows the connection of the Southern beam – labeled 15" I @42# on the frame – to the test column 27, the actual base flange depth, b_f, of the I-beam is measured to be approximately 6.70 inches. Once the actual flange depth was approximated, a copy of the *AISC Shapes Database Version 14.0 Historic* Excel spreadsheet was used to find a matching standard section. This AISC excel spreadsheet details steel elements from AISC steel manuals for the past 100 years – including editions from Historic to 13th Edition. The earliest labeled AISC edition in the spreadsheet is ASD5 which was published in 1962 [2]. Since Haskett Hall was erected in 1925, the "Historic" edition was used to find the correct standard sections used in the test frame. Given the estimated data of the 15" I @42# beam, there existed multiple historical sections in the spreadsheet that could have been used in the frame. The options are summarized in Table 5.1.

Table 5.1: 15-inch deep cross sections from AISC v14.0 historic spreadsheet

Historic Member	***A* (in.^{2})**	***d* (in.)**	**t_w (in.)**	**b_f (in.)**	**t_f (in.)**	**Wt. (lb)**
S 15x42	12.48	15.00	0.410	5.500	0.622	42.0
S 15x42	12.40	15.00	0.400	5.500	0.590	42.0
S 15x42	12.35	15.00	0.410	5.500	0.620	42.0
B 15x42	12.41	**15.00**	0.360	**6.740**	0.550	**42.0**

From the Excel spreadsheet, the properties of steel section B15x42 most closely matched calculated dimensions, shown in bold in Table 5.1. Since the other two beams within the Western frame of Haskett Hall – 18" I @55$^{\#}$ and 24" BI @73.5$^{\#}$ – existed on upper floors, and therefore away from the testing location, details of these beams were not documented through photographs. They were mostly covered by masonry or concrete. Therefore, it was assumed that these beams were also B-sections to match Historic elements and for uniformity when modeling the frame in SAP2000. By cross referencing depth and rated weight values of Haskett beams to the Historic spreadsheet, the following beams are selected in Table 5.2.

Table 5.2: Historic beams assigned to the Western frame

Historic Member	***A* (in.^{2})**	***d* (in.)**	**t_w (in.)**	**b_f (in.)**	**t_f (in.)**	**I_x (in.^{4})**
B15x42	12.41	15.00	0.360	6.740	0.550	464.9
B18x55	16.19	18.12	0.390	7.532	0.630	889.9
B24x73.5	21.56	24.00	0.390	9.000	0.701	2095.7

The B24x73.5 values within Table 5.2 were averaged amongst the three possible sections available within the AISC spreadsheet.

5.4 Column Section Properties

No section property details of the columns within the building could be located. Determining the column details was in collaboration with the undergraduate student, J. Wade. To estimate the geometric properties of columns within the perimeter frame, the building plans were initially used to make note that the columns within the building were built-up I-sections. Each column had an I-section bracketed by two channel sections on the I-section flanges to provide a greater moment of inertia and a relatively square shape for the overall column (Section 2.6). Photographs taken before and after the experiment were the primary source to estimate column dimensions while the undergraduate student J. Wade used an AutoDesk AutoCAD analysis to check measurements.

Primarily, experimental pictures were used to conduct pictorial analyses – the same procedure described in Section 5.3 to determine the beam properties within the frame. By using Equation 5.1, column properties were estimated through pictorial analysis of columns 26, 27, and 38 on the Western frame. Pictures of each respective column that were used for column dimension estimates can be found in Appendix B. The properties that were estimated include: overall depth of the composite section, d_o (which is a summation of the I-section depth and the two channel web thicknesses), inner I-section base flange width, b_f, channel depth, d, channel flange length, w, and channel flange thickness, t_f. Dimensions were measured by hand on the photographs with an engineering ruler with increments of $1/60^{th}$ of an inch and also through AutoCAD. By

comparing and averaging measurements, the results of the pictorial analyses of Western frame columns are shown in Table 5.3.

Table 5.3: Column dimension estimates using pictorial analysis

Column	**d_o (in.)**	**Channel d (in.)**	**I-Section b_f (in.)**	**Channel w (in.)**	**Channel t_f (in.)**
26	21.0	15.85	5.0	4.13	0.50
27	21.0	15.85	6.0	4.13	0.50
38	16.0	13.56	Not Available	3.00	0.50

Based off of these measurements, sections were chosen from the *AISC Shapes Database v14.0 Historic* Excel spreadsheet. Within the Historic version of the AISC database, the primary I-section is a Standard S-Beam. Because the overall depths of the columns d_o, include the thicknesses of the channels, it was assumed that the channels had a uniform thickness between the flange and web. Therefore, in order to match measured dimensions to the sections within the spreadsheet, to be consistent with measurements it was assumed that the channels had a thickness of 0.50 inches to assign the I-sections to be S20 for columns 26 and 27, and S15 for column 38.

The general section sizes were checked with undergraduate student J. Wade's independent AutoCAD results. The AutoCAD analysis was used to size the remaining columns on the Western frame. By analyzing the structural floor plans, provided in Figures A.13 through A.15 in Appendix A, it was estimated that there are three different

column sizes on the Western frame. Columns 7 and 15 were measured to be the smallest with an estimated depth of 12.0 inches. Columns 6, 14 and 38 were measured to have an average estimated depth of 15.0 inches, and columns 26 and 27 were measured to be the largest columns with an estimated depth of 20.0 inches.

5.4.1 Selection of Column I-Sections

The next step to determine column geometric details was to select the weight of the S-sections for each of the three columns. To select which specific I-sections to assign to the columns, the estimated depths, flange widths, and web and flange thicknesses were matched with the AISC Historic spreadsheet values. For each column section there were countless weight options. To narrow the section option choices, footnotes within the spreadsheet were used. For each steel section a footnote indicates the year that the section was manufactured and by what company. It was assumed that the column sections for Haskett Hall were manufactured in 1923, one year before construction of the building began – in 1924. The resulting I-sections for the Western frame – chosen from best fit estimates for the dimensions and manufacturing year – are shown in Table 5.4.

Table 5.4: Column assignments using AISC historic spreadsheet

Column	**Section**	***d* (in.)**	**t_w (in.)**	**b_f (in.)**	**t_f (in.)**	**A (in.^{2})**	**I_x (in.^{4})**
7, 15	S12x45	12.00	0.583	5.373	0.660	13.24	285.7
6, 14, 38	S15x81.3	15.00	0.800	6.400	1.034	23.91	795.5
26, 27	S20x90	20.00	0.747	6.897	0.950	26.47	1569.0

5.4.2 Selection of Column Channel Sections

The last detail to complete the built-up column section properties was to determine the properties of the bracketing channels. These channels were attached to the column I-section flanges using bolts distributed over the height of the column (Figure B.1.4 from Appendix B) Within the Historic version of the AISC spreadsheet there are no channel sections. The oldest channel sections are detailed in ASD7, which was published in 1969 – 44 years after Haskett Hall's erection was completed. Because the earliest channel sections within the spreadsheet were manufactured after the building was constructed, the AISC Excel spreadsheet was not used to determine channel section properties. Instead, channels were assigned geometric properties based on the measured values. There were many column photographs – located in Appendix B – to allow for determination of channel section properties. Channel section properties shown in Table 5.5 are used in the building model.

Table 5.5: Channel designs based off of measured values

Column	**Channel *d* (in.)**	**Channel t_w (in.)**	**Channel *w* (in.)**	**Channel t_f (in.)**
7, 15	13.00	0.500	3.00	0.500
6, 14, 38	13.50	0.500	3.00	0.500
26, 27	15.50	0.500	4.00	0.500

5.5 Loads Applied on the Frame

The loads on the Western perimeter frame were grouped into two categories: roof and wall loads and floor loads. The roof and wall loads were calculated by undergraduate student J. Wade who analyzed the roof and façade details – shown in Sections 2.3 and 2.5, respectively. The floor loads were calculated by analyzing the floor layout detailed in Section 2.4.

5.5.1 Roof and Wall Loads

Summarizing calculations conducted by undergraduate student J. Wade, the roof loads were calculated by referencing Figure A.16 which shows the roof framing plan. The purlins that run in the East-West direction on the roof act similar to joists, resulting in roof slabs being treated as one-way slabs. The material densities within the composite roof deck – wood with a density of 3.5 pounds per cubic foot (pcf) and steel with a density of 490 pcf – were determined and converted to a uniformly distributed surface load. In result, a value of 27.7 pounds per square foot (psf) for the distributed roof dead load was used in this research.

Wall loads were calculated by first determining the overall cross-sectional area of the façade and then by subtracting window areas. Windows are detailed in Figures A.2 and A.5 while the façade is detailed in Figure A.9 in Appendix A. Windows had a height of 8.0 feet and width of 5.23 feet (5 ft-2.75 in.), thickness of 0.1875 feet ($3/16^{th}$ inches) and a glass density of 160 pcf. Within the façade, sections were filled with concrete for fire protection. It was assumed that the façade had a constant thickness of 1.083 feet (13 inches) and that the density of limestone was comparable to brick (101 pcf). A distributed wall dead load of 64 psf is used in this thesis. Before the experiment, the demolition

company removed a part of the perimeter façade, exposing the Northern side of the Western perimeter frame and the second floor beams along the frame (Figure 5.1). From Figure 5.1, by removing the wall and exposing the perimeter this resulted in those areas of the frame having no wall loads. Roof load hand calculations can be seen in Figures C.2.1 through C.2.4 in Appendix C.

5.5.2 Floor Loads

Within the floor layout there existed beams running in the East-West direction, concrete slabs, occasional trapezoidal joists that ran below slabs and superimposed dead loads. The beams that ran between the columns in the East-West direction were considered point loads on the perimeter frame columns. Point loads from beams were calculated using Equation 5.2.

$$P_{beam} = \frac{1}{2}\left(Weight_{beam} \times Length_{beam}\right) \tag{5.2}$$

In Equation 5.2 the weight of a beam was measured in pounds per linear foot (plf) while the length for each beam running in the East-West direction was 22 feet- 9.5 inches (22.79 ft).

The majority of the slabs on the perimeter frame were located on the second floor. On the third and fourth floors, the slabs became point loads due to there being few beams along the perimeter frame to support the distributed loads (Figure 2.4). The reinforced concrete slabs had a density of 150 pcf with thickness ranging from 0.42 to 0.58 feet (5.0 to 7.0 inches). The slabs were reinforced with #4 rebar spaced at an average spacing of 10.0 inches (Figure A.18 in Appendix A). The product of the reinforced concrete density and slab thickness resulted in a value of 87.5 psf for the slab uniformly distributed dead load. The reinforced concrete slabs that ran in the North-South direction parallel to the

Western frame had one-way or two-way slab distributions. A one-way slab can be defined as the length to width ratio exceeding 2.0 and resulting in a uniformly distributed load along the short direction. When this ratio is less than 2.0, the slab is considered a two-way slab, resulting in a trapezoidal distributed load applied to beams on the perimeter frame. The peak distributed loads from one- and two-way slabs were calculated using Equation 5.3.

$$w_{1,2-way_{peak}} = \frac{1}{2} Width_{slab} \times \gamma \times t_{slab} \tag{5.3}$$

In Equation 5.3, γ is the reinforced concrete density and *t* is the thickness of the slab.

Within a two-way trapezoidal distributed load, there exist two equal horizontal lengths where the load increases from zero to the peak distributed load. The horizontal length is equal to one-half the slab width. When a reinforced concrete one-way slab ran in the East-West direction – the slab width being located along the perimeter frame – the slab became two point loads on the frame. Along the second floor of the frame, the conjoined slabs 2A-2B just North of column 38, conjoined slabs 2R-2S just South of column 15, and slab 2AJ just North of column 14 were each considered two point loads on the perimeter frame (Figure A.13 in Appendix A). The point loads from slabs were calculated using Equation 5.4.

$$P_{slab} = \left(\frac{1}{2} Width_{slab} \times \frac{1}{2} Length_{slab} \right) \times \gamma \times t_{slab} \tag{5.4}$$

In Equation 5.4, the slab area (product of width and length) was restricted to what would affect the perimeter frame. In other words, the distance measured on the East-West direction did not exceed 22 ft- 9.5 in. Reinforced concrete joists ran below slabs mainly on the third and fourth floors. The joists were reinforced with #9 rebar and had a range of

0.5 to 1.0 feet (6.0 to 12.0 inches) in depth while the slabs had a depth of 0.208 feet (2.5 inches). By running under the floor slabs, the joists turned the slab to a series of one-way slabs with a uniformly distributed load. Because the third and fourth floors did not have many beams along the perimeter frame, these distributed loads became point loads by using Equation 5.4. The joists also contributed to the point loads on the frame by being calculated using Equation 5.5.

$$P_{joist} = \frac{N}{2} \times Area_{joist} \times Length_{slab} \times \gamma \tag{5.5}$$

In Equation 5.5, N is the number of joists that ran along the slab area.

Superimposed dead loads were applied along each floor level. These dead loads were assumed to hold a value of 15 psf to account for the lighting, pipes, vents, and miscellaneous utilities hung from the ceiling of each respective floor. Due to the testing laboratory, no superimposed dead load was applied on the third and fourth floors from columns 6 to 14. Depending on whether the respective floor had beams running along the perimeter frame determined whether the superimposed dead loads were considered point loads or distributed loads. All load calculation information and values calculated using Equations 5.2 to 5.5 are detailed in Tables C.2.1 through C.2.8 in Appendix C.

Figure 5.1: Partially removed Western façade to expose the frame

CHAPTER 6: SAP2000 MODELING

6.1 Introduction

Chapter 6 discusses modeling of the two-dimensional Western perimeter frame of Haskett Hall in SAP2000. This chapter describes how the beams, columns and connections were modeled in SAP2000. Furthermore, details of the loading conditions and member cross-sections are included.

6.2 SAP2000 Frame Model

SAP2000 (2012) is a structural analysis computer program used in this research to analyze progressive collapse potential by following GSA guidelines [10]. The Western frame layout was modeled in SAP2000 following the details discussed in Section 5.2. Because the North and South elevations varied along the frame, these elevations were averaged to become the constant height of 49.47 feet for the roof within SAP2000. The foundations were described in Section 2.7 and are modeled to be rigid supports at the bottom of columns in the first story. Point and distributed load values were calculated using Equations 5.2 through 5.5 and are summarized in Tables C.2.5 through C.2.7 in Appendix C. These loads were entered on the SAP2000 frame model. The Western frame layout within SAP2000 can be seen in Figures 6.1 and 6.2, without and with loads, respectively.

Once the two-dimensional model was complete it was analyzed to evaluate the effects of the dead loads on the frame. As the building was unoccupied when the test column was removed there existed no live loads. The load case scale factor for the dead loads was entered as 1.0 for the purpose of accurately representing the building's response to its natural weight.

6.3 Frame Element Properties in SAP2000

The assigned sections and property values of beams and columns for the Western frame were detailed in Sections 5.3 and 5.4, the I-sections being chosen from the *AISC Shapes Database v14.0 Historic* Excel spreadsheet. Using the *Historic* Edition resulted in the sections being too outdated to import into SAP2000. Instead, the I-sections were re-defined in SAP2000 by either creating a new simple section or using the "Section Designer" function for built-up sections. All of the standard beam types were designed by creating a simple section. The partially reinforced beams – located along the second floor spanning from columns 15 to 38 (discussed in Section 2.6) – along with the built-up columns were designed using the "Section Designer."

When defining I-sections in SAP2000, defined property values – such as the cross-sectional area (A) and moment of inertia (I) – were matched with values within the AISC spreadsheet, as presented in Sections 5.3 and 5.4. Properties were matched within 0.1% (by slightly altering the web and flange thickness values). It was important to match cross-sectional area and moment of inertia values to allow for strain, moment, and demand-capacity ratio calculations from SAP2000 to accurately represent the response of the building based on the section properties established (Tables 5.2 and 5.4).

6.3.1 Beam Properties in SAP2000

The simple beam I-section dimensions and properties can be seen in Figures 6.3 through 6.5. These figures compare the AISC spreadsheet values with the SAP2000 values. Along the second floor, the three beams between columns 15 and 38 were composite beams – the beams were partially encased in unreinforced concrete while supporting a reinforced concrete slab (Figure 2.6b). The steel I-sections for the composite beams were assigned to be B15x42 members from the AISC spreadsheet (discussed in Section 5.3). The concrete that partially encased the B15x42 members had a specified strength of 4000 psi. Original building plans and pictures of beams were used to verify the area of the unreinforced concrete fillings in the I-section web. As seen in Figure 6.6, the concrete encompassed the top base flange of the beam as well as on the side of the web that was oriented towards the interior of the building. The unreinforced concrete that existed in the web was assumed to have cracked due to bending. Therefore, the composite beam was modeled in SAP2000 so that the unreinforced concrete was no longer filled in the web (Figure 6.7). The composite beam cross-section shown in Figure 6.8 varied with respect to the effective flange width of the slab. For composite beams, the effective width of the reinforced concrete slabs can be determined from ACI 318 (2008) by using Equation set 6.1 [1].

$$b_{effective} \leq \begin{cases} 1/4 \text{ span length} \\ b_w + 16h_f \\ \text{beam spacing} \end{cases} \tag{6.1}$$

In Equation set 6.1, for the purpose of this research the span length is the length of the composite beam, b_w is the base flange of the I-section, h_f is the thickness of the reinforced concrete slab, and the beam spacing is the distance between the perimeter frame and the

next beam parallel to the composite beams that would be supporting the slab. For each composite beam, b_w was 6.740 inches, h_f was 7.0 inches, and beam spacing was 9 feet- 7 inches (115 inches). The controlling parameter for the composite beams was the span length. The effective widths for each of the three composite beams are shown in Table 6.1.

Table 6.1: Effective concrete lengths and moments of inertia for composite beams

Beam between Columns (#, #)	**Span Length (in.)**	b_{eff} **(in.)**	I **(in.^{4})**
15, 26	242.5	60.63	1896
26, 27 (North Beam)	324.0	81.00	2030
27, 38 (South Beam)	301.0	75.25	1995

In SAP2000, the moments of inertia of the composite sections were calculated by the program in the "Section Designer." The moment of inertia was used to transform each beam section into an equivalent steel section.

SAP2000 is unable to perform calculations using composite members. Therefore, by transforming a composite member to be completely steel, SAP2000 calculations would become more accurate. To transform the composite beam to a steel member, Equation 6.2 was used.

$$n = \frac{E_C}{E_S} \tag{6.2}$$

In Equation 6.2, n is the scale factor ratio between moduli of elasticity. E_S is the modulus of elasticity for A36 steel (E_S = 29,000 ksi), while E_C is the modulus of elasticity for 4000 psi concrete (E_C = 3645 ksi). This resulted in a ratio, n, of approximately 0.126. The effective widths of the steel overlay using n and the moments of inertia (I) are shown in Table 6.2.

Table 6.2: Effective steel lengths for composite beams

Beam between Columns (#, #)	**Span Length (in.)**	**Concrete b_{eff} (in.)**	**Steel b_{eff} using n (in.)**	**Steel b_{eff} using I (in.)**
15, 26	242.5	60.63	7.62	**5.50**
26, 27 (North Beam)	324.0	81.00	10.18	**7.30**
27, 38 (South Beam)	301.0	75.25	9.46	**8.00**

As it was more important to match the original moments of inertia, the steel effective widths were defined by using I, bolded in Table 6.2. The composite beam cross-section with a transformed steel slab can be seen in Figure 6.9.

6.3.2 Column Properties in SAP2000

To design the built-up column sections, it was required to use the SAP2000 "Section Designer" function. This function primarily enabled I-sections to be designed and checked based on property values assigned from the AISC spreadsheet. Secondly, the function allowed for channel sections to be designed based on the values established in Section 5.4 (Table 5.5) and then be added as brackets to the respective I-sections. Lastly,

the “Section Designer” automatically calculated the new cross-sectional areas and moments of inertia for each built-up column. Column I-section dimensions and properties can be seen in Figures 6.10 through 6.15. Figure 6.16 shows the typical built-up column section.

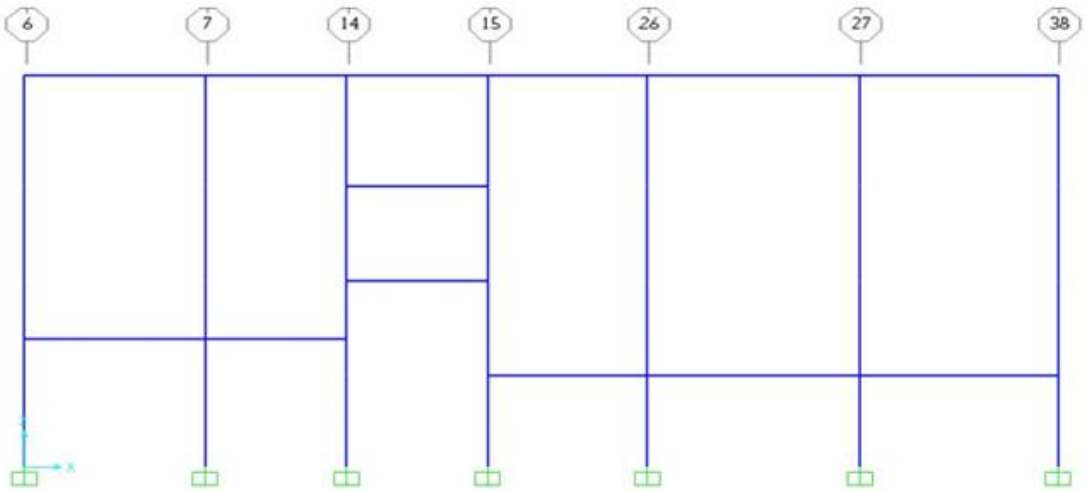

Figure 6.1: SAP2000 Western frame layout (from North to South)

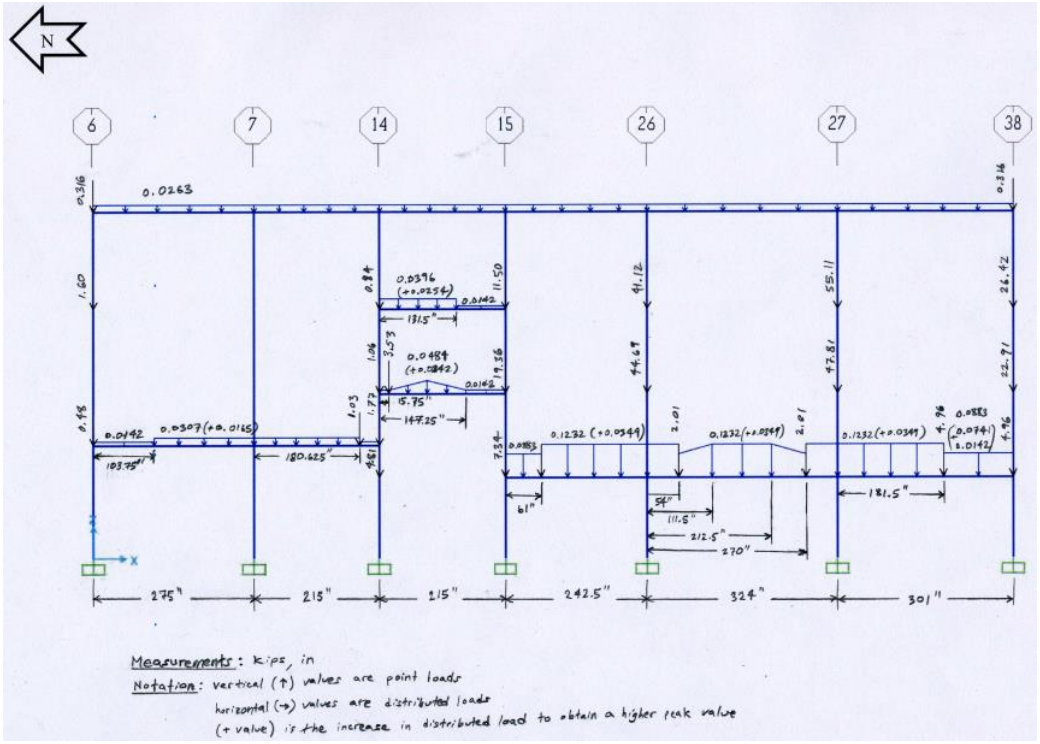

Figure 6.2: SAP2000 Western frame layout with load values and distances

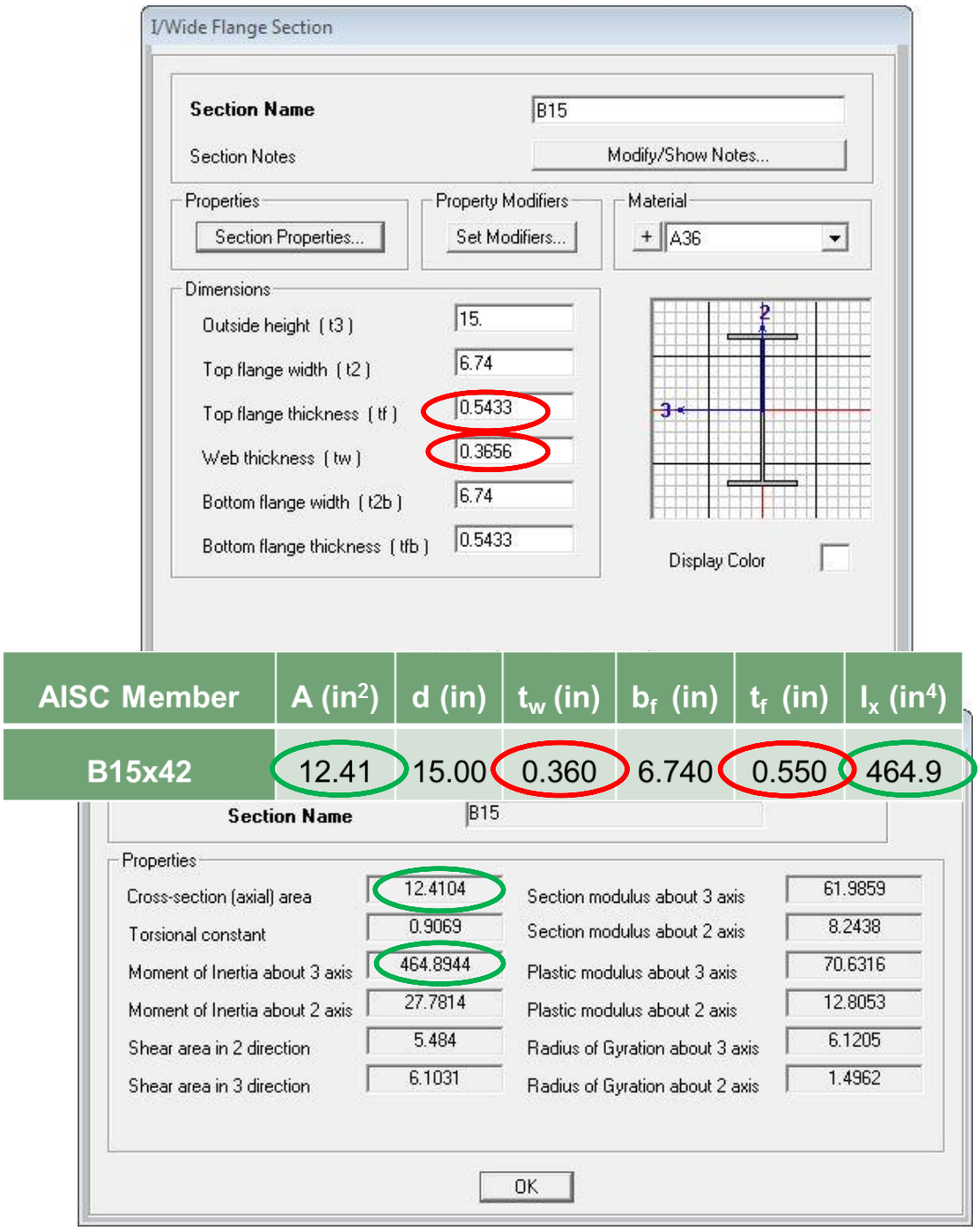

Figure 6.3: B15x42 SAP2000 property values compared to AISC specifications

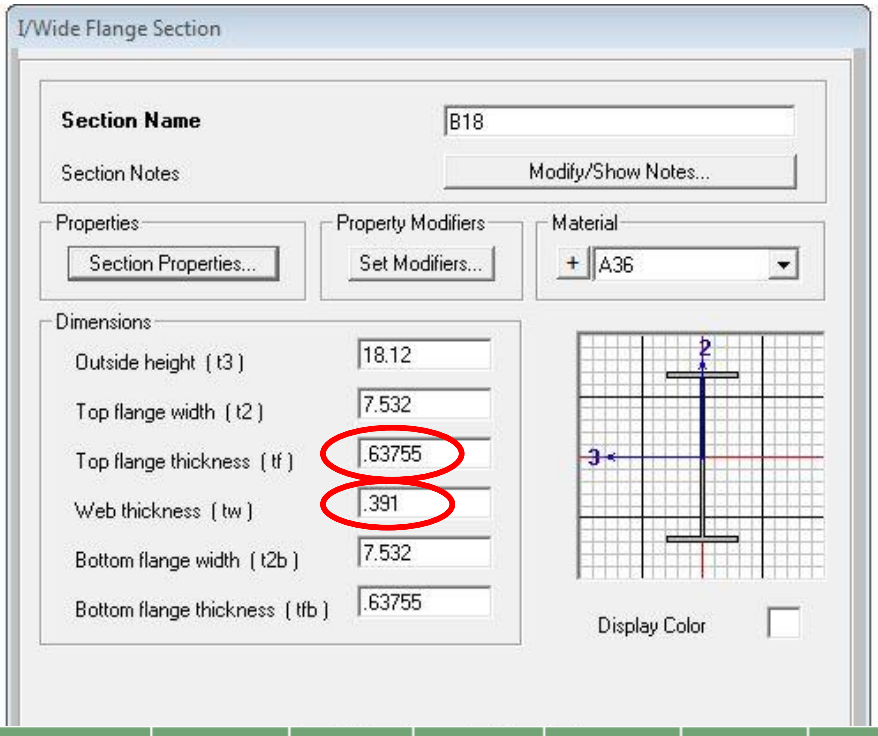

AISC Member	A (in^2)	d (in)	t_w (in)	b_f (in)	t_f (in)	I_x (in^4)
B18x55	16.19	18.12	0.390	7.532	0.630	889.9

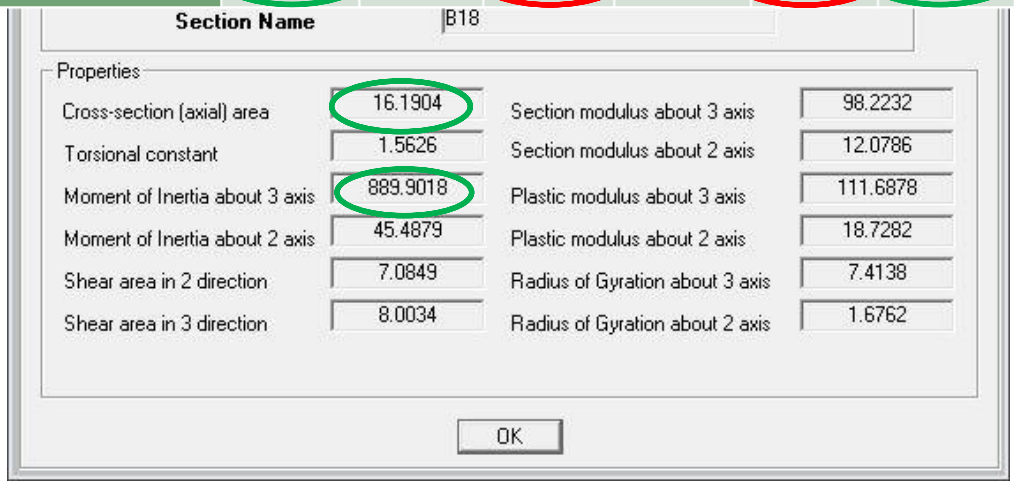

Figure 6.4: B18x55 SAP2000 property values compared to AISC specifications

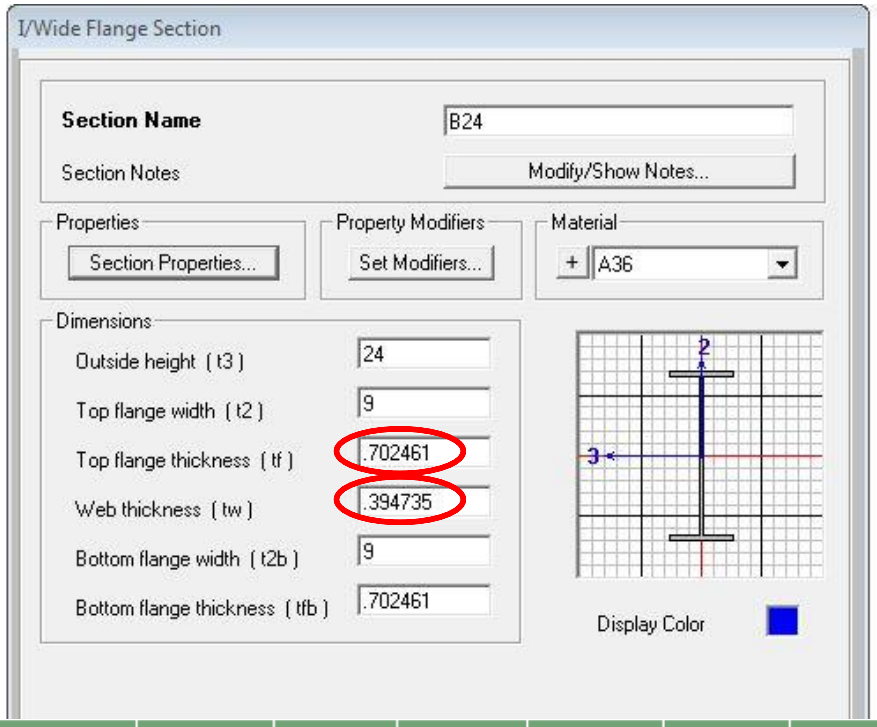

AISC Member	A (in^2)	d (in)	t_w (in)	b_f (in)	t_f (in)	I_x (in^4)
B24x73.5	21.56	24.00	0.390	9.000	0.701	2095.7

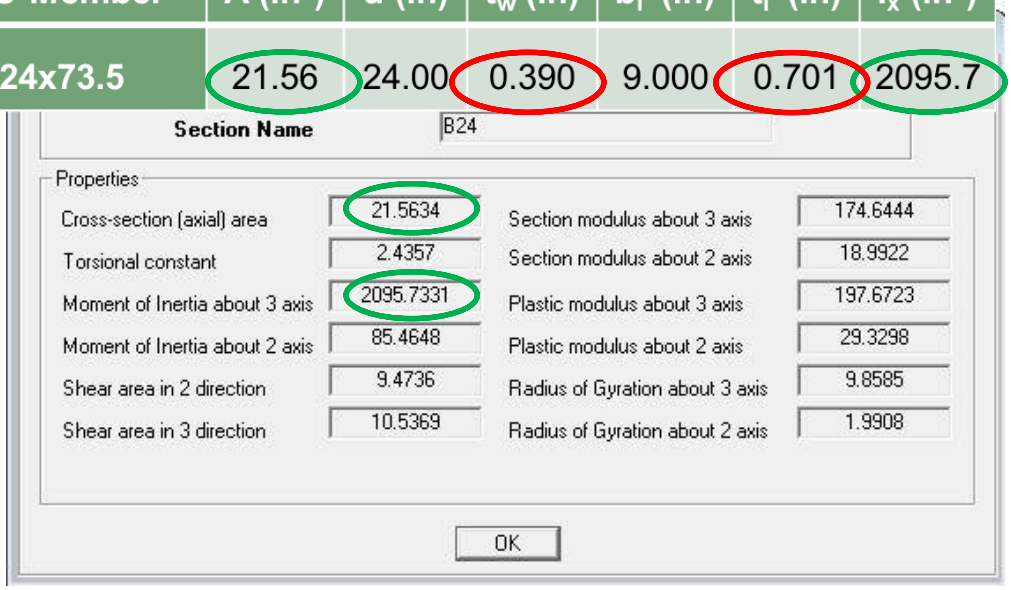

Figure 6.5: B24x73.5 SAP2000 property values compared to AISC specifications

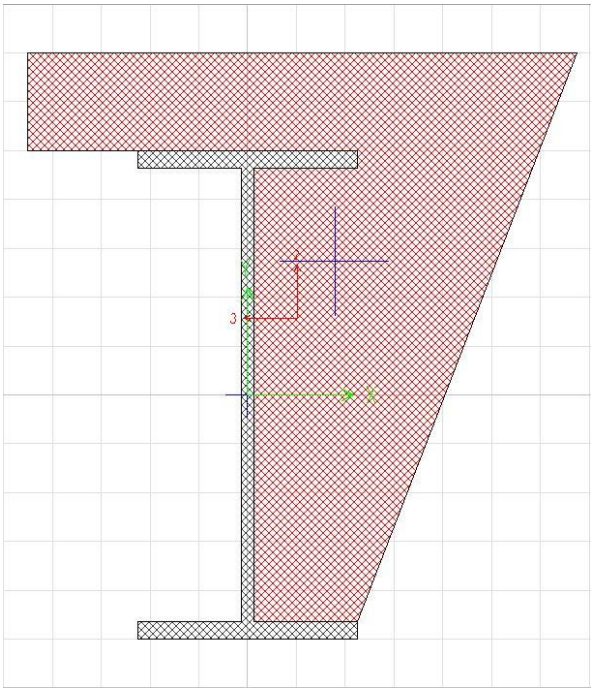

Figure 6.6: Composite beam, B15x42 with unreinforced concrete

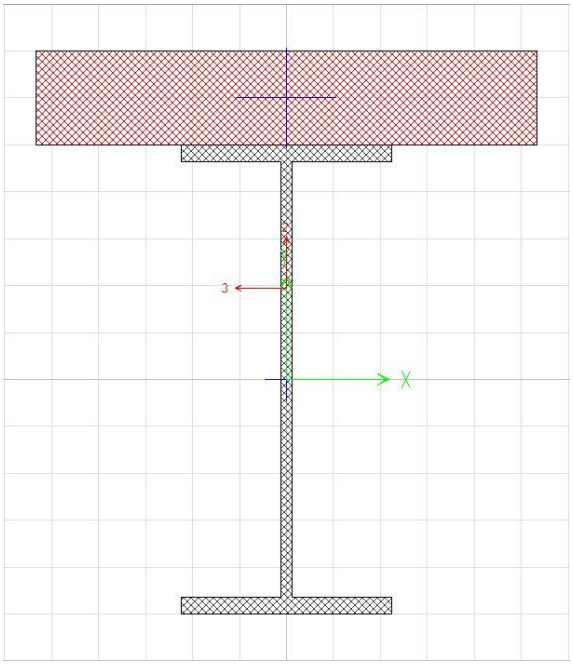

Figure 6.7: Composite beam, B15x42 with modified unreinforced concrete

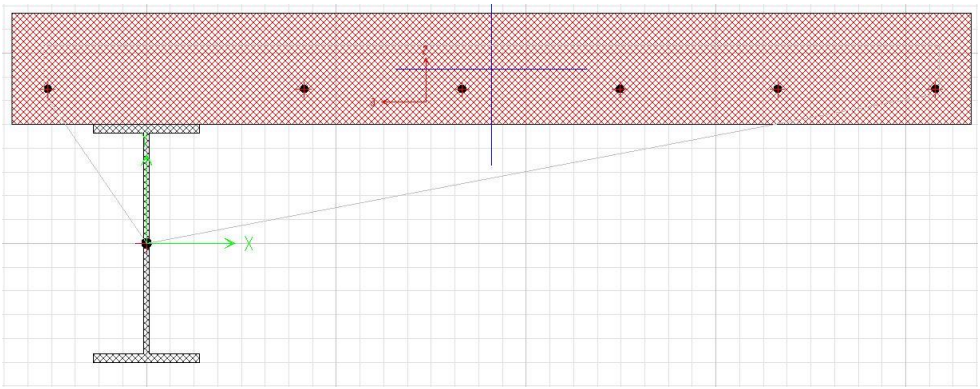

Figure 6.8: Composite beam with effective width of reinforced concrete slab

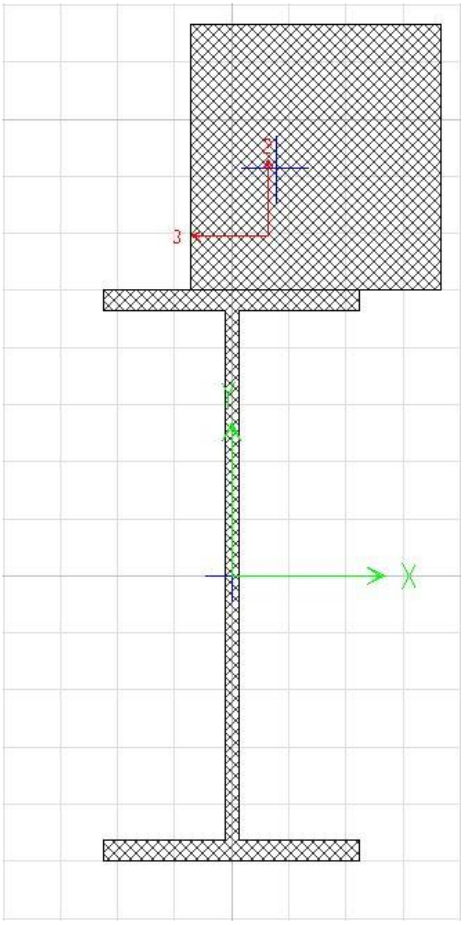

Figure 6.9: Composite beam with effective width of transformed steel slab

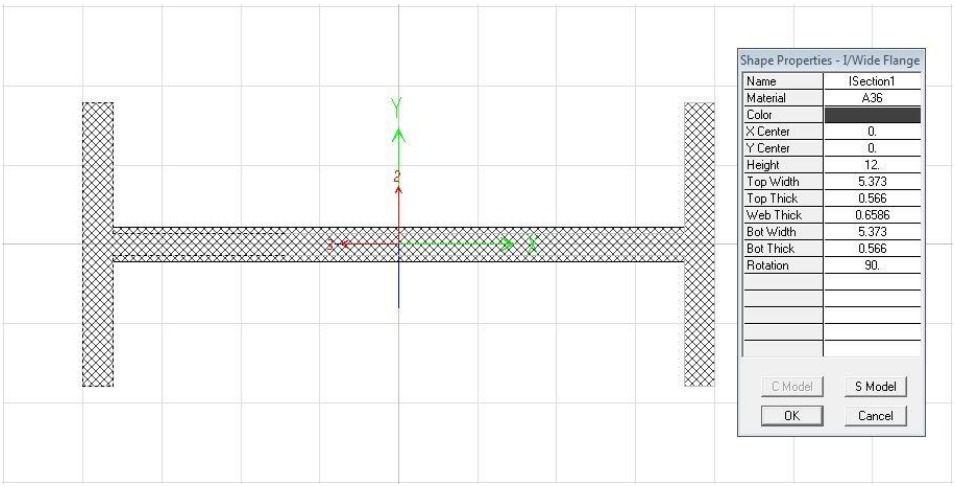

Figure 6.10: S12x45 column I-section dimensions

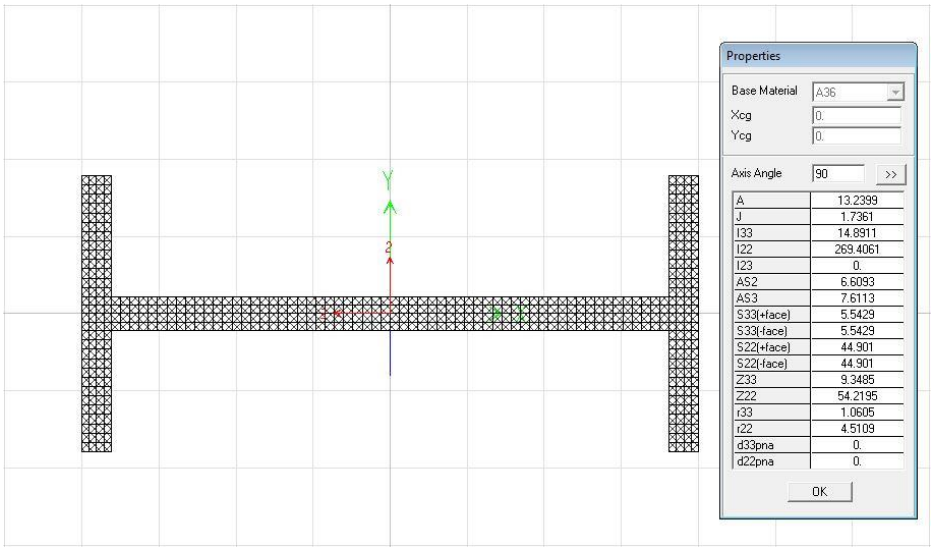

Figure 6.11: S12x45 column I-section minor axis property values

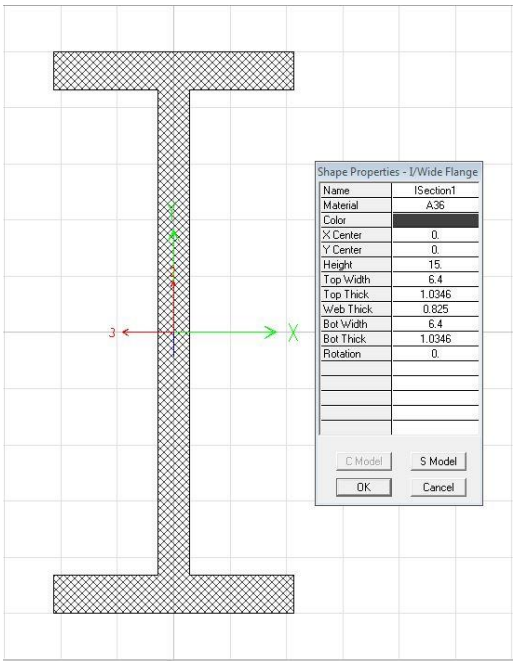

Figure 6.12: S15x81.3 column I-section dimensions

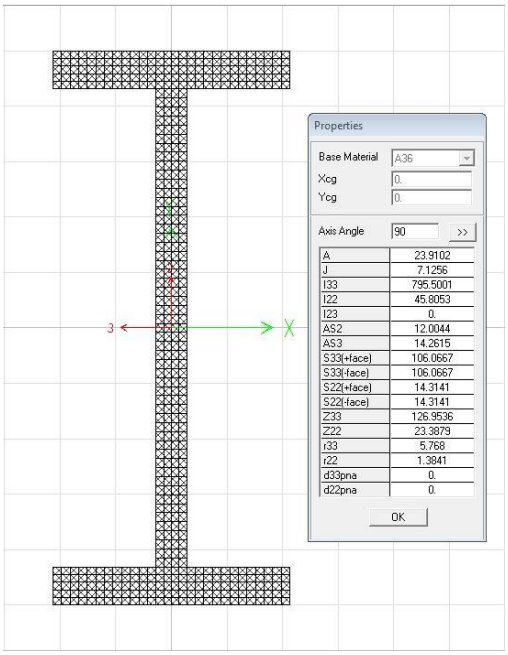

Figure 6.13: S15x81.3 column I-section major axis property values

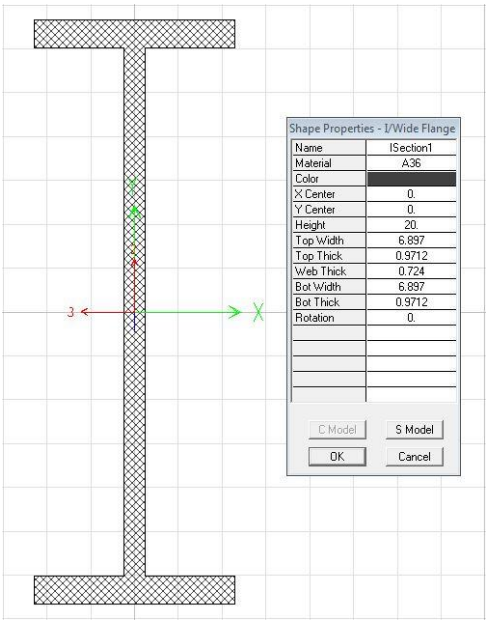

Figure 6.14: S20x90 column I-section dimensions

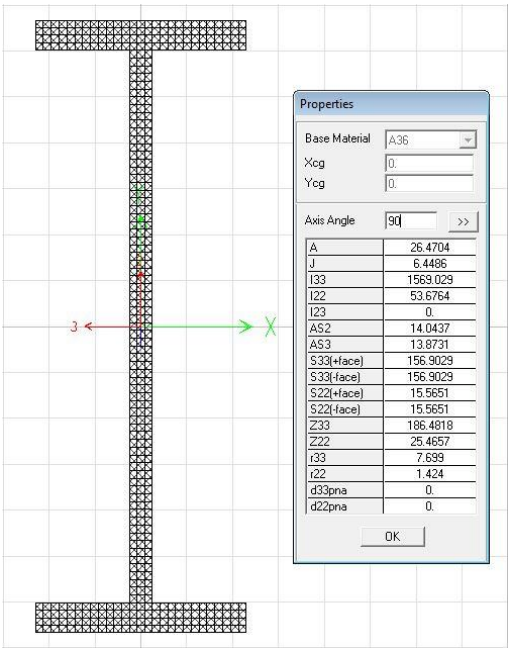

Figure 6.15: S20x90 column I-section major axis property values

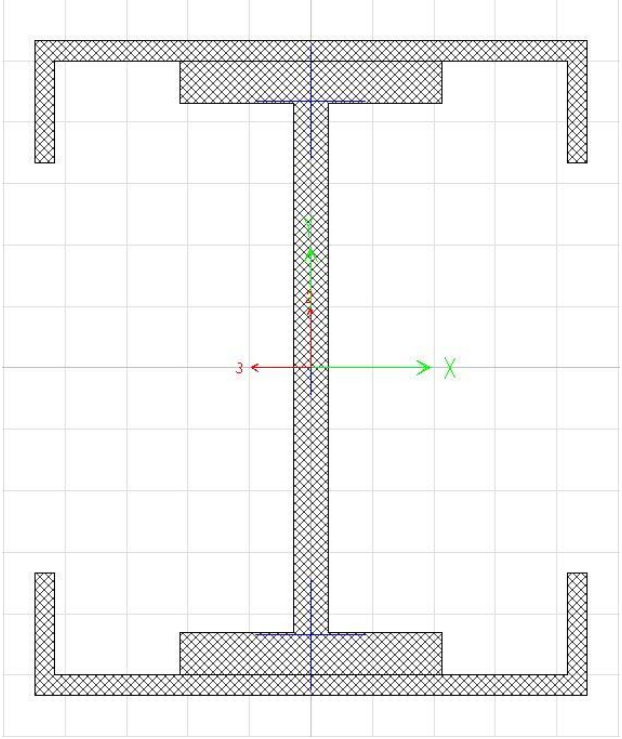

Figure 6.16: Standard built-up column section

CHAPTER 7: SAP2000 ANALYSIS AND TEST DATA COMPARISON

7.1 Introduction

Chapter 7 discusses the analysis results from SAP2000. Shear, moment, strain and displacement values calculated from SAP2000 are discussed. Experimental and theoretical strain and displacement values are compared with data from progressive collapse analysis of the frame in SAP2000. Lastly, GSA guideline was followed to calculate the Demand-Capacity Ratios of the frame members before and after the column was removed.

7.2 SAP2000 Analysis

To compare experimental data from the building with data calculated from SAP2000 model, the column removal process was simulated in SAP2000. To reenact the column removal process on the two-dimensional computer frame model, two models were developed: one model designed with the first-story test column in place and one model designed without the first-story test column. These two models represent the Western frame of the building during its natural static equilibrium (with column) and its potential progressive collapse static equilibrium after the column is removed from the original model. The experimental data needed to be compared with the change in

calculated data (i.e., data from model with the removed column subtracted by data from complete model).

7.3 Calculated Shear and Moments

Shear is force acting parallel to an element's cross-section while a moment is the product of force and distance to that axial force on the element's cross-section. Figures 7.1 through 7.4 show the calculated shear and moments on the frame before and after the column was removed. From Figures 7.1 and 7.3, for the frame with the test column, it can be seen that each element has typical shear and moment distribution under gravity loads. In other words, the beams connected to the removed column have maximum positive moment at mid-span and negative moment over the supports. Once the column was removed, as seen in Figures 7.2 and 7.4, the shear and moment distributions were altered. Examining the beams connected to the removed column in these figures, the entire length of the two beams act as a single beam with maximum positive moment at mid-span, which are the ends of the beams originally connected to the removed column. In other words, the negative beam moments immediately above the removed column became positive moments after the column was removed.

Between pre- and post-column removal, the shear across the North and South beams changed from 25 kips across one beam to 86 kips across both beams (244% increase). As for the moments within the beams, the magnitudes changed from a minimum of -1361 kip-inches (k-in.) across one beam to -11051 k-in. across both beams (712% decrease). It should also be noted that when the column was removed the magnitude of shear and moment in the two adjacent columns (columns 26 and 38) increased significantly. The shear in the first-story of column 26 decreased from -2.93

kips to -61.20 kips (1990% decrease), and shear in the first-story of column 38 increased from 5.91 kips to 65.98 kips (1016% increase). These increases in magnitude are in result of the axial load that was initially being supported by column 27 now being distributed across the frame. The axial change in the first-story of column 26 was -148 kips to -234 kips (58% decrease), and the axial change of the first-story of column 38 decreased from -86 kips to -177 kips (104% decrease). Before the test column was removed, the total axial load between columns 26, 27 and 38 was -405 kips while the total axial load between columns 26 and 38 after the column was removed was -411 kips (1.48% difference). Lastly, analyzing the North side of the frame, the shear and moment values minimally change in magnitude. This indicates that the distribution in forces from removing the column had little effect on the North side of frame.

7.4 Comparison of Experimental and Calculated Strains

A total of 16 strain gauges were used to collect experimental data. Within the Western perimeter frame there were twelve strain gauges: six on columns and six on beams (detailed in Section 3.3). The other four strain gauges were attached on the transverse beam and an interior column. SAP2000 was used to determine theoretical strain at locations where the twelve strain gauges were attached.

7.4.1 Strains Calculated from SAP2000 Model

The stress at the neutral axis of frame members can be calculated in SAP2000. To calculate strain values from the SAP2000 model, calculated stress values from the model were inputted into Equation 7.1 – an adaption of Equation 4.1.

$$\varepsilon = \frac{\Delta\sigma}{E} \tag{7.1}$$

In Equation 7.1, ε is the strain (measured in 10^{-6} in./in.), $\Delta\sigma$ is the change in stress calculated from SAP2000 analysis (measured in ksi), and E is the modulus of elasticity for steel (29,000 ksi). The stress change $\Delta\sigma$ is calculated by subtracting the stress from the complete model with the column (σ_{before}) from the stress from the model without the test column (σ_{after}). For the composite beams connected to the removed column, transformed cross-section was used. The modulus of elasticity was assumed to be that of steel (29,000 ksi). Stress diagrams of the frame before and after the column was removed can be seen in Figures 7.5 and 7.6. The stresses and calculated strain values at strain gauge locations are shown in Tables 7.1 and 7.2.

Table 7.1: Stress and strains from SAP2000 at strain gauge locations on columns

Gauge #	**Member**	**Height on Column**	**σ_{before} (ksi)**	**σ_{after} (ksi)**	**σ_{after} - σ_{before} (ksi)**	**Strain (x10^{-6} in./in.)**
1, 2	Column 26	3 ft-1 in.	-3.30	-10.70	-7.40	-255
4, 5, 6	Column 38	6 ft-2 in.	-2.94	-14.21	-11.27	-389
7	Column 38	4 ft-7 in.	-2.87	-13.42	-10.55	-364

Table 7.2: Stress and strains from SAP2000 at strain gauge locations on beams

Gauge #	**Member**	**Distance from Column 27**	**σ_{before} (ksi)**	**σ_{after} (ksi)**	**σ_{after} - σ_{before} (ksi)**	**Strain ($x10^{-6}$ in./in.)**
11, 12	(N) Beam	1 ft-11.15 in.	-6.77	67.64	74.41	2566
13, 14	(S) Beam	1 ft-11.15 in.	-6.94	70.17	77.11	2659
15	(S) Beam	13 ft-7.5 in.	6.23	5.98	-0.25	-8.62
16	(N) Beam	13 ft-7.5 in.	5.41	7.19	1.78	61.38

For strain gauges located on the North- and South-directed beams (strain gauges #11 through #16), the distance from the centerline of the test column was determined by adding one-half the distance of the overall test column depth (10.5 inches) to the original strain gauge distance from the column (detailed in Section 3.4).

Table 7.1 indicates that the two neighboring columns (26 and 38) were calculated to be in compression, resulting in a negative strain. Comparing the calculated strain values with the yield strain ($1240x10^{-6}$ in./in.) the strain in the model does not exceed the yield strain at the strain gauge locations before or after the column removal. Analyzing the full height of the column, the stress values do not exceed the yield stress of the frame (36 ksi), suggesting that the frame is not susceptible to progressive collapse only if one column is removed.

From Table 7.2, at a location nearest the removed column, the strain values are positive (indicating tension) while at a location near mid-span the strain values are nearing negative (indicating compression) on the bottom face of the bottom beam flange.

Comparing the calculated strain with the yield strain ($1240x10^{-6}$ in./in), at the removed column the North and South connecting beams exceeded the yield values by factors of 2.07 and 2.14, respectively (strain gauges #11 through #14). These results from the SAP2000 model indicate that these beams yielded and deformed significantly, suggesting that immediately above the removed column the beams were susceptible to failure and progressive collapse.

7.4.2 SAP2000 and Experimental Strain Comparison Analysis

Tables 7.3 and 7.4 compare the measured and calculated strains from the SAP2000 model, and the percent error. Comparison of experimental and calculated strain values show that no experimental strain value that was measured in columns is likely to lead to progressive collapse – all measurements being under the yield strain ($1240x10^{-6}$ in./in.). Whereas the predicted strains in the North and South beams were much larger than the yield strain, suggesting large deformations and possibly failure. Between the strain values on the beams and columns, at strain gauge #15 and #16 the experimental and predicted data varied in sign convention. In Section 4.3, it was discussed that strain gauge #15 should have the same response as the other gauges while strain gauge #16 did not (Figure 4.7). Furthermore, strain gauge #16 was oscillating between positive and negative measurements, suggesting that the readings were somewhat ambiguous (Figure 4.8).

Table 7.3: Comparison of experimental and calculated strains for columns

Gauge #	Steel Member	Height on Column	Experimental (E) Strain ($x10^{-6}$ in./in.)	Calculated (C) Strain ($x10^{-6}$ in./in.)	% Error (C-E)/E
1, 2	Column 26	3 ft-1 in.	-32, -54	-255	>372
4, 5, 6	Column 38	6 ft-2 in.	-31, -7, -61	-389	>538
7	Column 38	4 ft-7 in.	-103	-364	253

Table 7.4: Comparison of experimental and calculated strains for beams

Gauge #	Steel Member	Distance from Column 27	Experimental (E) Strain ($x10^{-6}$ in./in.)	Calculated (C) Strain ($x10^{-6}$ in./in.)	% Error (C-E)/E
11, 12	(N) Beam	1 ft-11.15 in.	136, 171	2566	>1401
13, 14	(S) Beam	1 ft-11.15 in.	252, 272	2659	>878
15	(S) Beam	13 ft-7.5 in.	81	-8.62	-111
16	(N) Beam	13 ft-7.5 in.	-10	61.38	-714

Tables 7.3 and 7.4 show that the overall strain measurements within the frame varied drastically between experimental to calculated data. This could be a result of the frame being modeled inaccurately in SAP2000 due to large load quantities or a misrepresentation of the composite beams that were connected to the test column. Because the frame did not have many beams, the majority of the loads were point loads

on the columns. These loads were partially distributed through the two connecting beams, increasing the stress and strain on the beams. This would also contribute to the increased stress and strain in the columns. In terms of the North and South composite beams, by potentially modeling the composite section incorrectly, this would result in a poor behavior for these beams in the model and ultimately lead to a greater inaccuracy.

7.5 Comparison of Data from SAP2000 and Experiment

The two vertical displacement sensors used to collect experimental data from the building were located under the North- and South-directed beams connected to the test column 27 as shown in Figure 3.11. The distances of these two displacement sensors from the test column were measured from the external face of the column's channels instead of the column's neutral axis. Within SAP2000, the distance of the two vertical displacement sensors were measured from the column's neutral axis and therefore required an additional distance along the beam of 10.5 inches (one-half the overall depth of the column). The displacement comparisons made in this section correspond to the same location. SAP2000 is able to calculate displacement values at any point on a selected element. The displacement values within the SAP2000 model are calculated using three conventions: "absolute", "relative to beam minimum" and "relative to beam end." The displacements that measure "absolute" and "relative to beam minimum" are a result of the building response in reference to the wire frame model. The displacements that measure "relative to beam end" are a result of the element response in reference to the moments applied to its two ends. For this research, displacements are calculated and reported following the convention of "absolute" displacement.

7.5.1 SAP2000 Displacement Data and Analysis

In terms of the "absolute" displacement convention, the second floor joint immediately above column 27 within the removed column model was measured to be displaced 4.31 inches in the negative z-direction (Figure 7.7). This large magnitude of displacement is apparent along the North- or South-directed beams connected to the removed column, especially at the displacement sensor locations. The North displacement sensor was located on the beam connecting columns 26 and 27 while the South displacement sensor was located on the beam connecting columns 27 and 38 (Figure 3.11). On the SAP2000 model at the position of the North displacement sensor the change in displacement – from 0.026 inches when the column existed to -4.20 inches when it was removed – was calculated to be -4.23 inches. At the position of the South displacement sensor, the change in displacement – from 0.026 inches when the column existed to -4.19 inches when it was removed – was calculated to be -4.26 inches.

The absolute displacement is assumed to have such a large magnitude because of the layout and magnitude of the loads on the frame and the overall load distribution. Because there were few beams that ran along the frame, most of the loads that existed on test column 27 were point loads. Combining loads from each floor, the axial load on column 27 had to be redistributed. At the same time, with such a high axial load, once the column was removed, there was minimal beam support to transfer loads and to counteract a change in displacements. The axial forces before and after the column was removed can be seen in Figures 7.8 and 7.9. Analyzing these figures, the axial load on column 27 was almost entirely divided between the adjacent columns 26 and 38 when column 27 was removed. Furthermore, no visible axial forces were found in the beams prior to removing the column. Once the column was removed, axial forces were distributed through the

North- and South-directed beams from the removed column. The axial load and displacement calculations presented in this section indicate the importance of three-dimensional (3D) model and 3D analyses to consider load distributions and contribution of slabs for more accurate representation of the building behavior after column removal.

7.5.2 SAP2000 and Experimental Displacement Comparison

To compare the experimental and calculated displacement data, the "absolute" convention was measured to be far greater than what was expected from the analysis. Experimental displacements do not exceed 1.0 inches, while the absolute theoretical displacements exceeded 4.0 inches, showing a drastic difference. Figures 7.10 and 7.11 compare the experimental and calculated displacements for the two vertical displacement sensors. The SAP2000 frame model was designed to have completely rigid connections. The actual Haskett Hall building had connections that were partially rigid – between being pinned and completely rigid. If the model could be designed with partially rigid connections, then the displacement comparisons would become more accurate.

7.6 SAP2000 Demand-Capacity Ratio Data and Analysis

This research analyzed the Western frame of Haskett Hall before and after the test column was removed. GSA (2003) uses Demand-Capacity Ratios (DCR) to analyze which structural elements will exceed their load carrying capacity and lead to progressive collapse. DCR can be calculated using Equation 7.2.

$$DCR = \frac{M_{\max}}{M_P} \tag{7.2}$$

In Equation 7.2, M_{max} is the maximum moment demand calculated using linear elastic static analysis from SAP2000, and M_P is the ultimate moment capacity – or plastic

moment. By GSA's guidelines, if DCR values for a given member exceed 2.0 for columns or 3.0 for beams (Figure 7.12), then the member is susceptible to failure [7]. In terms of a structure, failing members result in the building being susceptible to progressive collapse. It should be noted that GSA suggests analyzing structures using a load factor of 2.0 for dead loads. For this research, the load factor for dead loads was 1.0 to represent the building's natural weight. Therefore, to analyze the failure capacity of the model, DCR values exceeding 1.0 for columns and 1.5 for beams within SAP2000 are susceptible to progressive collapse or the calculated M_{maz} values can be multiplied by 2.0 because all loads are dead loads on the structure. SAP2000 automatically calculates DCR values for every member when prompted to conduct a "Steel Design/Check of Structure." Within SAP2000, the assigned DCR value to indicate failure is 1.00. Figures 7.13 and 7.14 show a structural check of the rigid Western frame before and after the column was removed with respective DCR maximum values of elements surrounding the removed column.

As seen in Figure 7.13, before the first-floor column 27 was removed, the frame's DCR values ranged from 0 to 0.50 and did not exceed SAP2000 failure value of 1.00. The maximum DCR value calculated within the SAP2000 model was located at the beam-column connection on the South-directed beam from the removed column with a value of 0.495. As seen in Figure 7.14, after column 27 was removed, the frame's DCR values ranged from 0 to greater than 1.00. To account for the varying DCR values based on axial loads and moments, beams and columns neighboring the test column have DCR values shown at the mid-span and section ends on Figure 7.14. The maximum DCR value calculated within the SAP2000 frame model was located on the North-directed beam

from the test column, specifically at the beam's North end connecting to column 15. The value was calculated to be 3.976. By GSA standards, these values indicated that the frame was structurally sound before removing column 27 and was susceptible to collapse after the column was removed.

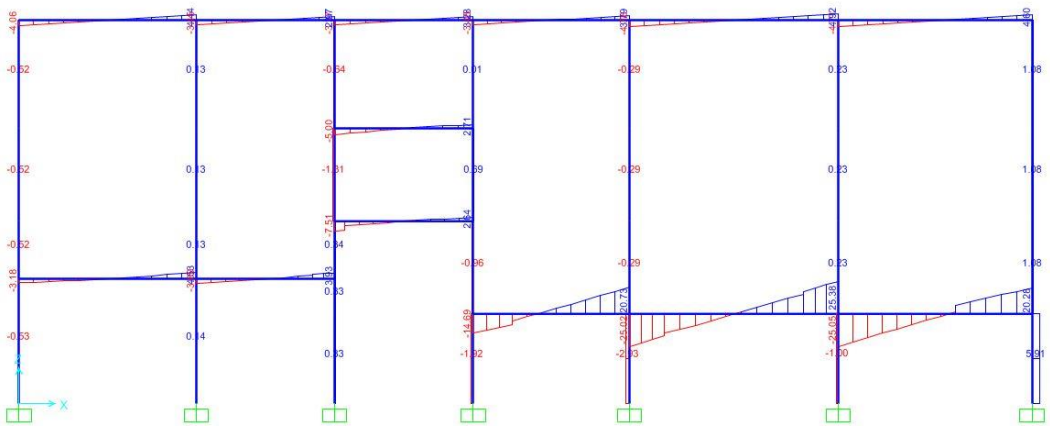

Figure 7.1: Shear distribution before the column was removed

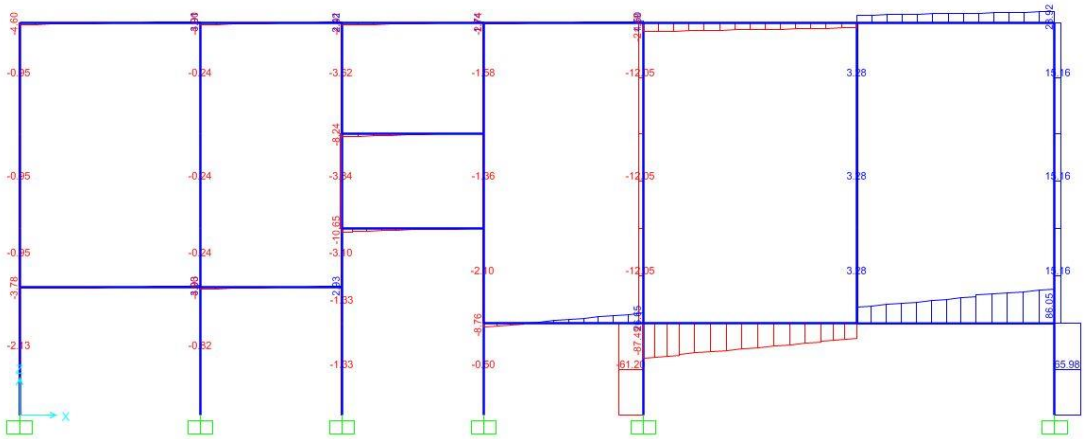

Figure 7.2: Shear distribution after the column was removed

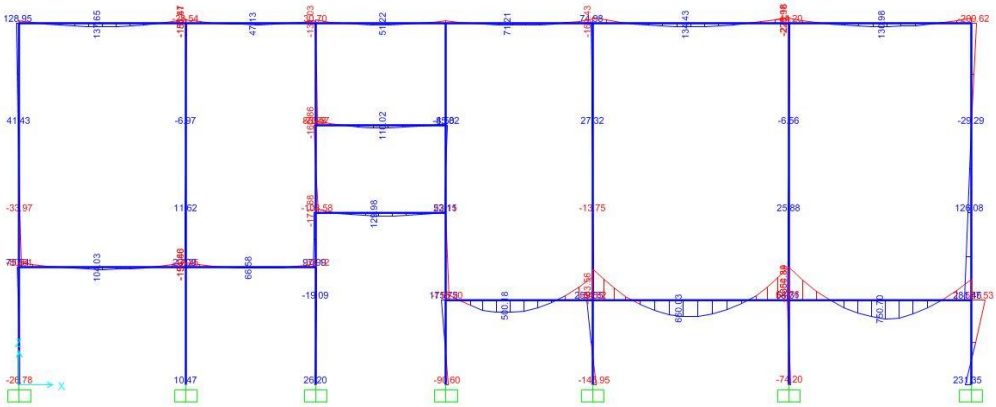

Figure 7.3: Moment distribution before the column was removed

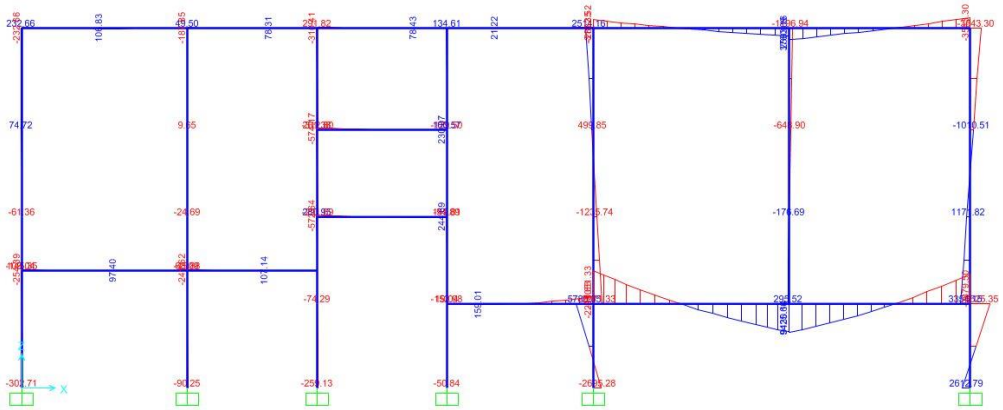

Figure 7.4: Moment distribution after the column was removed

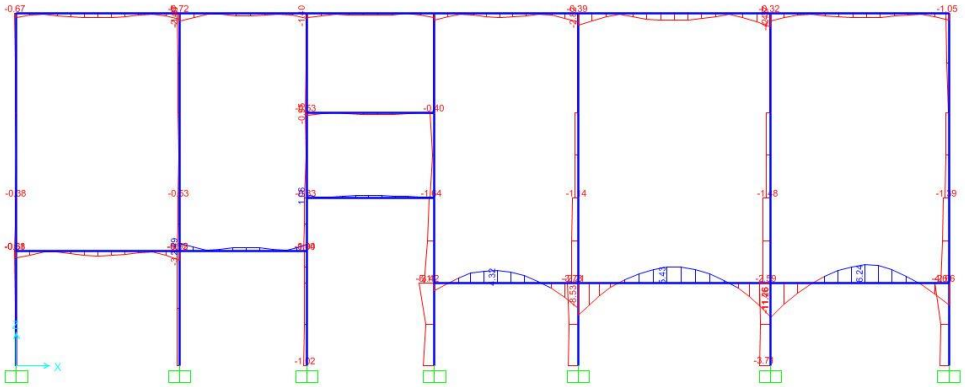

Figure 7.5: Stress distribution before the column was removed

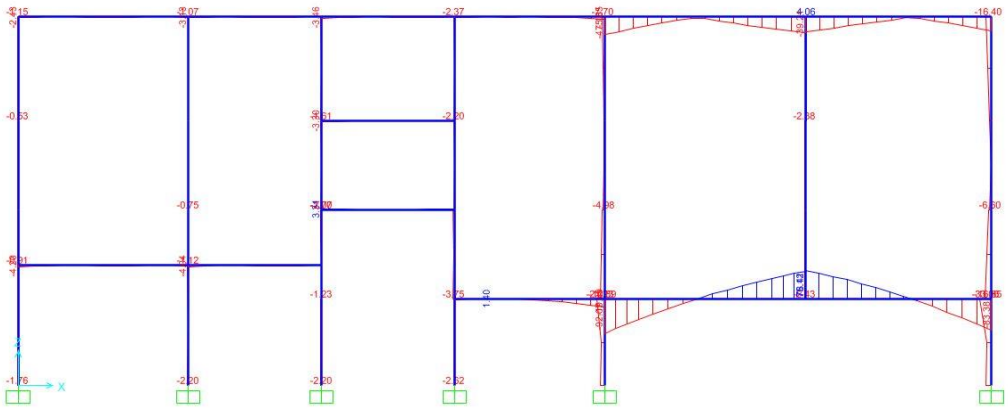

Figure 7.6: Stress distribution after the column was removed

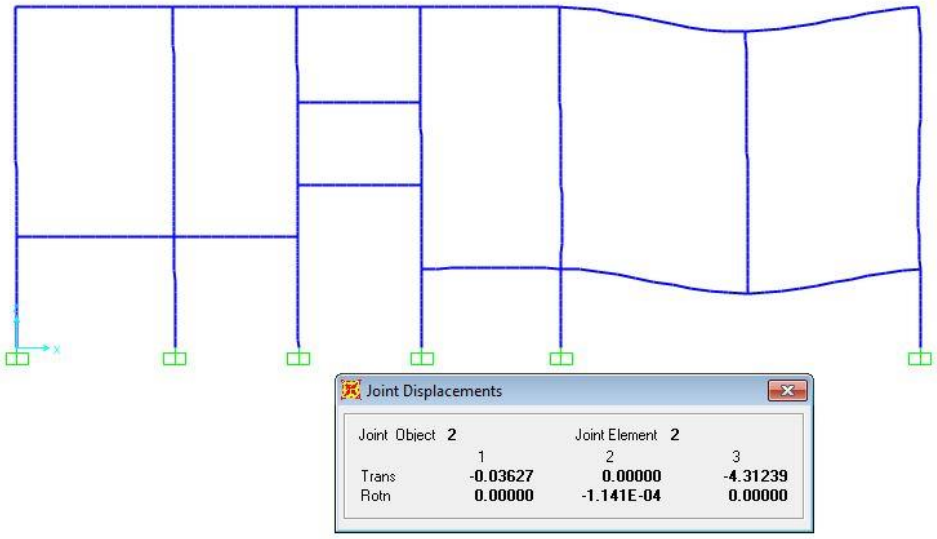

Figure 7.7: Joint displacement immediately above the removed column

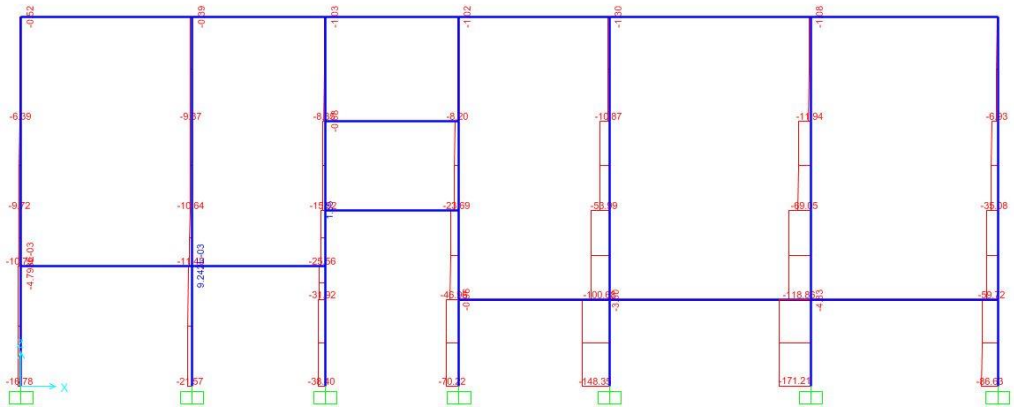

Figure 7.8: Axial force distribution before the column was removed

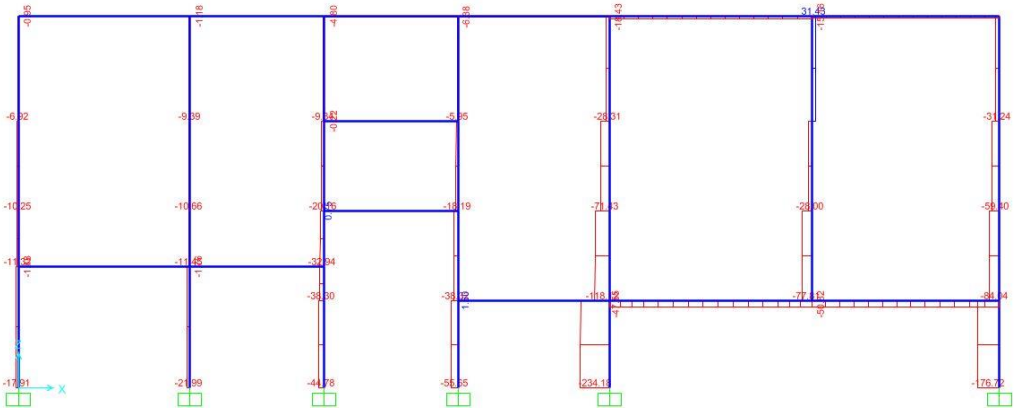

Figure 7.9: Axial force distribution after the column was removed

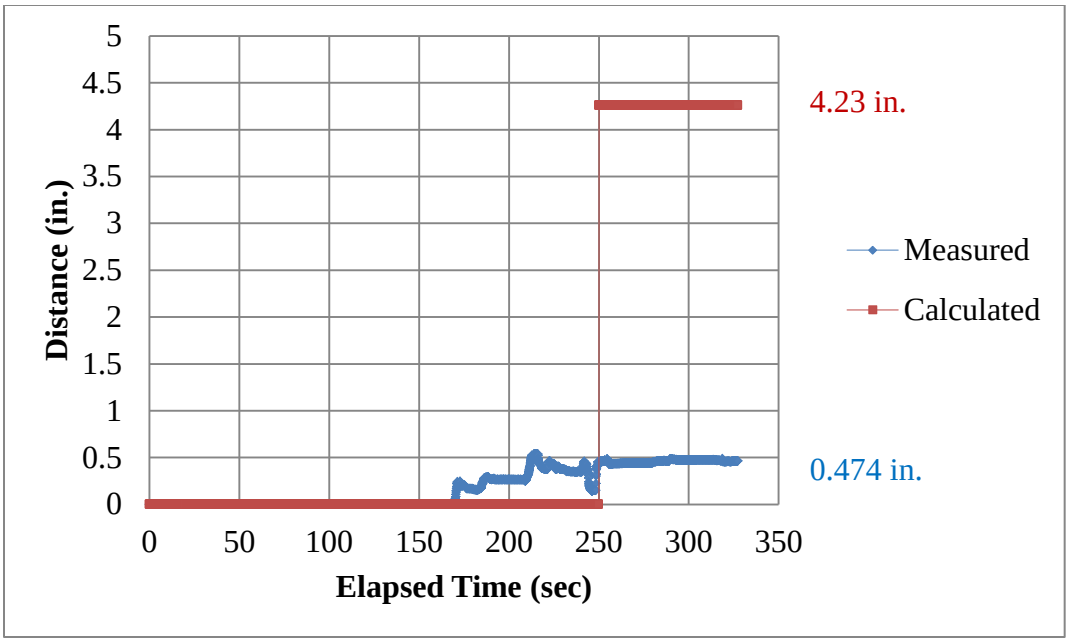

Figure 7.10: Experimental and calculated displacement comparison at North sensor located 39.25 inches away from the neutral axis of the removed column

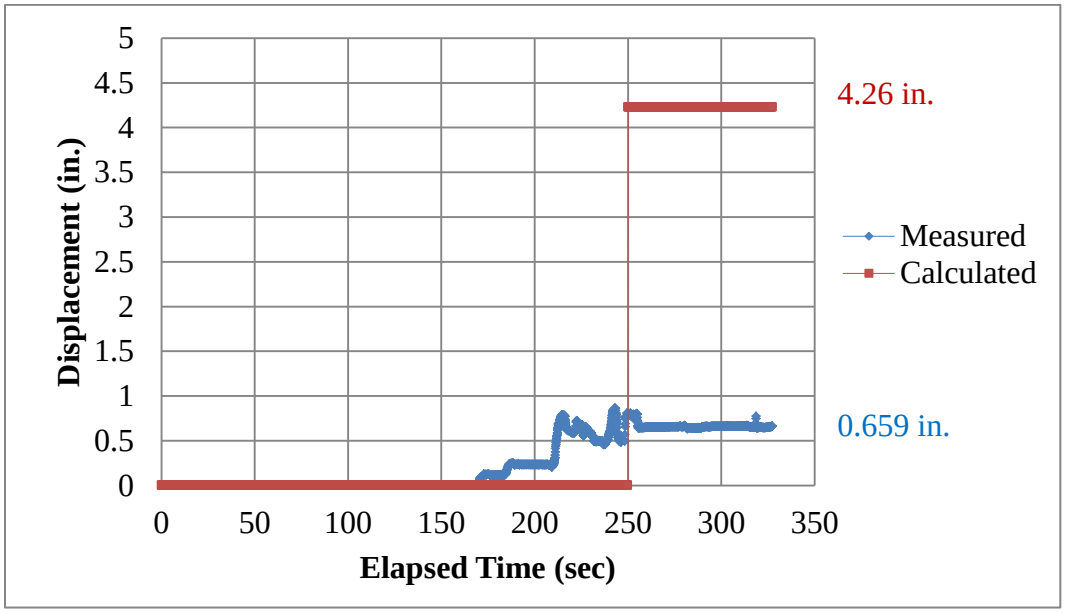

Figure 7.11: Experimental and calculated displacement comparison at South sensor located 28.50 inches away from the neutral axis of the removed column

Component/Action	Values for Linear Procedures *DCR*
Beams – flexure	
a. $\frac{b_f}{2t_f} \le \frac{52}{\sqrt{F_{ye}}}$ and $\frac{h}{t_w} \le \frac{418}{\sqrt{F_{ye}}}$	3
b. $\frac{b_f}{2t_f} \ge \frac{65}{\sqrt{F_{ye}}}$ or $\frac{h}{t_w} \ge \frac{640}{\sqrt{F_{ye}}}$	2
c. Other	Linear interpolation between the values on lines a and b for both flange slenderness (first term) and web slenderness (second term) shall be performed, and the lowest resulting value shall be used.
Columns – flexure	
For $0 < P/P_{CL} < 0.5$	
a. $\frac{b_f}{2t_f} \le \frac{52}{\sqrt{F_{ye}}}$ and $\frac{h}{t_w} \le \frac{300}{\sqrt{F_{ye}}}$	2
b. $\frac{b_f}{2t_f} \ge \frac{65}{\sqrt{F_{ye}}}$ or $\frac{h}{t_w} \ge \frac{460}{\sqrt{F_{ye}}}$	1.25
c. Other	Linear interpolation between the values on lines a and b for both flange slenderness (first term) and web slenderness (second term) shall be performed, and the lowest resulting value shall be used.

Figure 7.12: GSA guidelines for maximum beam and column DCR values

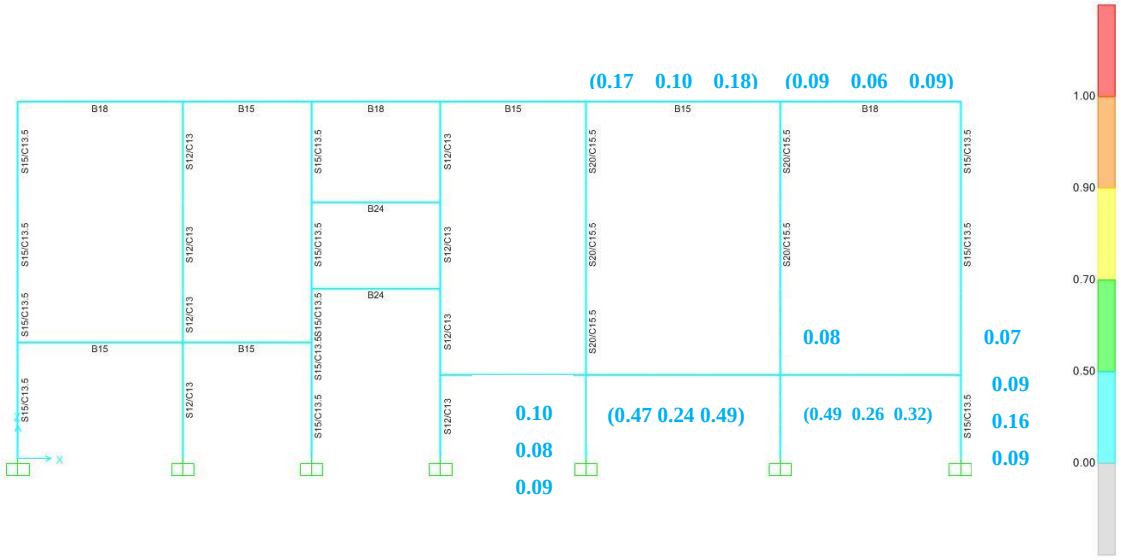

Figure 7.13: Structural check and neighboring mid-span and endpoint DCR values before column was removed

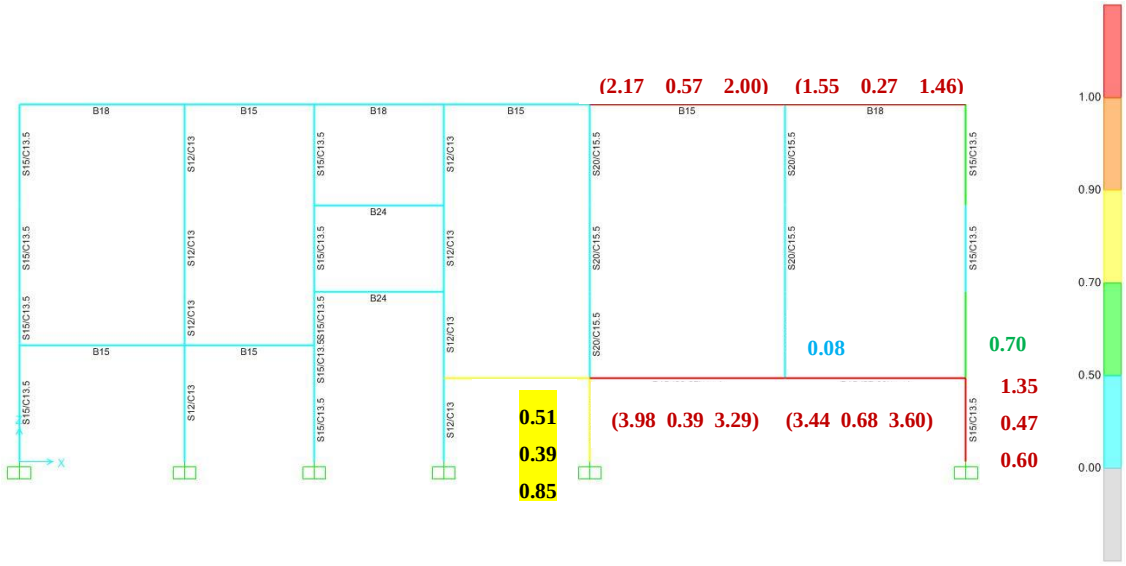

Figure 7.14: Structural check and neighboring mid-span and endpoint DCR values after column was removed

CHAPTER 8: SUMMARY AND CONCLUSION

8.1 Summary

This research investigated the progressive collapse potential of a steel building, Haskett Hall, by removing a first-story column before the building was demolished. Strain and displacement values were recorded from strain gauges and displacement sensors installed on the beams and columns neighboring the removed column. Experimental data was analyzed to test the progressive collapse response of the building. Analysis results indicated that the building was not susceptible to collapse. This data was then compared with data from analyses of a two-dimensional SAP2000 computer model.

As there were limited building design specifications and drawings, the building's beams and columns were modeled by determining geometric properties from drawings and pictorial analyses. In SAP2000, the building was modeled to simulate the column removal process by creating two models of the two-dimensional frame: before and after the first-story column was removed. The SAP2000 model was analyzed for linear static analysis of progressive collapse. Compared to experimental data, the calculated data indicated that the structure had some potential for progressive collapse with strain values exceeding the yield strain.

Following General Service Administration (GSA) guidelines, the demand-capacity ratios (DCR) were calculated within SAP2000 to measure the potential collapse of the frame model before and after removing the column. It was noted that SAP2000

does not consider composite beams, but the DCR values still exceeded GSA guidelines to suggest potential collapse. The experiment conducted, data analyzed, and errors observed in this research will be used to improve future linear static progressive collapse research.

8.2 Conclusion

Haskett Hall was designed and completed in the 1920s revealing unique as well as outdated design methods. It is suggested that, whenever possible, future projects be given fully detailed structural building plans to eliminate the possibility for modeling errors. In the case that section dimensions are not specified, pictorial analyses are a possible alternative. Such dimensional analyses should be further explored. Analyses were run in SAP2000 for linear static analysis by considering DCR values. Analyzing the experimental and calculated responses of the two-dimensional frame model, the SAP2000 results drastically exceeded the field results due to the discrepancy in structural designs, three-dimensional slab contributions and load redistributions resulting in possible inaccuracy of two-dimensional load distributions, and the various inconsistences of the experiment during the column removal process. With the discrepancy between experimental and calculated data, it was concluded that through two-dimensional analyses it is uncertain whether Haskett Hall was susceptible to progressive collapse after removing one first-story column.

8.3 Recommendations for Future Research

To analyze Haskett Hall for progressive collapse it is suggested that this research be expanded to explore three-dimensional, non-linear and dynamic analyses in the hopes

of creating more accurate simulations. Furthermore, models should be designed with partially-rigid connections to account for real behavior and building specifications.

REFERENCES

[1] ACI 318-08. 2008. *Building code requirements for structural concrete and commentary.* American Concrete Institute (ACI). Farmington Hills, MI.

[2] "AISC Shapes Historic Edition." *AISC Shapes Database Version 14.0 Historic*. American Institute of Steel Construction, 2013. Web. 17 Apr. 2013. <http://www.aisc.org/WorkArea/showcontent.aspx?id=17622>.

[3] ASCE 7-05. 2005. *Minimum design loads for buildings and other structures*. Report: ASCE/SEI 7-05. American Society of Civil Engineers (ASCE). Reston, VA.

[4] DoD. 2005. *Design of buildings to resist progressive collapse*. Unified Facilities Criteria (UFC) 4-023-03, Department of Defense (DoD)

[5] Giriunas, K. A. 2009. *Progressive collapse analysis of an existing building*. Honors Thesis. Department of Civil and Environmental Engineering and Geodetic Science. The Ohio State University, Columbus, OH.

[6] Griffiths, H., Pugsley, A., Saunders, O. 1968. *Report of inquiry into the collapse of flats at Ronan Point, Canning Town*. Ministry of Housing and Local Government. Her Majesty's Stationary Office. London, United Kingdom.

[7] GSA. 2003. *Progressive collapse analysis and design guidelines for new federal office buildings and major modernization projects*. General Services Administration (GSA).Washington, D.C.

[8] Hertenstein, J. P. (1993). *Facility audit report Haskett hall, building 027* [Data file]. Retrieved from http://fod.osu.edu/bldg_audit/Haskett_Hall-93.pdf

[9] Nair, R. S. 2004. Progressive collapse basics. *Proceedings of North American Steel Construction Conference (NASCC)*. March 24-27. Long Beach, CA.

[10] SAP2000. 2012. SAP 2000 Advanced structural analysis program, *Version 15*. Computers and Structures, Inc. (CSI). Berkeley, CA, U.S.A.

[11] Song, B. I. 2010. *Experimental and analytical assessment on the progressive collapse potential of existing buildings*. Master's Thesis. Department of Civil, Environmental, and Geodetic Engineering. The Ohio State University, Columbus, OH.

APPENDIX A: STRUCTURAL BUILDING PLANS

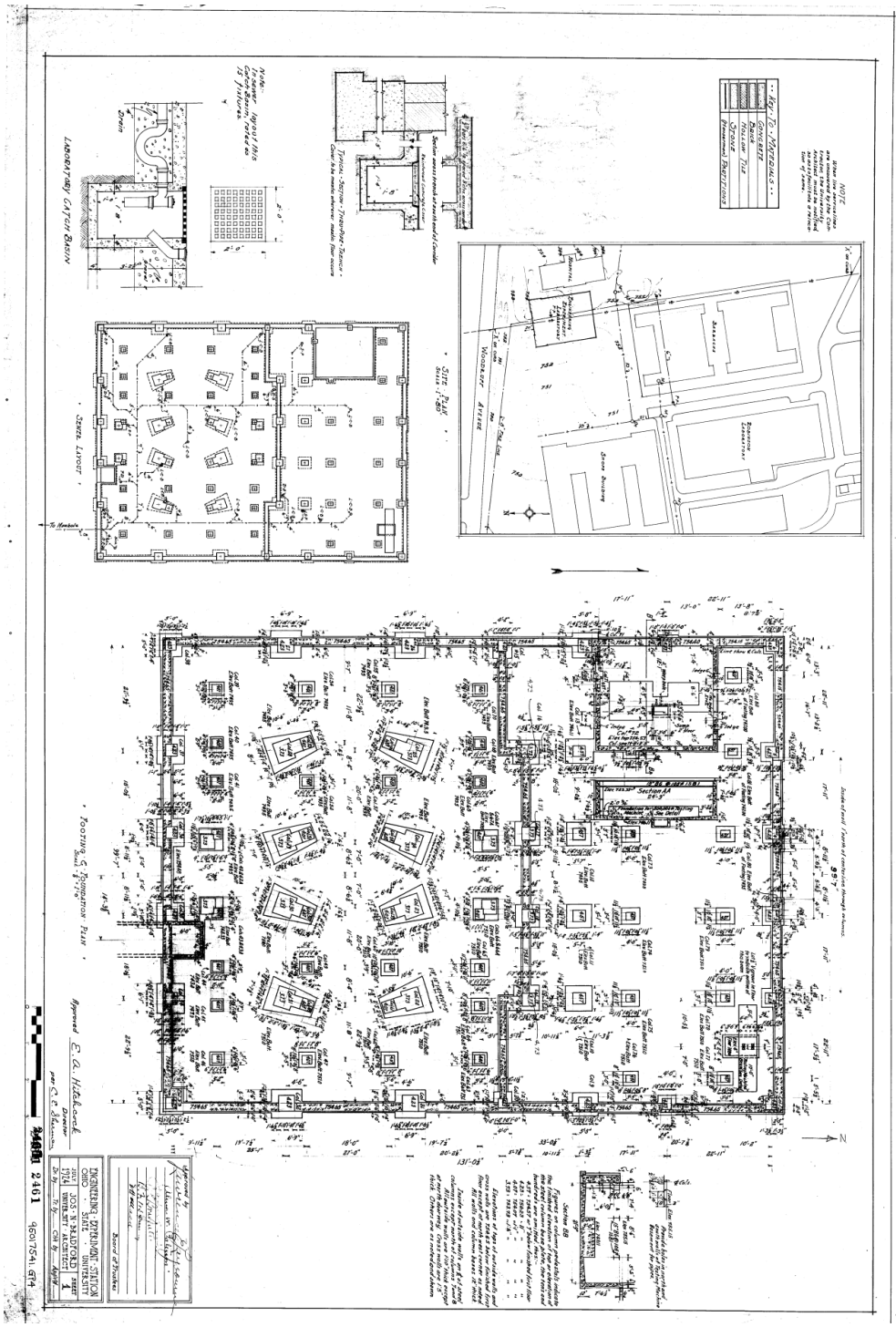

Figure A.1: Footing and foundation plan

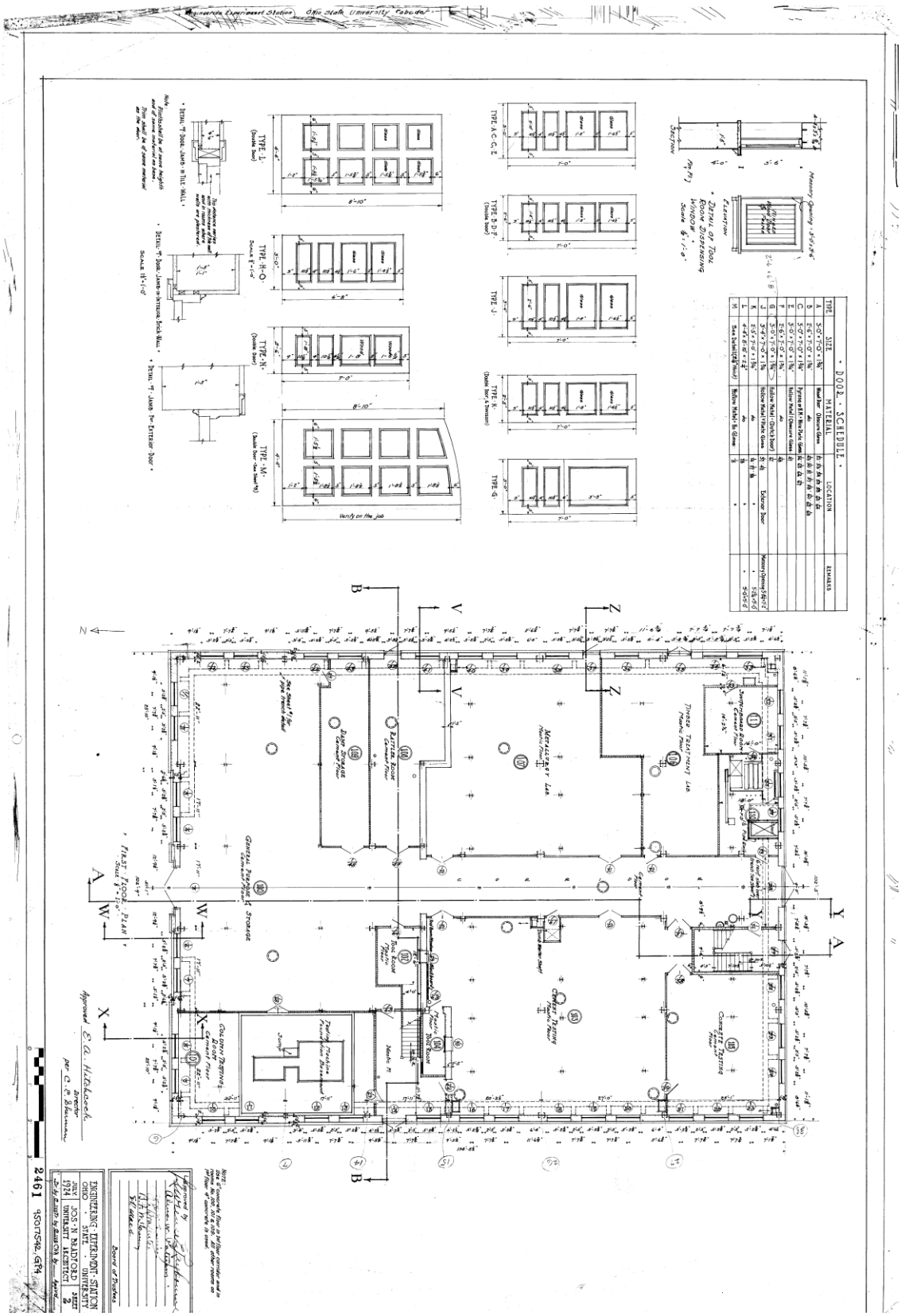

Figure A.2: Door schedule

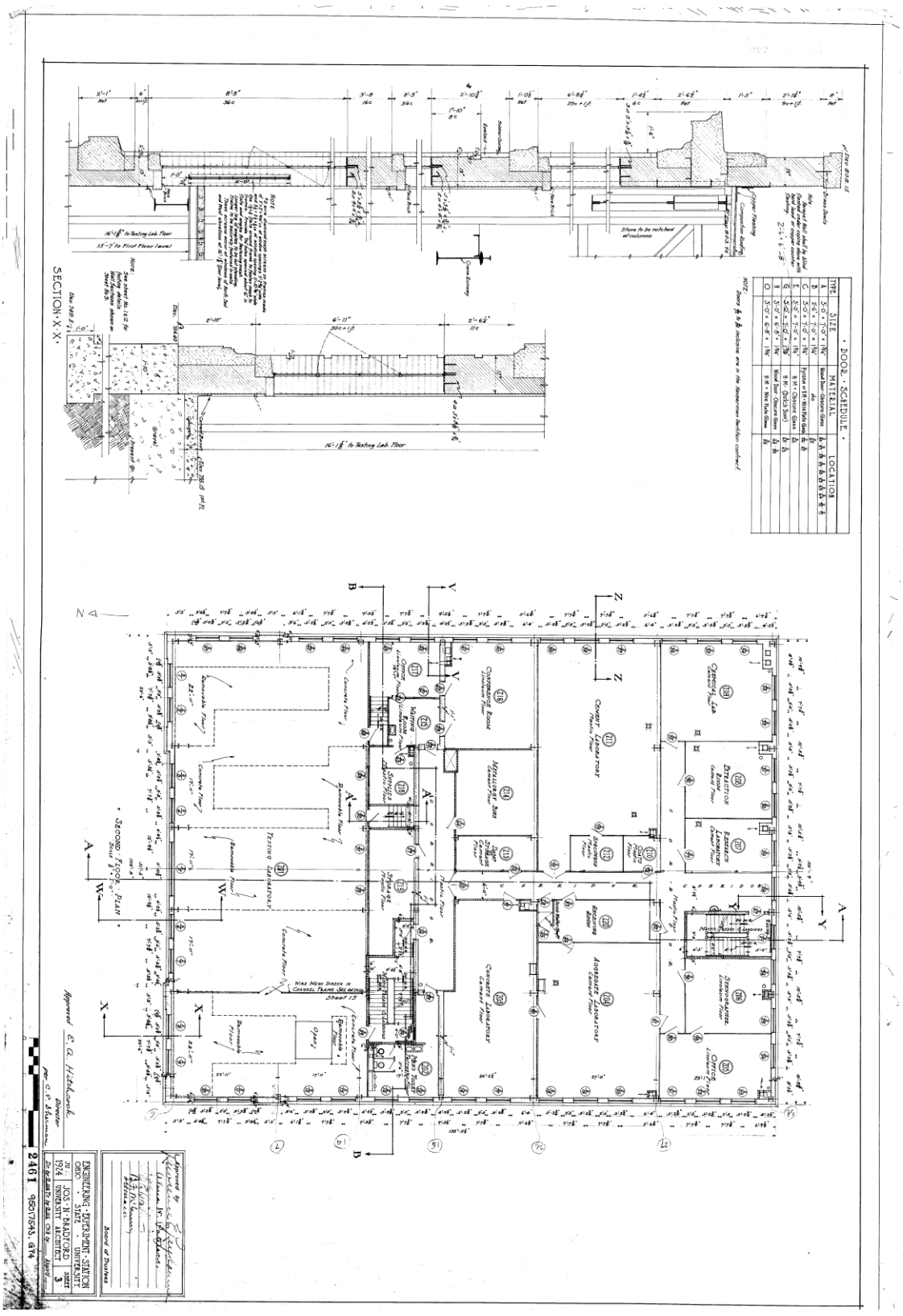

Figure A.3: Second floor room descriptions and X-X cross-section

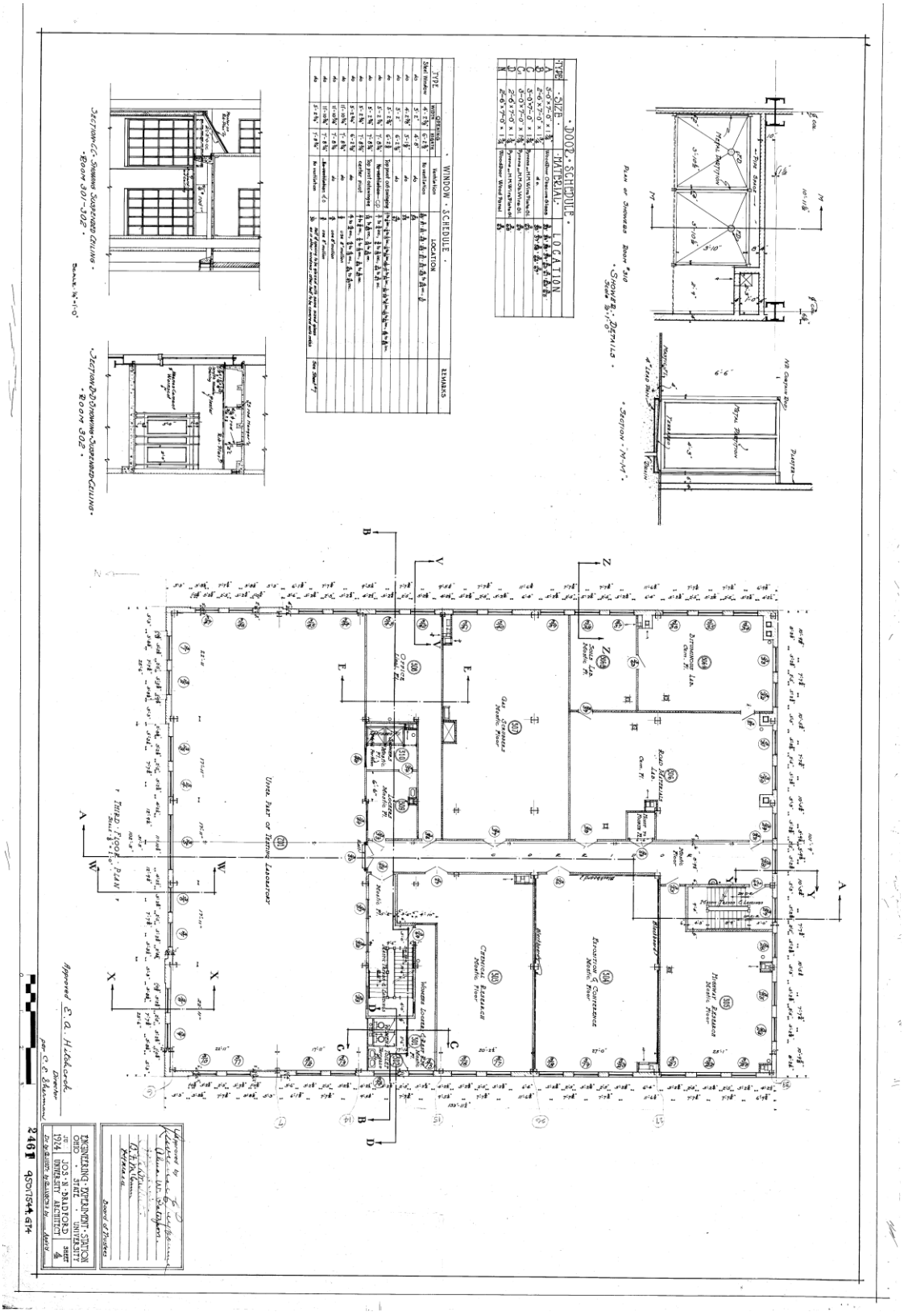

Figure A.4: Third floor room descriptions and window and door schedules

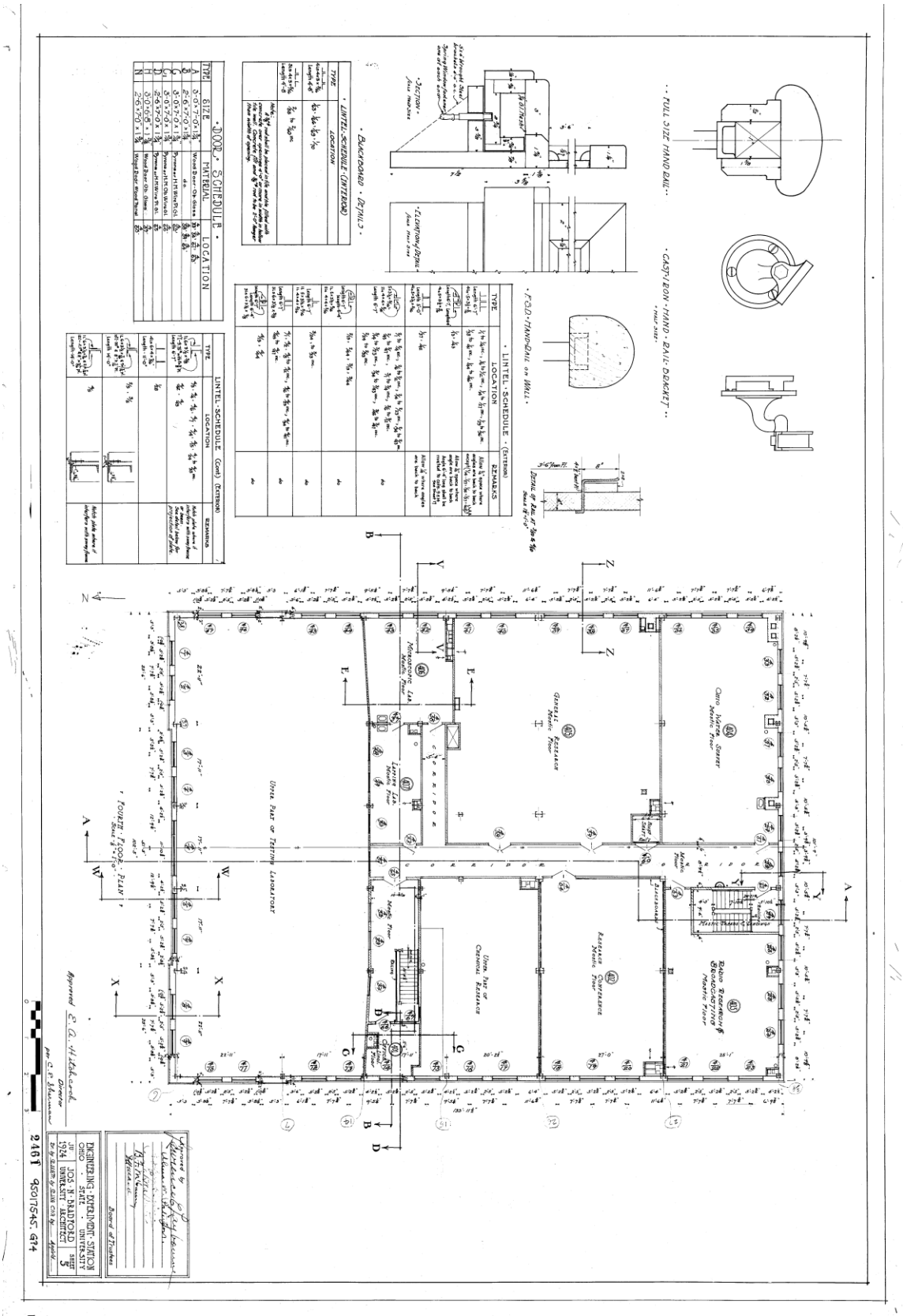

Figure A.5: Fourth floor room descriptions

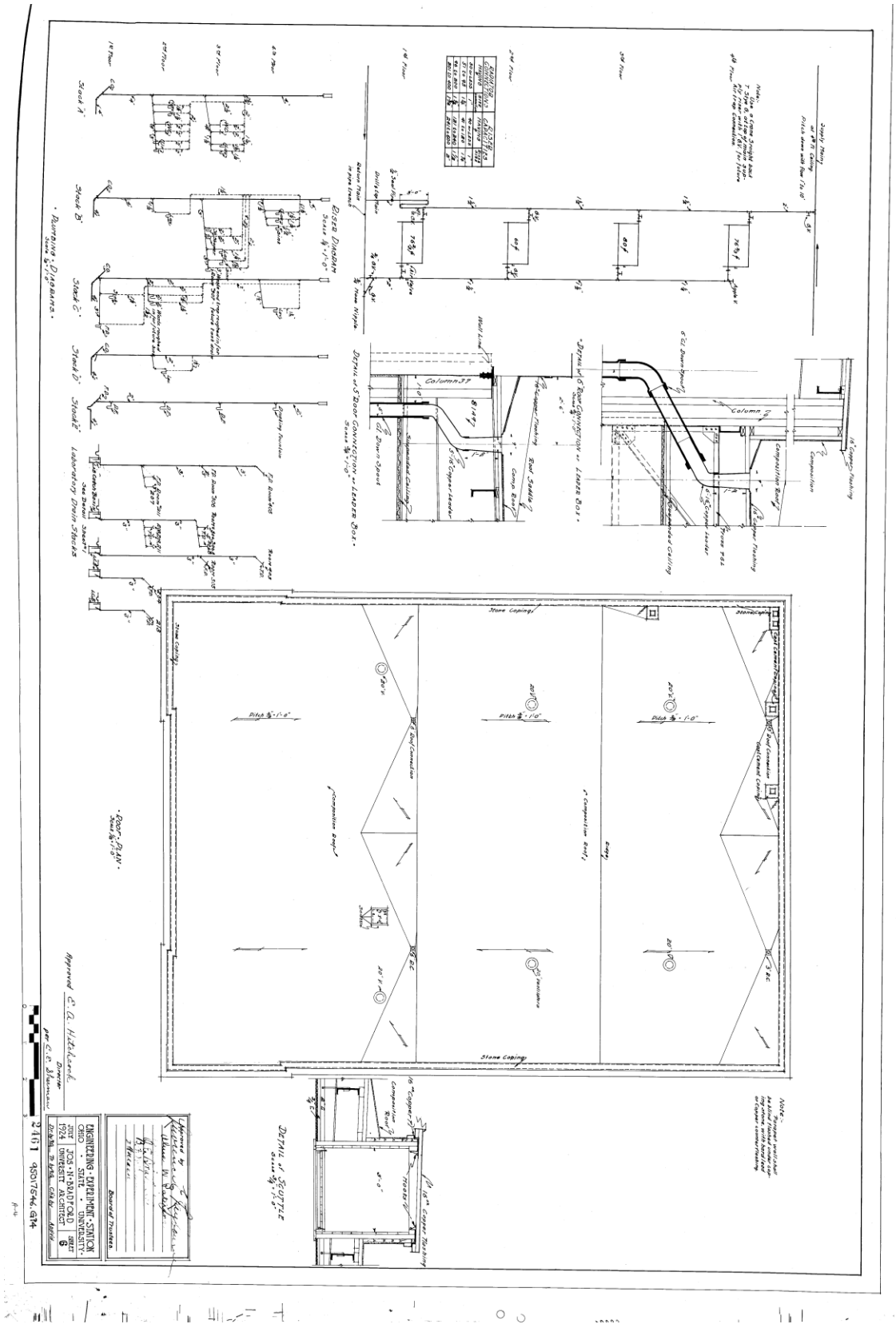

Figure A.6: Plumbing diagrams

Figure A.7: Haskett Hall elevations

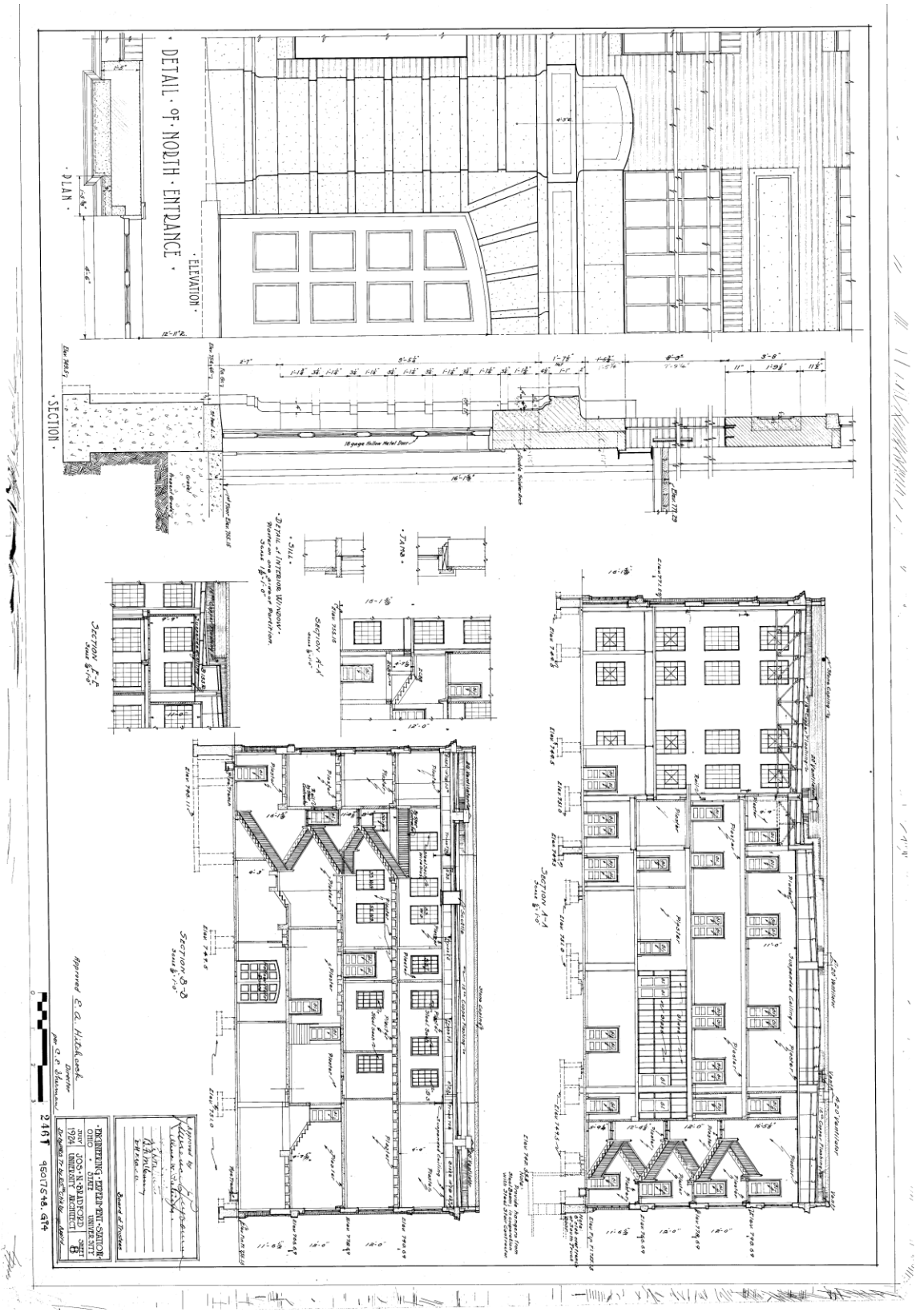

Figure A.8: Elevation section cuts A-A and B-B

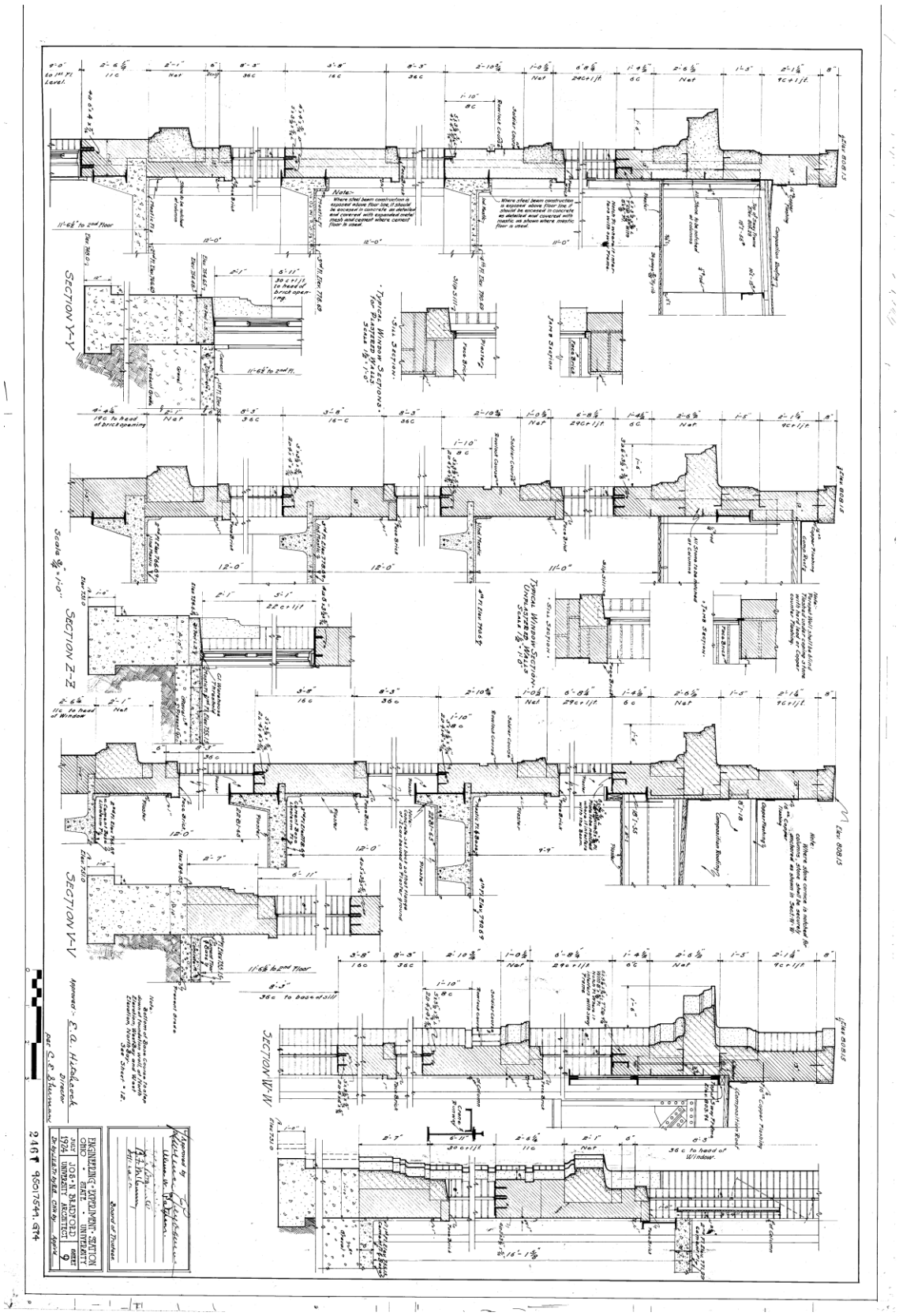

Figure A.9: Façade cross-sections

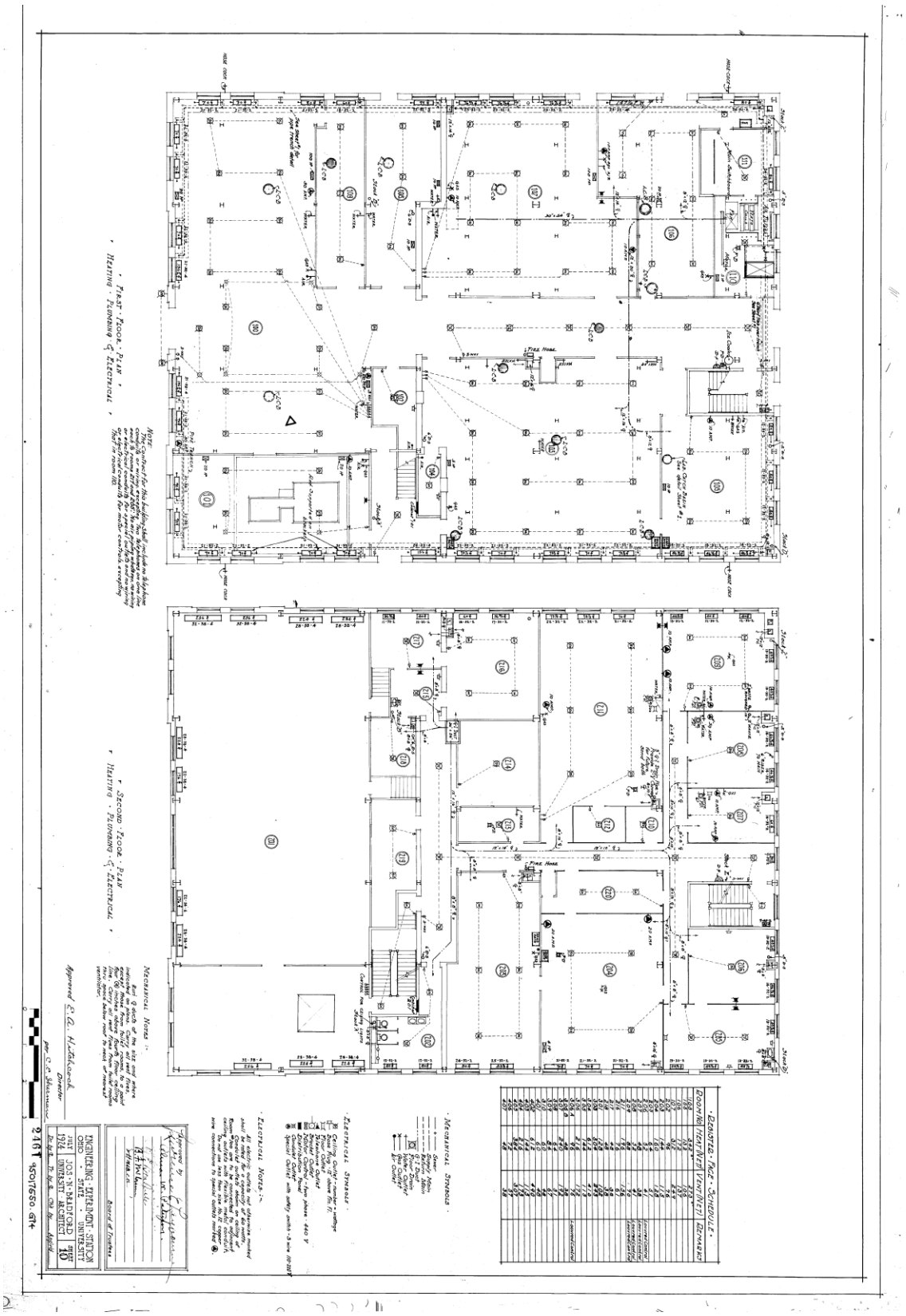

Figure A.10: First and second floor heating, plumbing and electrical plans

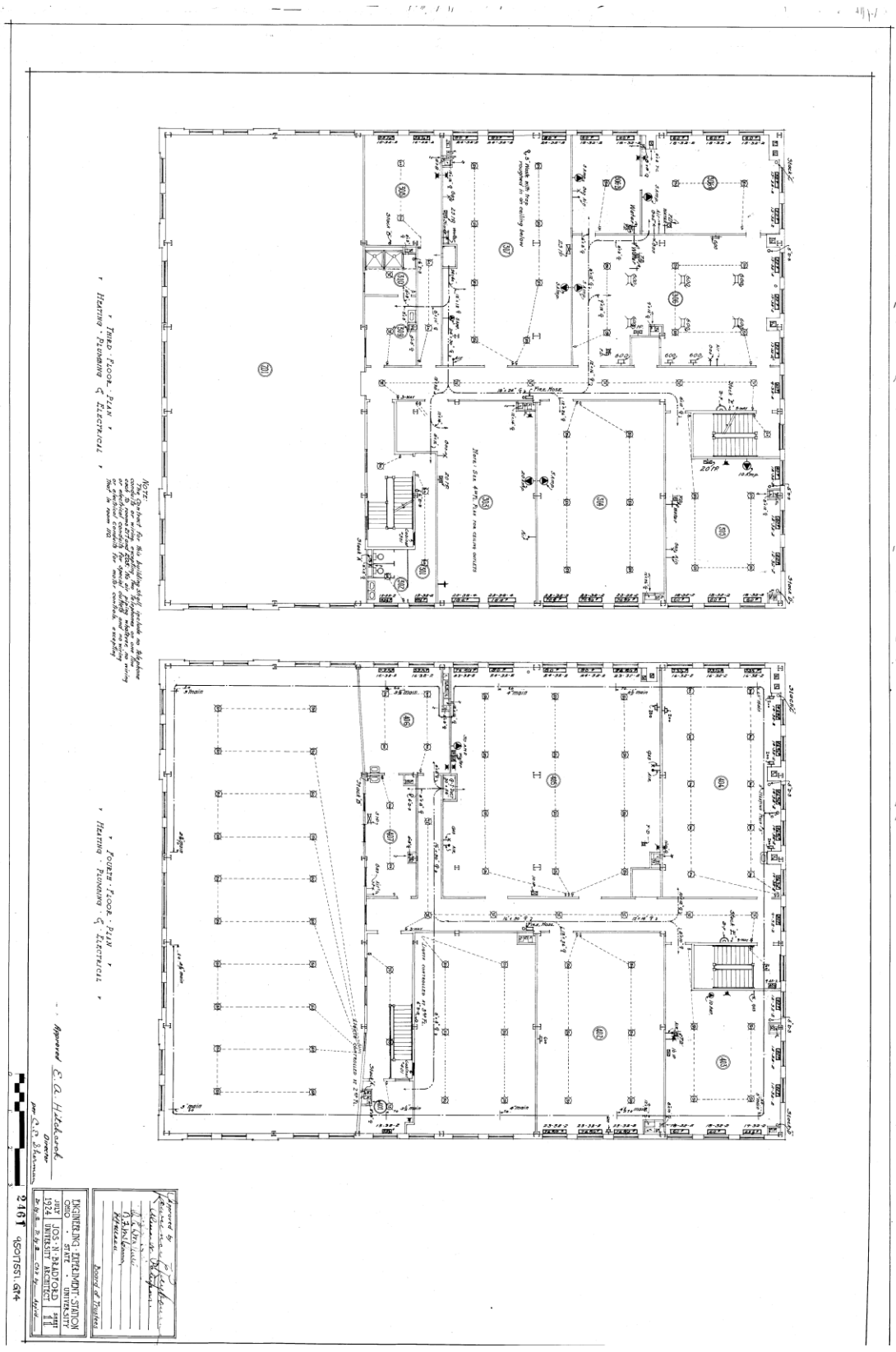

Figure A.11: Third and fourth floor heating, plumbing and electrical plans

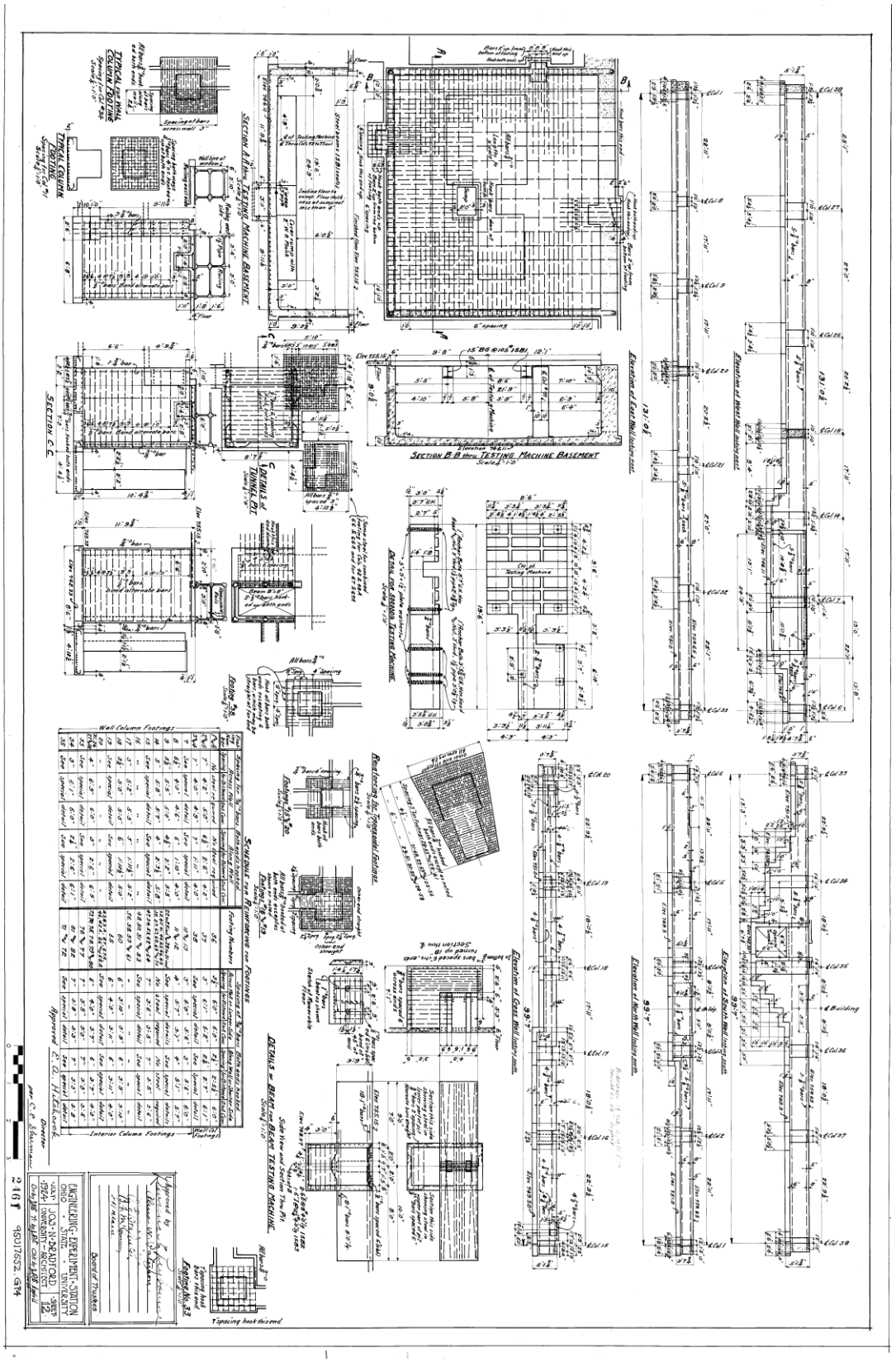

Figure A.12: Column footings

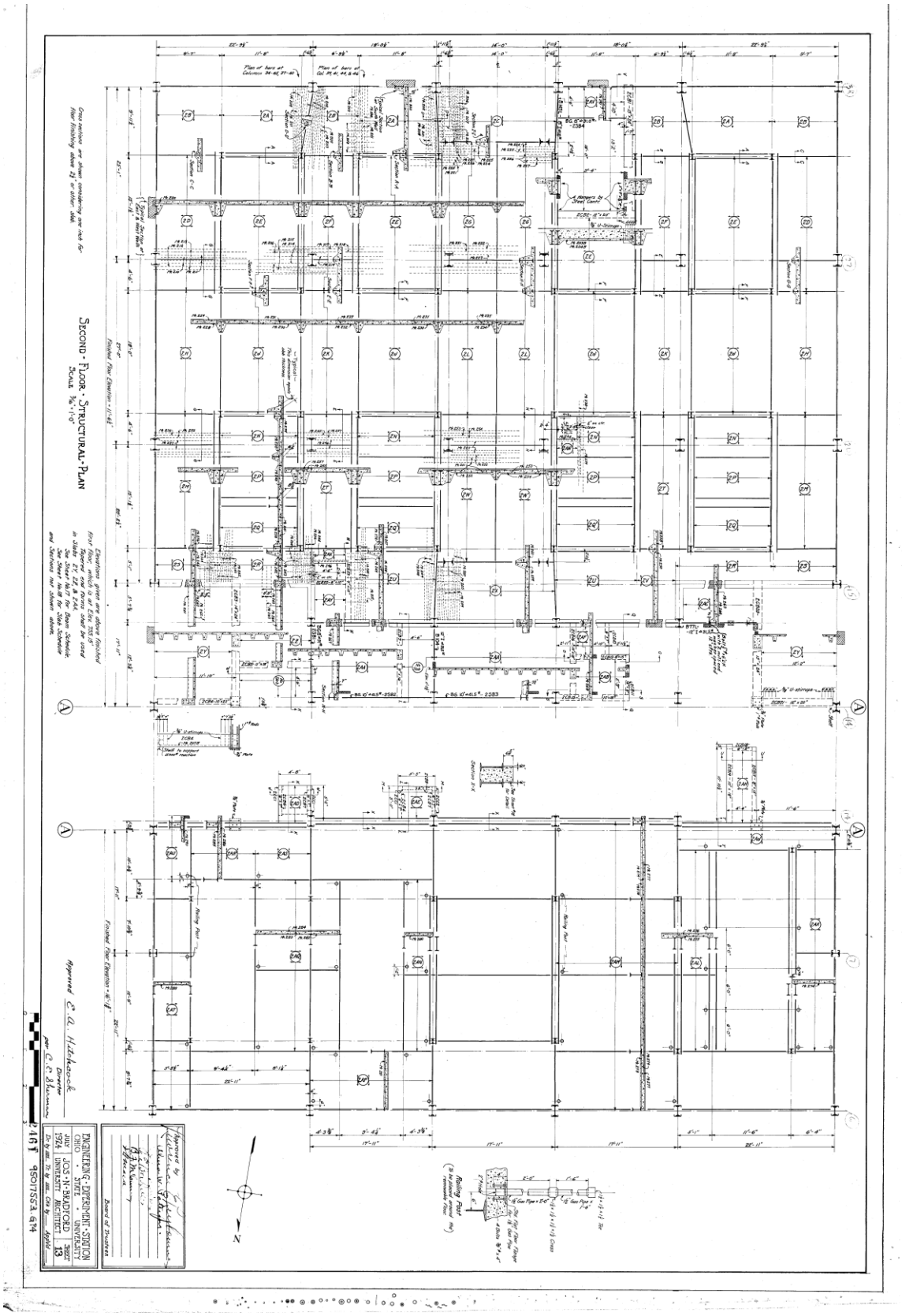

Figure A.13: Second floor structural plan

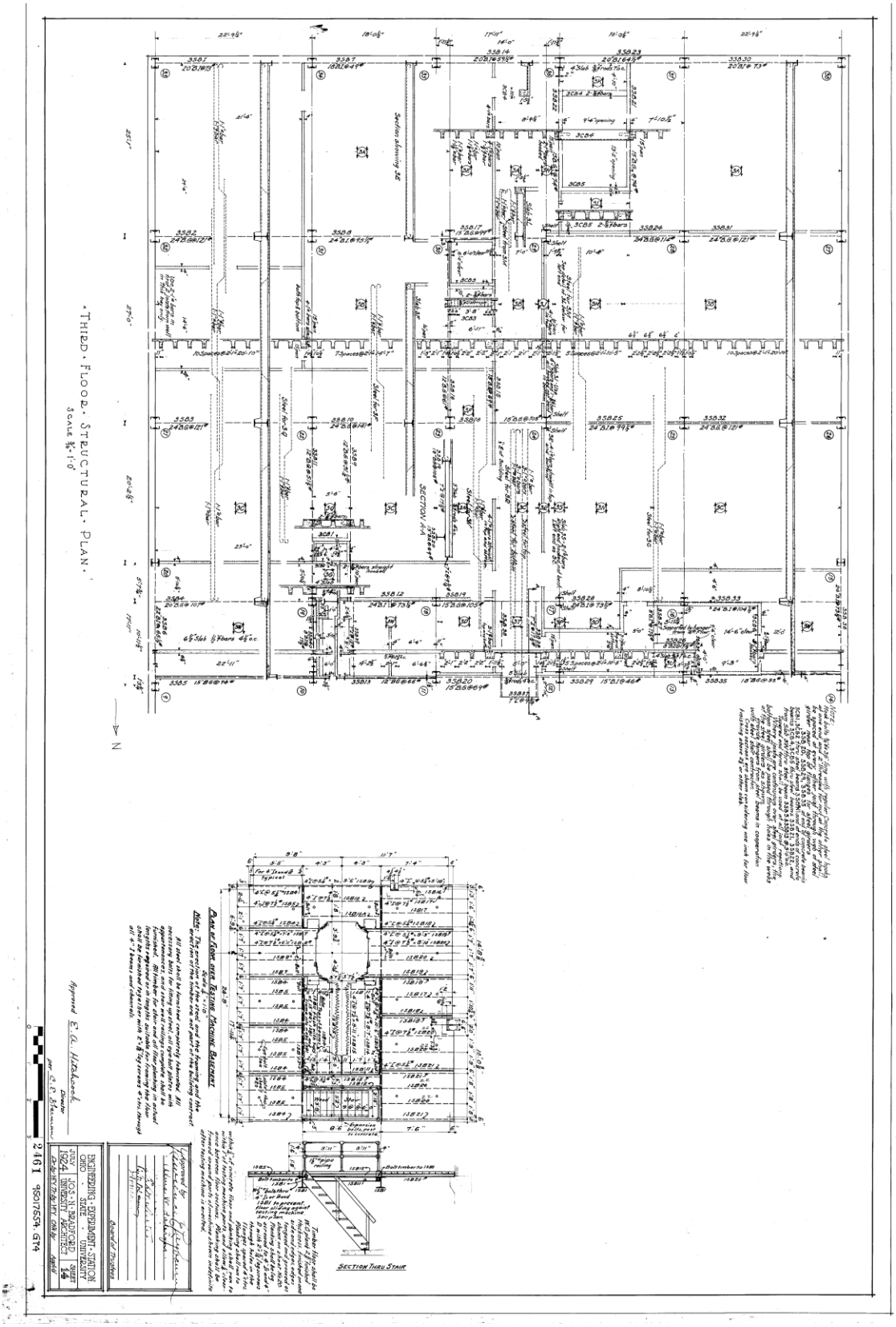

Figure A.14: Third floor structural plan

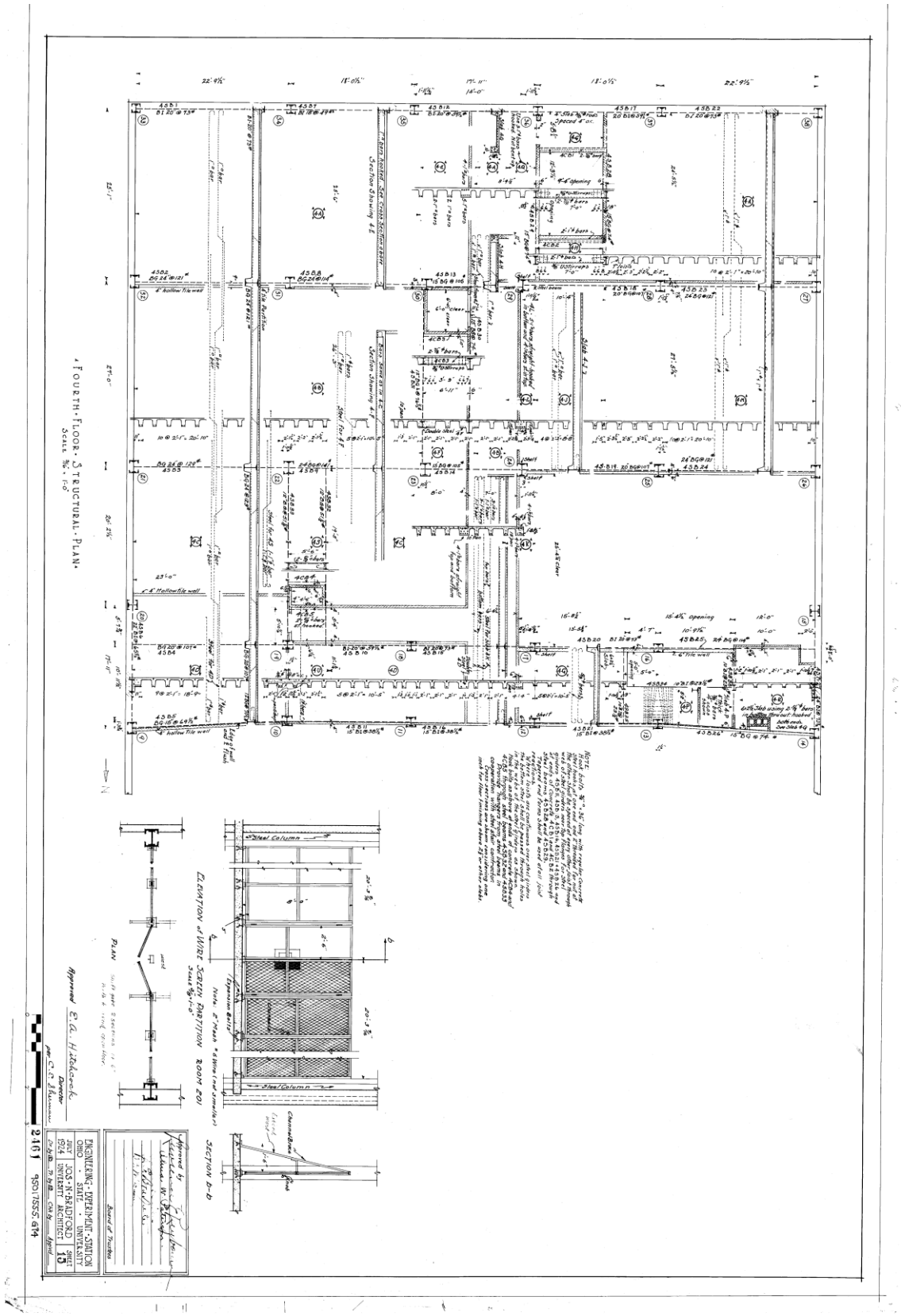

Figure A.15: fourth floor structural plan

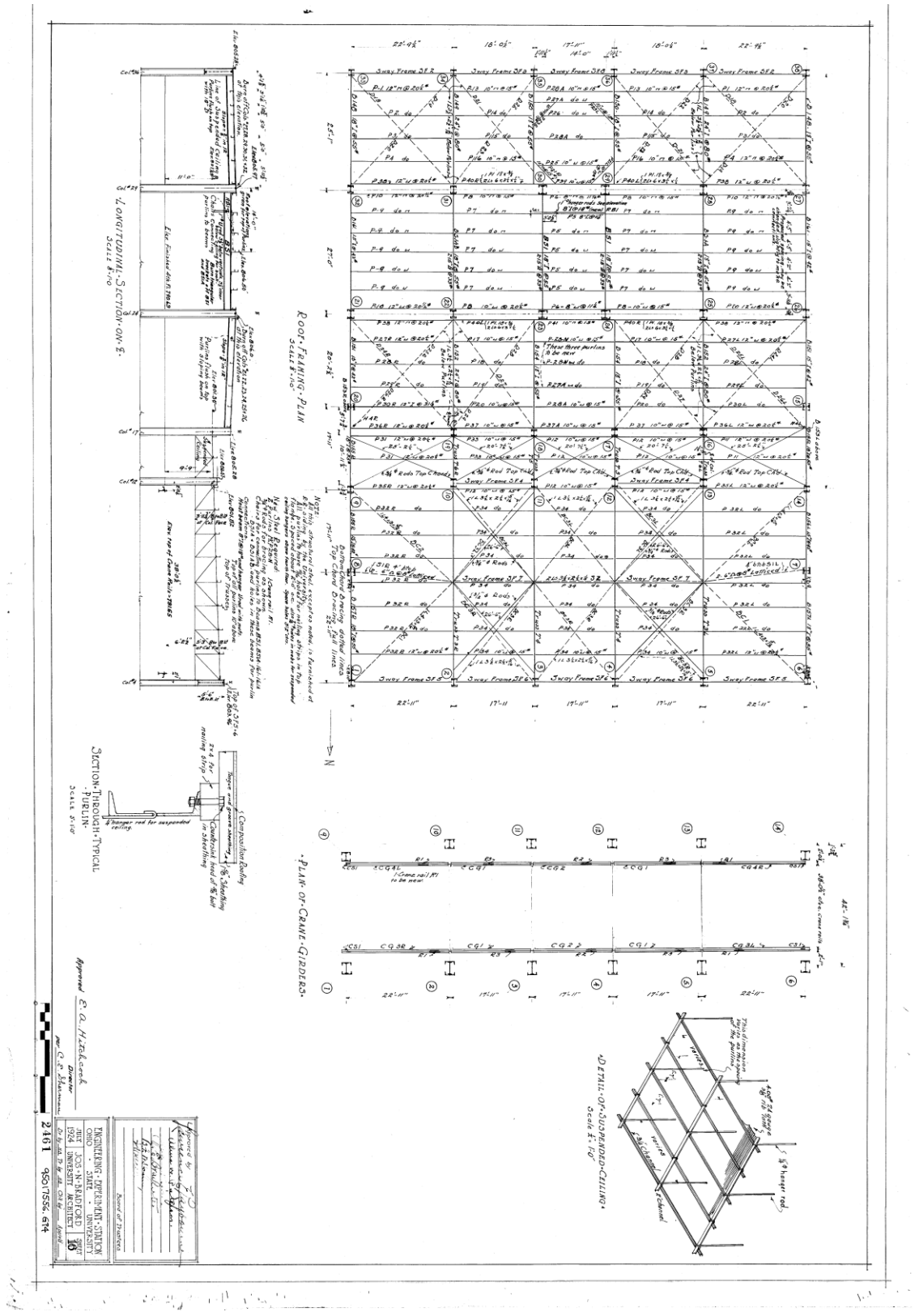

Figure A.16: Roof framing plan

Figure A.17: East and west frame sections and elevations

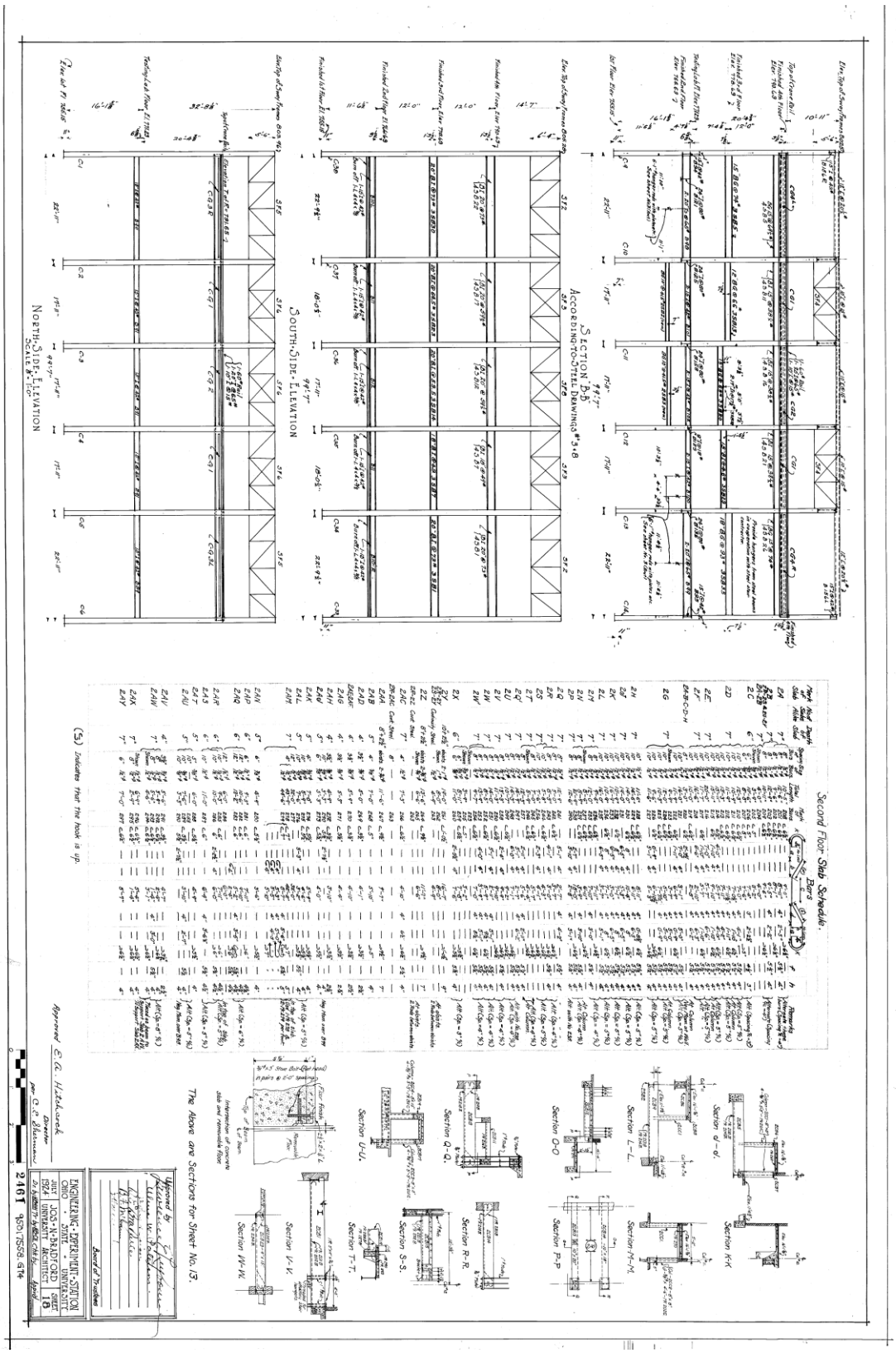

Figure A.18: North and South frame sections and elevations with second floor slab schedule

Figure A.19: Section A-A and old steel schedule

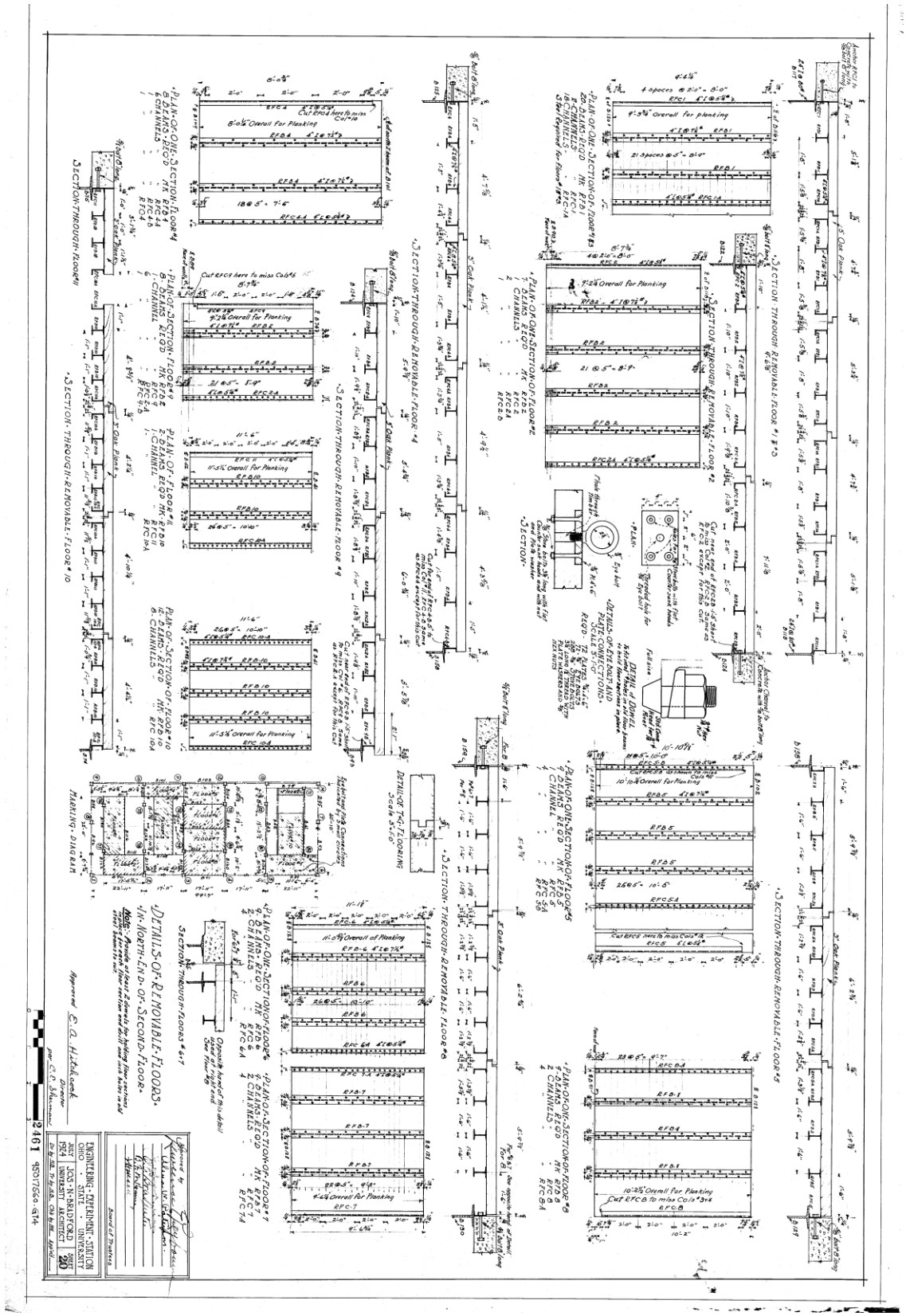

Figure A.20: Details of removable floors in North end of second floor

APPENDIX B: EXPERIMENTAL PICTURES OF COLUMNS AND BEAMS

B.1 North Column 26 Pictures

Figure B.1.1: North column 26 seen from South-direction. Used to estimate bracketing channel depth

Figure B.1.2: North column 26 seen from East-direction. Used to estimate overall column depth (I-section and two channels)

Figure B.1.3: North column 26 seen from Southeast-direction. Used to estimate base flange length

Figure B.1.4: North column 26 seen from Northeast-direction. Used to estimate I-section base flange length and channel flange thickness

B.2 Removed Column 27 Pictures

Figure B.2.1: Removed column 27 seen from South-direction. Used to estimate column channel depth and beam base flange length

Figure B.2.2: Removed column 27 seen from North-direction. Used to estimate overall column depth

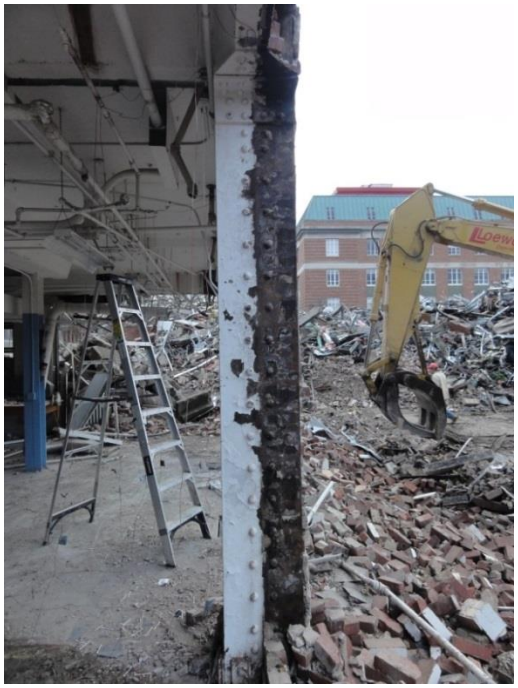

Figure B.2.3: Removed column 27 seen from North-direction. Used to estimate bracketing channel depth

Figure B.2.4: Removed column 27 seen from Northeast-direction. Used to estimate I-section base flange length and channel flange thickness

B.3 East Column 28 Pictures

Figure B.3.1: East column 28 seen from East-direction. Used to estimate overall depth and channel flange length

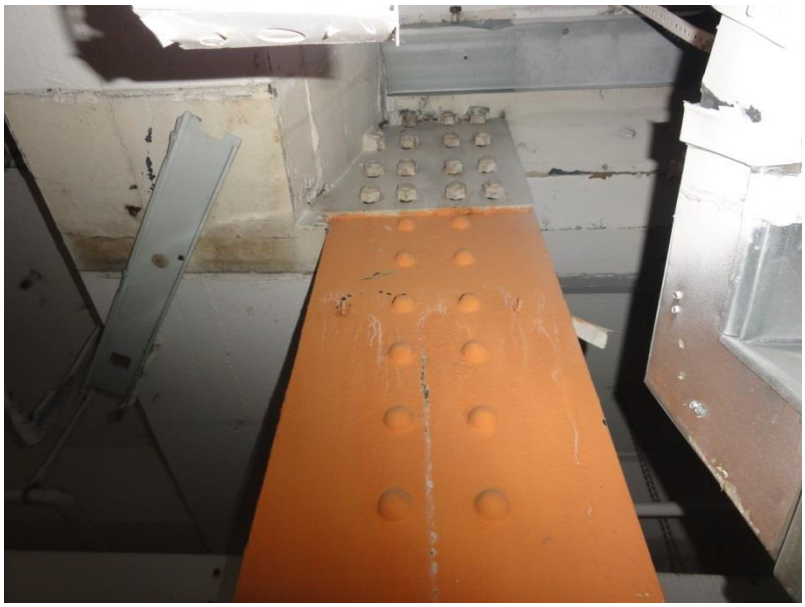

Figure B.3.2: East column 28 seen from East-direction. Used to estimate bracketing channel depth

B.4 South Column 38 Pictures

Figure B.4.1: South column 38 seen from East-direction. Used to estimate overall depth and channel flange length

Figure B.4.2: South Column 38 seen from Northeast-direction. Used to estimate channel thickness and show beam partial concrete reinforcement

Figure B.4.3: South column 38 seen from North-direction. Used to estimate bracketing channel depth

B.5 Beam Pictures

Figure B.5.1: Beam-column connection with rivets through angles on beam bottom flange and web

APPENDIX C: ORIGINAL DISPLACEMENT DATA AND LOAD CALCULATIONS

C.1 Displacement Sensors

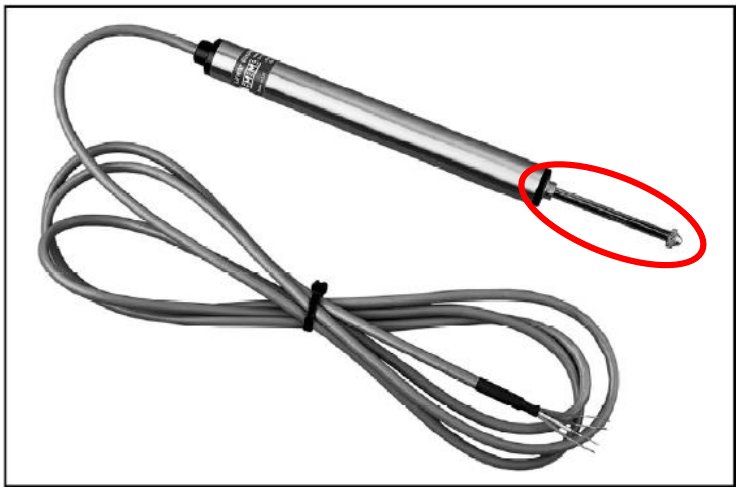

Figure C.1.1: Linear Variable Differential Transformer (LVDT) with plum bob (red)

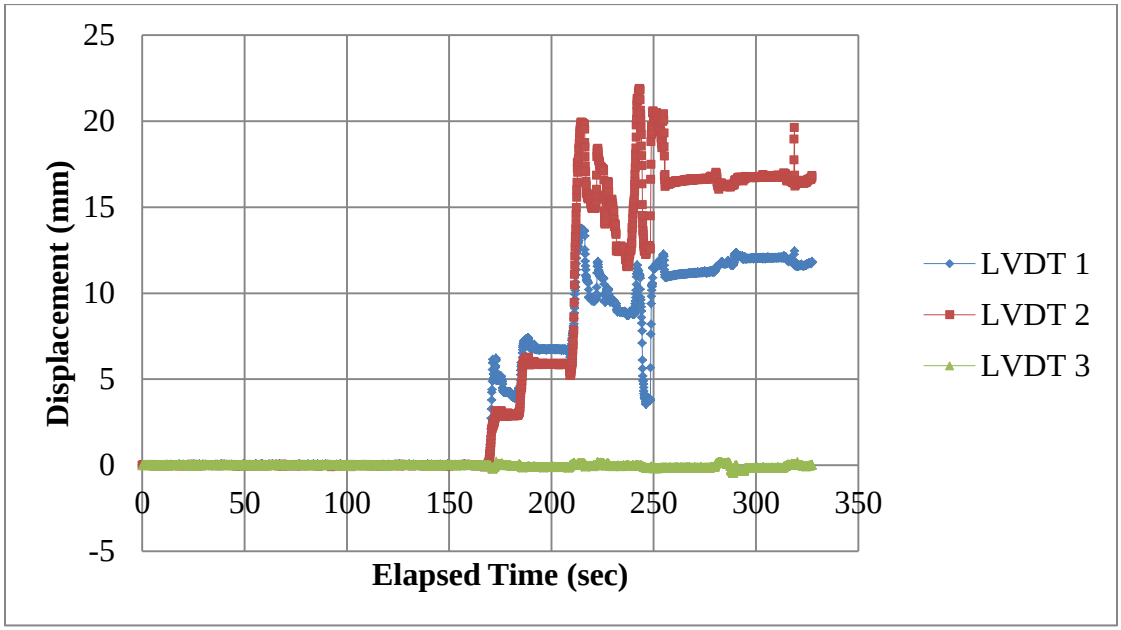

Figure C.1.2: Original displacement versus time plot of vertical (1 and 2) and horizontal (3) LVDTs

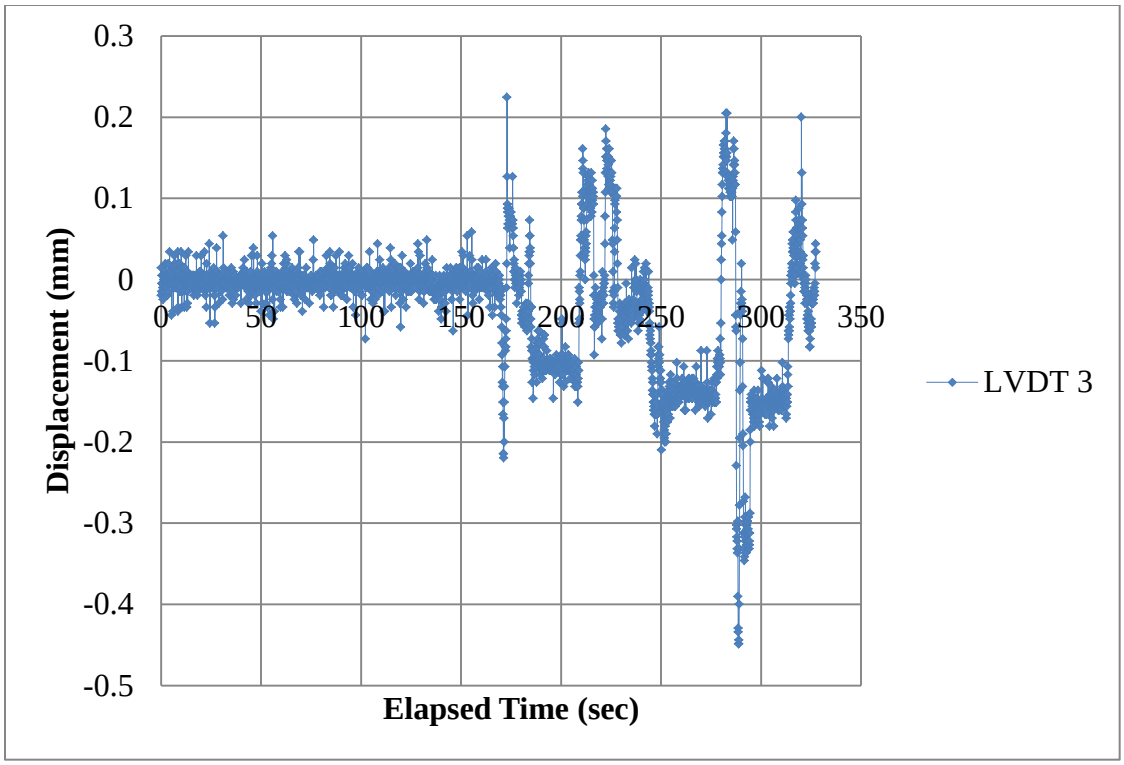

Figure C.1.3: Original displacement versus time plot of horizontal LVDT

C.2 Load Calculations

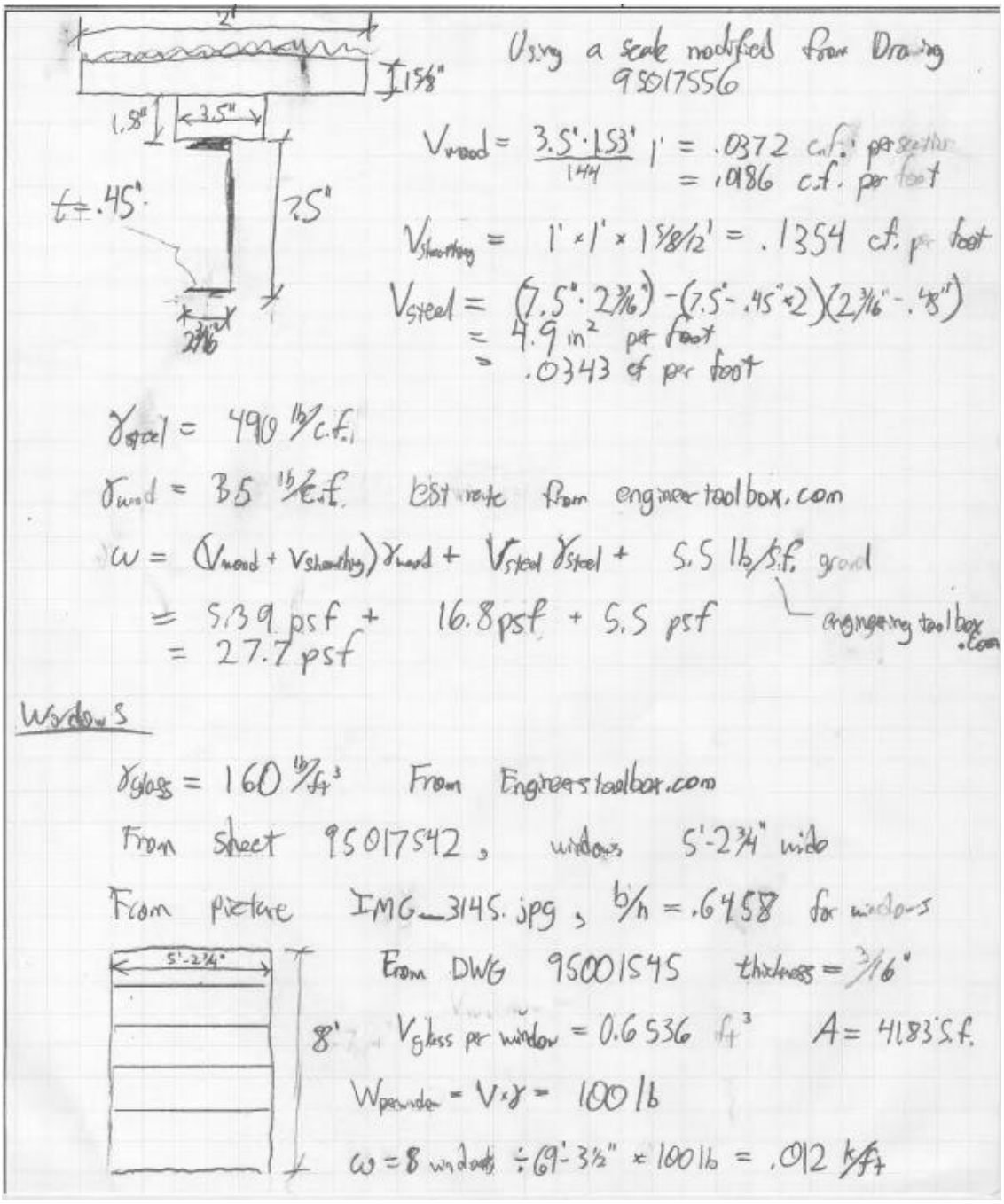

Figure C.2.1: Calculations for roof and wall loads – roof density and window layout

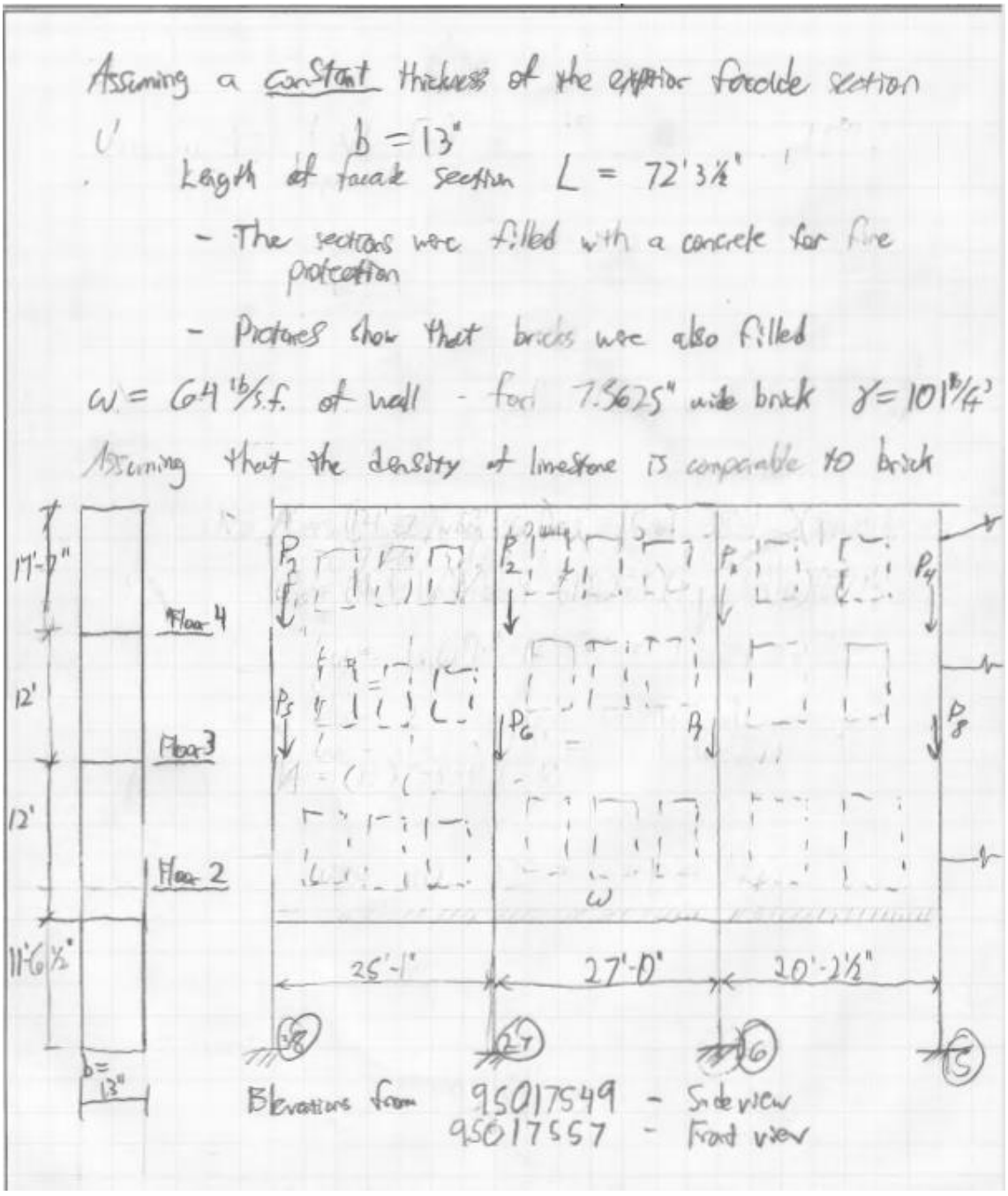

Figure C.2.2: Calculations for roof and wall loads – wall density and façade area

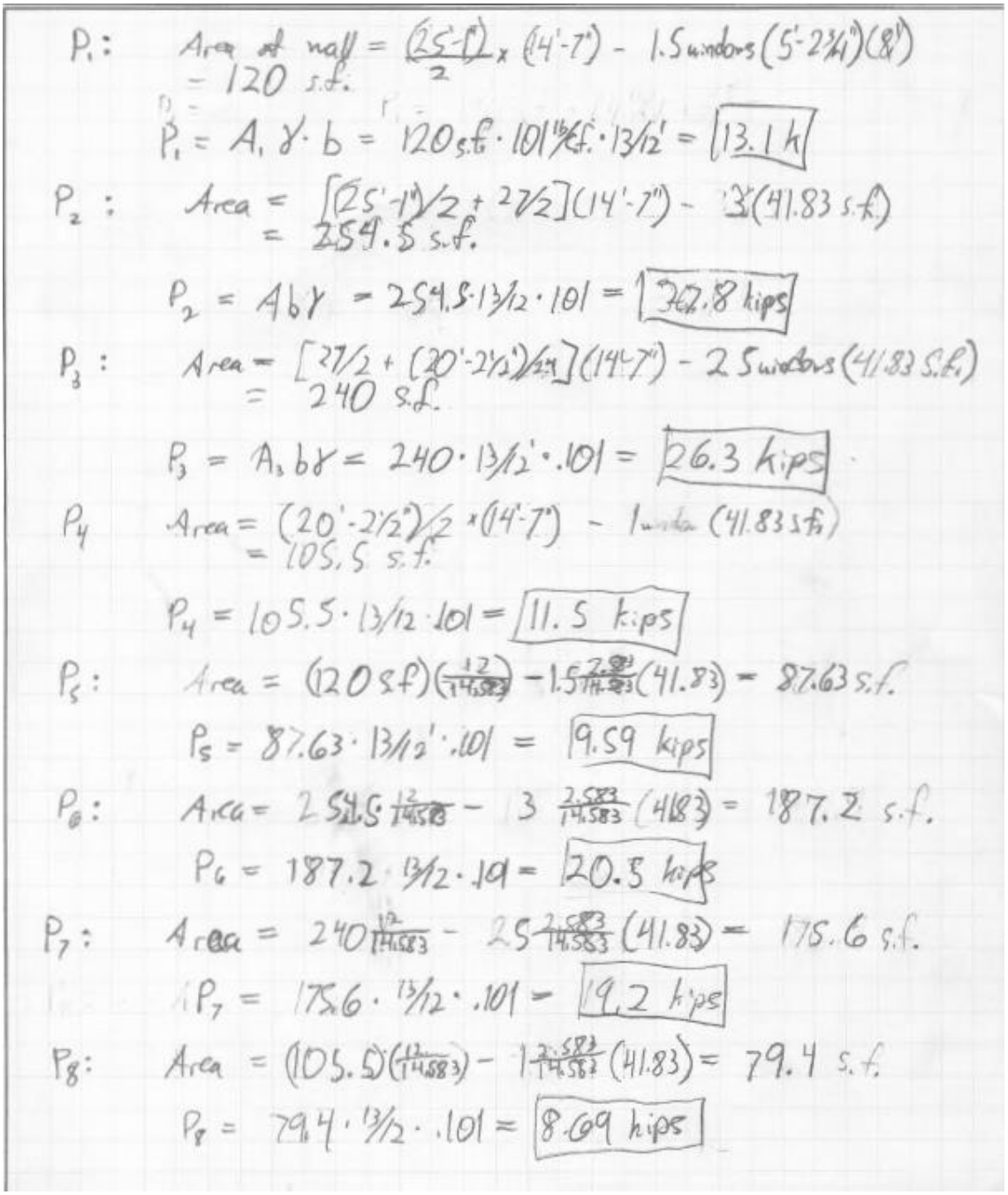

Figure C.2.3: Calculations for roof and wall loads – wall gravity loads on columns

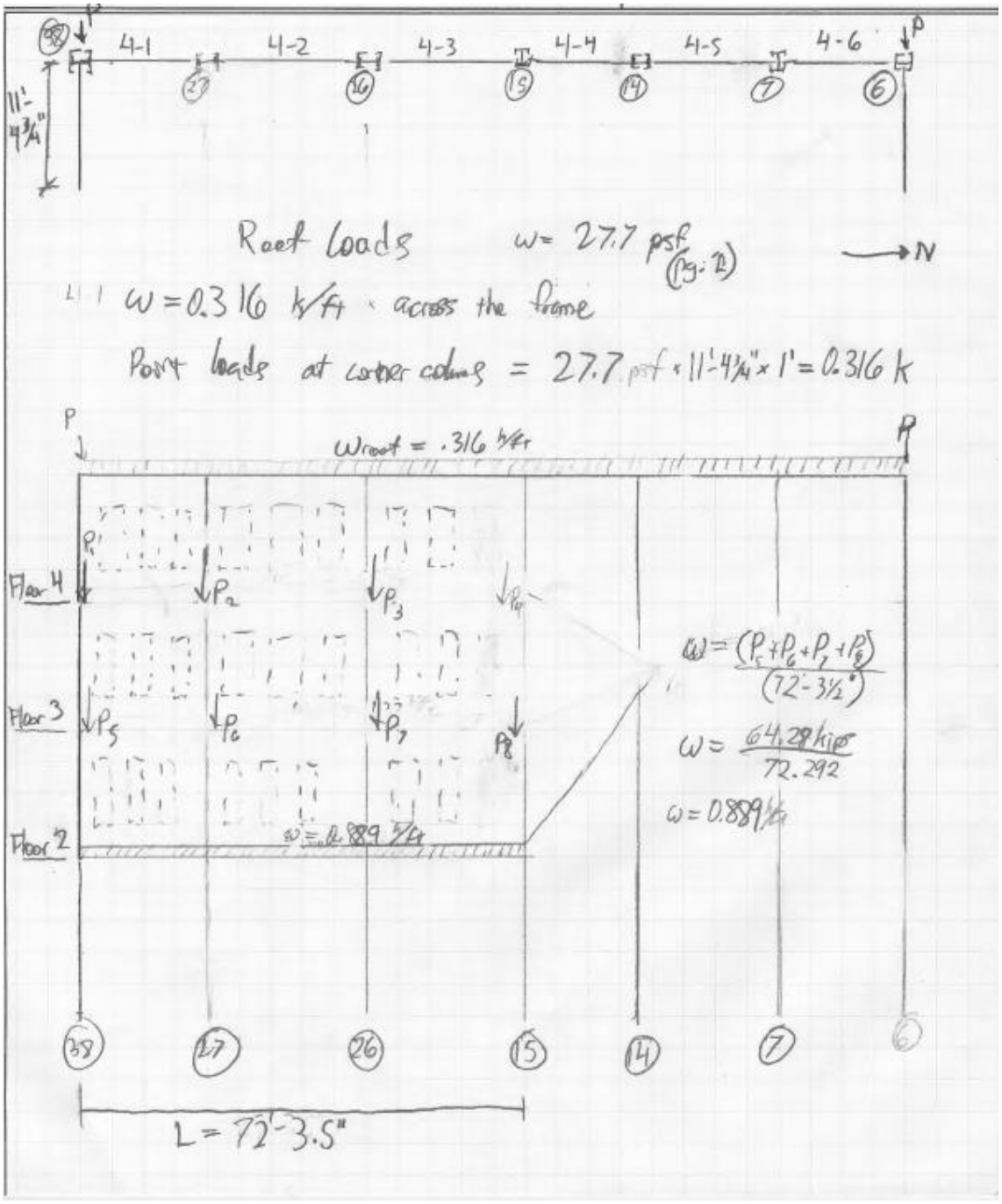

Figure C.2.4: Calculations for roof and wall loads – final load distributions

Table C.2.1: Point loads from East-West beams using Equation 5.2

	Column	East-West Beam (Y/N)	East-West $Weight_{beam}$ (plf)	East-West $Length_{beam}$ (ft)	East-West P_{beam} (lb)
Fourth Floor	6	Y	140	22.79	1595.42
	7	N	N/A	N/A	N/A
	14	Y	74	22.79	843.29
	15	N	N/A	N/A	N/A
	26	Y	121	22.79	1378.90
	27	Y	121	22.79	1378.90
	38	Y	73	22.79	831.90
Third Floor	6	N	N/A	N/A	N/A
	7	N	N/A	N/A	N/A
	14	Y	93	22.79	1059.81
	15	N	N/A	N/A	N/A
	26	Y	121	22.79	1378.90
	27	Y	121	22.79	1378.90
	38	Y	73	22.79	831.90
Second Floor	6	Y	42	22.79	478.63
	7	N	N/A	N/A	N/A
	14	Y	65	22.79	740.73
	15	N	N/A	N/A	N/A
	26	N	N/A	N/A	N/A
	27	N	N/A	N/A	N/A
	38	N	N/A	N/A	N/A

NOTE: Third floor East-West beam on column 14 is offset by 1 ft- 3.75in. to the South

Table C.2.2: Floor slab information to use in Equations 5.3 and 5.4

Slab	**Between Columns (#, #)**	***Width*$_{slab}$ (ft)**	***Length*$_{slab}$ (ft)**	**Direction**	**Joists (Y/N)**	**t_{slab} (in.)**	**#-way**
4R	**14, 15**	10.96	12.00	E-W	Y	2.5	1
4M	26, 27	22.79	27.00	N-S	Y	2.5	1
4A	27, 38	22.79	25.08	N-S	Y	2.5	1
3W	**14, 15**	10.96	12.00	E-W	N	6.0	2
3C	15, 26	20.21	22.79	E-W	Y	2.5	1
3B	26, 27	22.79	27.00	N-S	Y	2.5	1
3A	27, 38	22.79	25.08	N-S	Y	2.5	1
2AK	**6, 14**	6.33	29.32	N-S	N	5.0	1
2AJ	**7, 14**	2.86	22.92	E-W	N	5.0	1
2Y	14, 15	10.92	17.92	N-S	Y	2.5	1
2S-2R	**15, 26**	5.08	22.79	E-W	N	7.0	1
2M	**15, 27**	9.58	19.63	N-S	N	7.0	1
2H	**26, 27**	9.58	18.00	N-S	N	7.0	2
2D	**27, 38**	9.58	19.63	N-S	N	7.0	1
2A-2B	**27, 38**	9.96	22.79	E-W	N	7.0	1

NOTE: A bolded column location indicates that a beam existed on the frame to support distributed loads

Table C.2.3: Floor slab peak distributed loads and point load values

Slab	**Between Columns (#, #)**	$Width_{slab}$ **(ft)**	$Length_{slab}$ **(ft)**	t_{slab} **(in.)**	**#-way**	**γ (pcf)**	w_{peak} **(plf)**	P_{slab} **(lb)**	$P_{triangle}$ **(lb)**
4R	**14, 15**	10.96	12.00	2.5	1	150	187	N/A	N/A
4M	26, 27	22.79	27.00	2.5	1	150	356	4807	N/A
4A	27, 38	22.79	25.08	2.5	1	150	356	4466	N/A
3W	**14, 15**	10.96	12.00	6.0	2	150	410	2465	2251
3C	15, 26	20.21	22.79	2.5	1	150	315	3598	N/A
3B	26, 27	22.79	27.00	2.5	1	150	356	4807	N/A
3A	27, 38	22.79	25.08	2.5	1	150	356	4466	N/A
2AK	**6, 14**	6.33	29.32	5.0	1	150	197	N/A	N/A
2AJ	**7, 14**	2.86	22.92	5.0	1	150	89.5	1025	N/A
2Y	14, 15	10.92	17.92	2.5	1	150	170	1528	N/A
2S-2R	**15, 26**	5.08	22.79	7.0	1	150	222	2534	N/A
2M	**15, 27**	9.58	19.63	7.0	1	150	419	N/A	N/A
2H	**26, 27**	9.58	18.00	7.0	2	150	419	N/A	2009
2D	**27, 38**	9.58	19.63	7.0	1	150	419	N/A	N/A
2A-2B	**27, 38**	9.96	22.79	7.0	1	150	435	4964	N/A

Table C.2.4: Joist point loads using Equation 5.5

Slab	**Between Columns (#, #)**	***Length*$_{slab}$ (ft)**	**t_{slab} (in.)**	**Joist Depth (in.)**	**Joist area (ft^2)**	***N* (joists)**	**γ (pcf)**	**w_{joists} (plf)**	**P_{joists} (lb)**
4R	**14, 15**	12.00	2.5	6.00	0.313	5	150	117	N/A
4M	26, 27	27.00	2.5	12.00	0.625	10	150	N/A	12656
4A	27, 38	25.08	2.5	12.00	0.625	10	150	N/A	11757
3C	15, 26	22.79	2.5	12.00	0.625	10	150	N/A	10683
3B	26, 27	27.00	2.5	12.00	0.625	10	150	N/A	12656
3A	27, 38	25.08	2.5	12.00	0.625	10	150	N/A	11757
2Y	14, 15	17.92	2.5	10.00	0.521	5	150	N/A	3499

Table C.2.5: Floor slab layouts and load distributions

Slab	Distribution	Between Columns (#, #)	Beam Length (in.)	Start Point (in.)	Distr. Peak Start (in.)	Distr. Peak End (in.)	End Point (in.)
4R	Uniform	**14, 15**	215	0	0	131.5	131.5
4M	Points	26, 27	324	0	N/A	N/A	324
4A	Points	27, 38	301	0	N/A	N/A	301
3W	Triangle	**14, 15**	215	15.75	81.5	81.5	147.25
3C	Points	15, 26	242.5	0	N/A	N/A	242.5
3B	Points	26, 27	324	0	N/A	N/A	324
3A	Points	27, 38	301	0	N/A	N/A	301
2AK	Uniform	**6, 7**	275	103.75	103.75	275	275
2AK	Uniform	**7, 14**	215	0	0	180.625	180.625
2AJ	Points	**7, 14**	215	180.625	N/A	N/A	215
2Y	Points	14, 15	215	0	N/A	N/A	215
2S-2R	Points	**15, 26**	242.5	0	N/A	N/A	61
2M	Uniform	**15, 26**	242.5	61	61	242.5	242.5
2M	Uniform	**26, 27**	324	0	0	54	54
2H	Trapezoid	**26, 27**	324	54	111.5	212.5	270
2D	Uniform	**26, 27**	324	270	270	324	324
2D	Uniform	**27, 38**	301	0	0	181.5	181.5
2A-2B	Points	**27, 38**	301	181.5	N/A	N/A	301

NOTE: Measurements are in reference to the North end of the beam.

Table C.2.6: Total floor slab distributed loads on perimeter frame beams

Floor	Between Columns (#, #)	Beam Length (in.)	Distr. Load Start (k/in.)	Distr. Peak (k/in.)	Distr. Load End (k/in.)	Source
Fourth	14, 15	215	0.0254		0.0254	Slab 4R
Third	14, 15	215	0	0.0342	0	Slab 3W
Second	6, 7	275	0.0165		0.0165	Slab 2AK
	7, 14	215	0.0165		0.0165	Slab 2AK
	15, 26	242.5	0.0349		0.0349	Slab 2M
	26, 27	324	0.0349		0.0349	Slab 2M
	26, 27	324	0	0.0349	0	Slab 2H
	26, 27	324	0.0349		0.0349	Slab 2D
	27, 38	301	0.0349		0.0349	Slab 2D

NOTE: Refer to Table C.2.5 to determine location of distributive loads on beams. A superimposed dead load of 0.0142 k/in. existed on each beam. A wall distributed load of 0.0741 k/in. existed on second floor beams located between columns 15 through 38.

Table C.2.7: Total point loads on perimeter frame beams

Floor	Between Columns (#, #)	Beam Length (in.)	Location (in.)	Point Load (kips)	Point Source
Third	14, 15	215	15.75	3.53	E-W Beam
Second	7, 14	215	180.625	1.03	Slab 2AJ
	15, 26	243	61	2.53	Slab 2S-2R
	26, 27	324	54	2.01	Slab 2H
	26, 27	324	270	2.01	Slab 2H
	27, 38	301	181.5	4.96	Slab 2A-2B

NOTE: Measurements are in reference to the North end of the beam

Table C.2.8: Total point loads on perimeter frame columns

Floor	Column	E-W P_{beam} (lb)	P_{slab} (lb)	P_{joist} (lb)	P_{wall} (lb)	$P_{superimposed}$ (lb)	P_{total} (lb)	P_{total} (kips)
Fourth	6	1595	N/A	N/A	N/A	N/A	1595	1.60
	7	N/A	N/A	N/A	N/A	N/A	0	0
	14	843	N/A	N/A	N/A	N/A	843	0.84
	15	N/A	N/A	N/A	11500	N/A	11500	11.50
	26	1379	4808	6328	26300	2308	41122	41.12
	27	1379	9274	12207	27800	4451	55111	55.11
	38	832	4466	5879	13100	2144	26421	26.42
Third	6	N/A	N/A	N/A	N/A	N/A	0	0
	7	N/A	N/A	N/A	N/A	N/A	0	0
	14	1060	N/A	N/A	N/A	N/A	1060	1.06
	15	N/A	3598	5342	8690	1727	19357	19.36
	26	1379	8406	11670	19200	4035	44690	44.69
	27	1379	9274	12207	20500	4451	47811	47.81
	38	832	4466	5879	9590	2144	22911	22.91
Second	6	479	N/A	N/A	N/A	N/A	479	0.48
	7	N/A	N/A	N/A	N/A	N/A	0	0
	14(N)	741	1026	N/A	N/A	N/A	1766	1.77
	14(S)	N/A	1528	1750	N/A	1531	4809	4.81
	15	N/A	4062	1750	N/A	1531	7343	7.34
	26	N/A	N/A	N/A	N/A	N/A	0	0
	27	N/A	N/A	N/A	N/A	N/A	0	0
	38	N/A	4965	N/A	N/A	N/A	4965	4.96

NOTE: On the second floor there existed two elevations for slabs running into column 14